Highly sensitive measurements of substrates and inhibitors on the basis of tyrosinase sensors and recycling systems

Dissertation

Zur Erlangung des akademischen Grades
Doktor der Naturwissenschaften
(Dr. rer. nat.)
in der Wissenschaftsdisziplin Analytische Biochemie

eingereicht an der
Mathematisch-Naturwissenschaftlichen Fakultät
der Universität Potsdam

von
Katrin Streffer

Potsdam, im September 2002

Acknowledgements

I wish to express my gratitude to Professor Dr. F. W. Scheller for his encouraging support of my work and for many fruitful discussions.

Furthermore, I wish to thank Dr. U. Wollenberger for her careful guidance, a lot encouragements and numerous advice.

I am also very grateful to Professor Dr. G. W. Canters for his kind support during my working stay in his laboratory.

My thousands of thanks to Dr. E. Vijgenboom and A. W. J. W. Tepper for teaching me in all things around molecular biology and protein purification.

My gratefulness to all the people in Prof. Dr. F. W. Schellers group as well as to all the people in the group of Prof. Dr. G. W. Canters, because I am not able to list them all. I will pick only some of them.

Special thanks to Dr. A. Makower, Dr. C. Bauer, Dr. A. V. Eremenko, Dr. W. F. M. Stöcklein, Dr. F. F. Bier and Dr. F. Kleinjung for their support of the work and helpful discussions.

Quite special thanks go to Dr. U. Kolczak for sharing her apartment with me during one of my stays in Leiden (The Netherlands), for her support, helpful discussions and all the things I do forget now!

Additionally I wish to express my gratitude to Prof. Dr. M. G. Peter, Dr. S. Haebel and H. Kaatz for fruitful discussions and especially for doing the synthesis of special tyrosinase inhibitors and for doing the mass spectroscopy of the enzymes.

Financial support from the Deutsche Forschungsgemeinschaft (INK16 A1-1) and from the BIOSET Concerted Action (EC Environment and Climate Programme) is gratefully acknowledged.

Finally, I would like to thank my whole family for their support which has accompanied me through all these years. I would particularly like to thank my parents (B. and H. Möller), my brother in law (C. Streffer) and my sister in law (C. E. Streffer) for the care and supervision of my two children. Furthermore, I wish to thank my parents in law (I. and M. Streffer) for their correction work. In the end I wish to thank my husband (R. M. F. Streffer) for his never ending encouragement, his understanding and all the unnamed things!

Contents

Abbreviations

AME	alternariol monomethyl ether
Amp	ampicillin
AOH	alternariol
AQ	see Eastman AQ 29D
BSA	bovine serum albumin
COE	Clark type oxygen electrode
COE_MT_PVA	mushroom tyrosinase electrode, in which tyrosinase entrapped in polyvinyl alcohol is immobilised on a Clark type oxygen electrode
COE_ST_PVA	tyrosinase electrode, in which tyrosinase from *S. antibioticus* entrapped in polyvinyl alcohol is immobilised on a Clark type oxygen electrode
CPE	carbon paste electrode
DMSO	dimethylsulfoxid
DNA	deoxyribonucleic acid
DTSP	3,3-dithiodipropionic acid-di-(N-succinimidylester)
Eastman AQ 29D	registered trademark of Eastman Kodak (Kingsport, Tennessee, USA) for a polyester-sulphonic acid cation exchanger
E. coli	Escherichia coli
EDC	N-ethyl-N-(3-diethylaminopropyl) carbodiimide
FAD	flavin adenine dinucleotide
FC	flow cell
FI-S	flow injection system
FMN	flavin adenine mononucleotide
G	amplification factor
GA	glutaraldehyd
GCDE	glassy carbon disk electrode
GCE	glassy carbon electrode
GC/MS	gas chromatography / mass-spectroscopy
GDE	graphite disk electrode
GDH	glucose dehydrogenase
GKM	glucometer (potentiostat)
Gm	gentamycin
HEPES	N-[2-hydroxyethyl]piperazine]-N′-[2-ethanesulfonic acid]
HPLC	high pressure liquid chromatography
IPTG	isopropyl-1-thio--D-galactopyranoside

kojic acid	5-hydroxy-2-hydroxymethyl-4H-4-pyrone
kojic acid 5-O-capryloate	octanoic acid 2-hydroxymethyl-4-oxo-4H-4-pyran-5-yl ester
kojic acid 7-O-capryloate	octanoic acid 5-hydroxymethyl-4-oxo-4H-4-pyran-2-yl-methyl ester
kojic acid 5,7-di-O-di-capryloate	octanoic acid 5-hydroxymethyl-4-oxo-2-(1-oxooctyloxymethyl)-4H-pyran-5-yl ester
kojic acid linker	11-aminoundecanoic acid (5-hydroxy-4-oxo-4*H*-pyran-2-yl)-methyl ester
LB	liquid medium (pH=7.0), contains bacto tryptone, bacto yeast extract and NaCl
MALDI	matrix assisted laser desorption / ionization
MALDI-MS	matrix assisted laser desorption / ionization mass spectrometry
MDC	mono- and diphenolic compounds
MEL 1-11	primer (see Table 7.1 at page 112)
MEL 1-14	primer (see Table 7.1 at page 112)
MEL 2-7	primer (see Table 7.1 at page 112)
m-GDH	membrane-bound glucose dehydrogenase
MT	mushroom tyrosinase (identical with tyrosinase from *Agaricus bisporus*)
MT/GDH-sensor	bienzyme electrode, in which mushroom tyrosinase and GDH entrapped in polyvinyl alcohol are immobilised on a Clark type oxygen electrode
MUT 5	primer (see Table 7.1 at page 112)
NAD^+	nicotinamide adenine dinucleotide oxidised form
NADH	nicotinamide adenine dinucleotide reduced form
$NADP^+$	nicotinamide adenine dinucleotide phosphate oxidised form
NADPH	nicotinamide adenine dinucleotide phosphate reduced form
Nafion	registered trademark of E. I. du Pont de Nemours and Company (Wilmington, Dellaware, USA) for a perfluorinated-sulphonated cation exchanger
NHS	N-hydroxysuccinimide
n.d.	not described
NT	neurotransmitter
par.	paragraph

pKS1 - pKS7	plasmids with inserts, constructed in the context of this work and listed in Table 4.8 at page 96
pMEL...	plasmids with inserts, used in the context of this work and listed in Table 4.8 at page 96
PCR	polymerase chain reaction
PQQ	pyrroloquinoline quinone
Q1, Q2	short-chain ubiquinones
Q6, Q9	long-chain ubiquinones
RVCE	reticulated vitreous carbon electrode
S. antibioticus	*Streptomyces antibioticus*
SAS plates	plates prepared with *S. antibioticus* sporulation medium
SCE	saturated calomel electrode
S. coelicolor	*Streptomyces coelicolor*
SDS-PAGE	SDS-polyacralamide gel electrophorese
s-GDH	soluble glucose dehydrogenase
SGE	solid graphite electrode
S. glaucescens	*Streptomyces glaucescens*
SH	salicylate hydroxylase
S. lividans	*Streptomyces lividans*
SPCE	screen printed carbon electrode
SPE	screen printed electrode
SPE_MT_N	mushroom tyrosinase electrode, in which tyrosinase entrapped in nafion is immobilised on a screen printed electrode
SPE_MT_PU	mushroom tyrosinase electrode, in which tyrosinase entrapped in polyurethane is immobilised on a screen printed electrode
SPR	surface plasmon resonance
S-S	stationary system
*ss*DNA	single stranded DNA
S.T.	tyrosinase from *S. antibioticus*
ST/GDH-sensor	bienzyme electrode, in which tyrosinase from *S. antibioticus* and GDH entrapped in polyvinyl alcohol are immobilised on a Clark type oxygen electrode
Tc	tetracycline
TYR	tyrosinase
TZ18R	primer (see Table 7.1 at page 112)
Xgal	5-bromo-4-chloro-3-indolyl--D-galactopyranoside
ZWG	Zentrum für Wissenschaftlichen Gerätebau

1 Introduction

One of the basic problems in analytical chemistry is the sensitive and selective quantification of a variety of chemical compounds. Especially highly polar or nonvolatile organic compounds are difficult to detect with classical analytical devices. On the other hand classical analytic chemistry is in most cases expensive, time consuming and combined with a high consumption of reagents. Today small analytical devices are needed which can be used in a continually expanding market of:

- environmental monitoring

- medical diagnostics

- health care

- quality control

Furthermore they should be easy to handle and they should offer the possibility for automation. In all these areas biosensors show their advantages.

Biosensors are devices that can detect chemical compounds through specific interaction with a biological sensing component, which is in close contact with a physical transducer. The biological component (e.g., enzymes, tissues, cells, organelles, receptors, antibodies or antigens) translates the specific molecular recognition of the compound into an easily measurable change of a chemical or physical parameter. This change is sensed by the transducer which generates an output signal [2, 3]. Transducers applied for biosensor development are often electrochemical, optical or thermal detectors. The most successful commercial developments are based on electrochemical transducers, especially amperometric electrodes [4].

Even the first biosensor type was an amperometric enzyme electrode [5]. In amperometric electrodes the redox-active compound is oxidised or reduced at the electrode poised at an appropriate electrical potential. Bare amperometric electrodes have in clean solutions and with a time consuming sample preparation a lower detection limit for low- molecular weight substrates of around 100nM. The introduction of an enzyme, which produces or consumes the redox-active compound leads to a clear improvement of selectivity.

On the other hand the enzyme containing matrix in front of these electrodes decreases the sensitivity typically by 2-3 orders of magnitude, due to the additional diffusion resistance. If effective mass transfer is provided and if a high enzyme activity within a thin layer is used, then measurements can be carried out down to 1μM [6]. A sensitivity of 1μM is sufficient for the determination of metabolites such as glucose, lactate and uric acid (standard value in blood for glucose 3-6.5mM, for lactate 0.6-2.4mM and for uric acid 180-420μM, standard

value in urine for glucose: 0.8-1.1mM and for uric acid 1.8-6.5mM/day), but for a large number of chemical compounds a much lower detection limit is demanded.

To overcome this problem of sensitivity one has to look for possibilities for the amplification of the measuring signal. In nature cyclic reactions present an important principle to amplify weak signals. The application of these kinds of reactions to analytical systems increases the sensitivity for enzyme electrodes more than three orders of magnitude [6]. In Figure 1.1 the sensitivities of different measurement principles are illustrated. The combination of the electrochemical detection principle and the recycling of the analyte was performed in a number of ways: the electrochemical (analyte regeneration between two electrodes), the bio-electrocatalytic (analyte regeneration between an electrode and an enzyme) and the biocatalytic recycling (analyte regeneration between two enzymes).
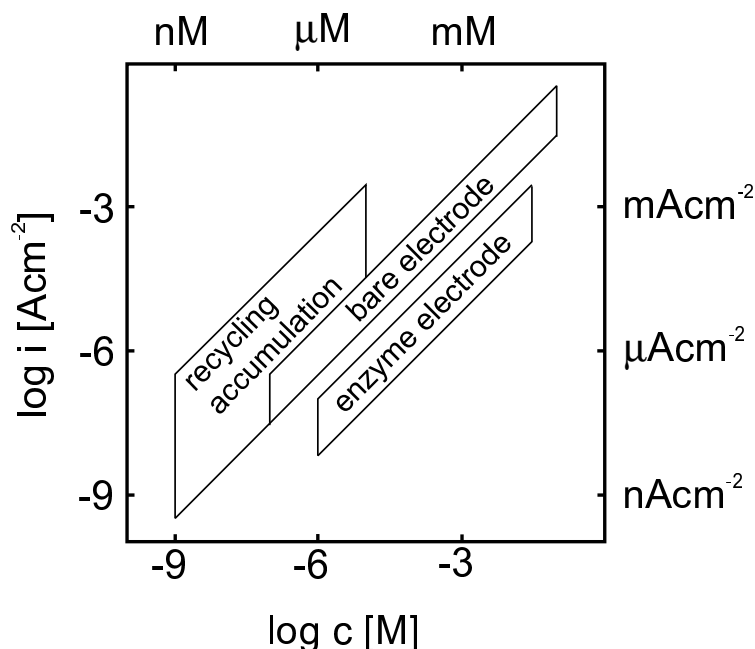
Figure 1.1: Comparison of sensitivities of bare amperometric electrodes with amperometric enzyme electrodes with and without an integrated amplification system (adapted from [7])

In the present work tyrosinase was used for the development of different amperometric enzyme electrodes. Tyrosinase possesses many attractive properties: it is commercially available, an amplification of the signal within the enzymatic and the electrochemical procedures can be observed and the enzyme offers rather broad specificity. There are numerous application areas for tyrosinase sensors, e.g., environmental monitoring, medical diagnostics and food control.

Tyrosinase is also an object of intensive studies in the fields of basic research as well as applied research, starting from investigations concerning the structure and mechanism of tyrosinase up to a possible use of tyrosinase inhibitors for cosmetics and anti-cancer drug design. This intensive work of various groups in completely different areas offers once more the possibility of learning from each other and of cooperation of basic and applied research. One possibility is the application of enzymatic engineering for the improvement of biosensor performance.

2   Target

The aim of the present studies is the development of a tyrosinase sensor, which allows the quantitative analysis of phenolic compounds in environmental analysis and in principle in clinical analysis. Special attention is paid to the development of tyrosinase sensors as sensitive as possible since the limits of phenolic compounds are very low in various samples, e.g. the limit of phenol in drinking water is 5nM according to the EU-Trinkwasserverordnung, 2001. Also the limit of dopamine (a catecholamine, which is important in medical diagnostics) is only 39μM in urine and 0.7nM in plasma. Therefore, the tyrosinase sensor developed in the context of this study have to determine phenolic compounds down to nanomolar concentrations. For comparison purposes different water samples have to be determined with a reference method (Standard Method DIN 38409-H16-1).

To accomplish these goals, different types of tyrosinase sensors will be investigated, sensors with as well as without an amplification system. A number of combinations of the electrochemical detection principle, used here, and the analyte recycling are known. Two of them are selected and examined, the bioelectrocatalytic and the biocatalytic recycling. Moreover it is investigated, whether one of the tyrosinase sensors can also be of use for the quantification of tyrosinase inhibitors, because several of them belong to a group of substances whose analysis is of great interest, e.g. thiourea, a compound which is generated by degradation of dithiocarbamate pesticides or respiratory toxins like azides and cyanids.

For the sensor development two tyrosinases were selected from a number of known tyrosinases, the tyrosinase from *Agaricus bisporus* and from *Streptomyces antibioticus*. They are examined in regard to their later application. In addition a pathway for the modification of the *S. antibioticus* tyrosinase by site directed mutagenesis (SDM) is investigated aiming at the site-oriented fixation (SOF) of the enzyme for further investigations. This may open the way for the introduction of a suitable linker molecule. Furthermore a site-to-site fixation of two enzymes is conceivable.

3 Foundations

3.1 Enzymes

Enzymes are proteins which possess the ability to catalyse specific substrate reactions extremely rapidly. They are classified according to their function and they are divided into six major classes: oxido-reductases, transferases, hydrolases, lyases, isomerases and ligases [8]. Oxido-reductases are mostly used for analytical purposes because of their electron transferring properties during catalysis. Oxido-reductases can be divided into four groups: oxidases, dehydrogenases, peroxidases and oxygenases. Enzymes belonging to the groups oxidases and dehydrogenases were used in this work and will be described in the following paragraphs (paragraph 3.1.1 and 3.1.2).

Oxidases are enzymes which transfer hydrogen from a substrate to molecular oxygen. All have a strongly bound co-factor and/or a prosthetic group. Based on the product formed during catalysis, oxidases can be divided into two groups: water producing (copper-containing-) and hydrogen peroxide producing (FAD- or FMN-containing)-oxidases. One oxidase from different organisms has been studied and will be discussed below: the copper-containing oxidase tyrosinase.

Dehydrogenases are enzymes which transfer hydrogen from a substrate to a co-factor. They can be distinguished by the binding of the co-factor, e.g., dehydrogenases of one group have bound co-factors (FMN, FAD, PQQ) and other dehydrogenases have soluble co-factors (NAD$^+$/NADH, NADP$^+$/NADPH).

3.1.1 Tyrosinase

Tyrosinase (EC 1.14.18.1) catalyses the aerobic regioselective oxidation of monophenols to o-diphenols (cresolase, monophenolase or hydroxylase activity) as well as the two-electron oxidation of o-di-phenolic compounds to o-quinones (catecholase or diphenolase activity) (Figure 3.1). From isotope labelling studies it is known, that both oxidation steps use molecular oxygen [9]. The two electrons
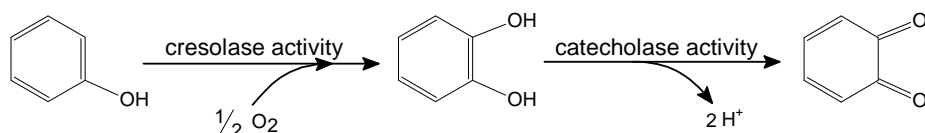
Figure 3.1: Illustration of the cresolase and catecholase activity of tyrosinase
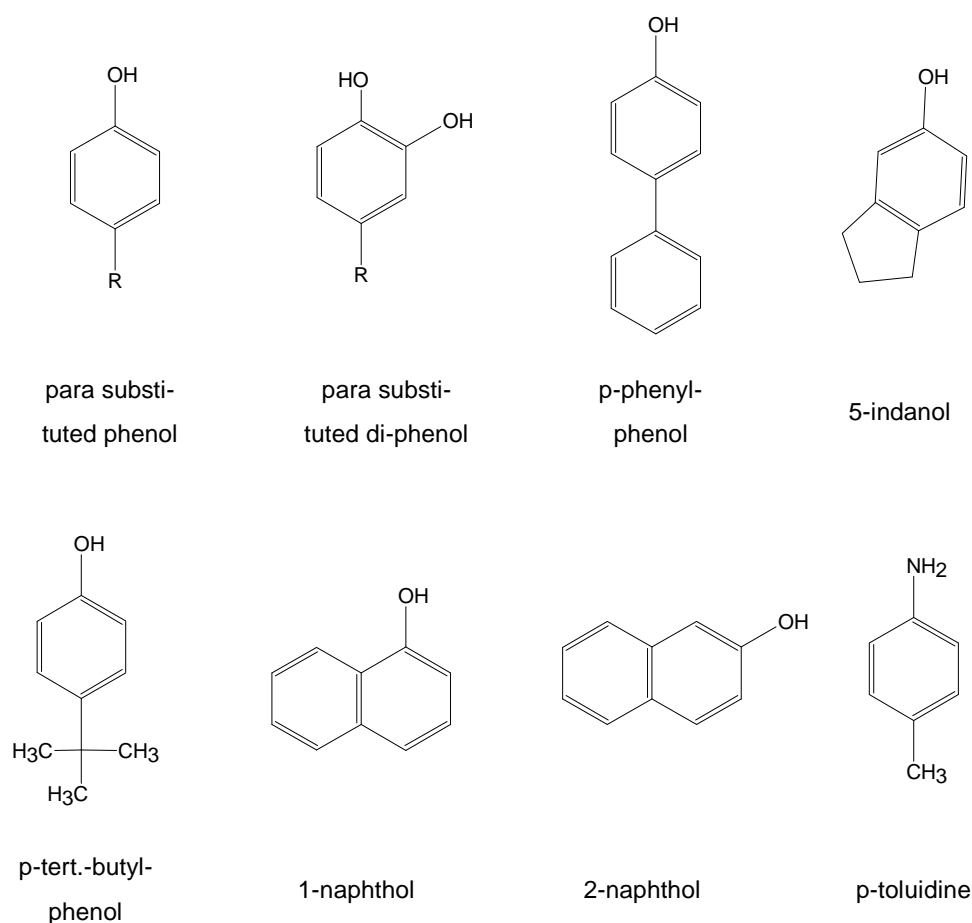
Figure 3.2: A selection of tyrosinase substrates

which are required to reduce the remaining oxygen atom to water are supplied by the substrate via a two electron process [10, 11]. The substrate range not only includes the physiologically important substrates tyrosine and L-dopa, but also other phenols and di-phenols, peptides [12] and even proteins [13]. The structures of the mentioned phenolic compounds are shown in Figure 3.2. The following coherence have been demonstrated for substituted phenols or catechols:

- The reactivity decreases upon a transition of the substituent in para-position from electron-donating to electron-withdrawing substituents or with other words, as the electron-withdrawing ability of the substituent increases, K_M and k_{cat} decreases in the order -H > -SCN > - $COCH_3$ > -CHO > -CN > NO_2 [14, 15].

- Bulky phenols (p-phenylphenol, 5-indanol, p-tert-butylphenol and 1- and 2-naphthols) were non-reactive [14].

- Among the substituted phenols also non-phenols, like p-toluidine, were oxidised [14].

The statement that the substituent in the ring must be in the para position [14] is disproved by, e.g., Brown et al., Krol and Bolton or Kahn and Miller [30, 34, 35]. The enzyme is widely distributed in bacteria, fungi, plants and animals. Here the commercially available tyrosinase from *Agaricus bisporus* (in the following called mushroom tyrosinase) and tyrosinase from *Streptomyces antibioticus* (in the following called *S. antibioticus* tyrosinase), which had to be isolated, have

Table 3.1: Comparison between tyrosinase from *Agaricus bisporus*, *Neurospora crassa* and from *Streptomyces antibioticus*

Tyrosinase from	*Agaricus bisporus*	*Neurospora crassa*	*Streptomyces antibioticus*
Structure	L_2H_2 [16] 4 Cu [15]	L [17] 2 Cu [19, 20]	L [18] 2 Cu [21]
Molecular weight	13.4kD / 43-48kD [16] 13kD / 46kD[a] 110kD [22]	46kD [17, 23, 24]	30.6kD[b][18]
Number of aa[c]	569 (LH) [25]	407 [24]	272 [18]
Isoelectric point	5,0 [26]	6,0 - 8,0 [27]	Above 9 [1]
pH-optimum	5.5 [28] 5.0 - 8.0 [29, 30] 7.0 [31]	5.0 - 8.0 [32]	7.0 [33]
pH-range	4.0 -10.0 [26]		6.0 - 7.0 [33]
Origin	Cytosolic protein [17]	Cytosolic protein [17]	Extracellular protein [18]
Hydropathy	Hydrophilic protein [1]	Hydrophilic protein [1]	Hydrophobic domains are exposed on the external surface of the folded polypeptide [18]

[a] see Figure 4.1 in paragraph 4.1.1 on page 45.
[b] see Figure 4.4 in paragraph 4.1.1 on page 49.
[c] aa = amino acid

been used. Some important characteristics of these tyrosinases are summarised in Table 3.1 and compared with the characteristics of the tyrosinase from *Neurospora crassa*, the best investigated tyrosinase.

S. antibioticus tyrosinase as well as tyrosinase from *Neurospora crassa* are monomeric proteins while tyrosinase from the common mushroom *Agaricus bisporus* is a tetrameric protein which consists of two different subunits (light and heavy) of the form L_2H_2. The *S. antibioticus* tyrosinase, with a molecular weight of about 30.6kD, is presumable one of the smallest tyrosinases followed by tyrosinase from *Neurospora crassa*, whereas mushroom tyrosinase with 120kD belongs to the big ones.

Until now there are no crystal structures available for any tyrosinase, but for all tyrosinases, described here, the nucleotide sequence is known (for mushroom tyrosinase see reference [25], for tyrosinase from *S. antibioticus* see reference [18] and for tyrosinase from *Neurospora crassa* see reference [24]).

The melanin operon (*melC* operon) of *S. antibioticus* is composed of two genes that encode MELC1 and MELC2 (apotyrosinase). MELC1 has been suggested as a transactivator which can facilitate the incorporation of copper into the apotyrosinase [36]. The overall G + C content of *melC* is with 70% well within the range of 62% - 74% for previously sequenced *S. antibioticus* genes [18].

Chemical and spectroscopic studies of tyrosinase have shown that its coupled bi-nuclear copper active site is very similar to that found in the hemocyanins [17, 37–40]. For several hemocyanins the crystal structures are available and much can be learned about their geometry and its contributions to the reactivity from correlations with hemocyanins. Especially the amino acid sequence of a part of the octopus hemocyanin and of *S. antibioticus* tyrosinase is similar. In Figure 3.3**A** the structure of octopus hemocyanin is shown and the part under the arrow in the Figure is the part of the structure in which the amino acid sequence of the hemocyanin is identical with the amino acid sequence of *S. antibioticus* tyrosinase [1]. Figure 3.3**B** shows the active centre of octopus hemocyanin which presumably is comparable with that one of tyrosinase [1].

According to previous reports His^{37}, His^{53} and His^{62} are assigned to be the copper ligands for Cu_A of *S. glaucescens* tyrosinase, whereas His^{189}, His^{193} and His^{215} are copper ligands for the Cu_B site of *S. glaucescens* tyrosinase. As these copper ligands are also conserved in the *S. antibioticus* tyrosinase and the tyrosinase of other organisms, they may have identical functions [41]. The binuclear copper site can be prepared in a variety of forms, the oxygenated form (*oxy*tyrosinase, E_{oxy}), the *met*tyrosinase (E_{met}) and the deoxygenated form (*deoxy*tyrosinase, E_{deoxy} or E_{red}). The resting form of tyrosinase, i.e. the enzyme as obtained after purification, is found to be a mixture of $\geq 85\%$ *met* and $\leq 15\%$ *oxy* forms [42]. In Figure 3.4 a scheme of the catalytic cycle of tyrosinase is given, which includes information about the valency of Cu ions in the various forms of tyrosinase.
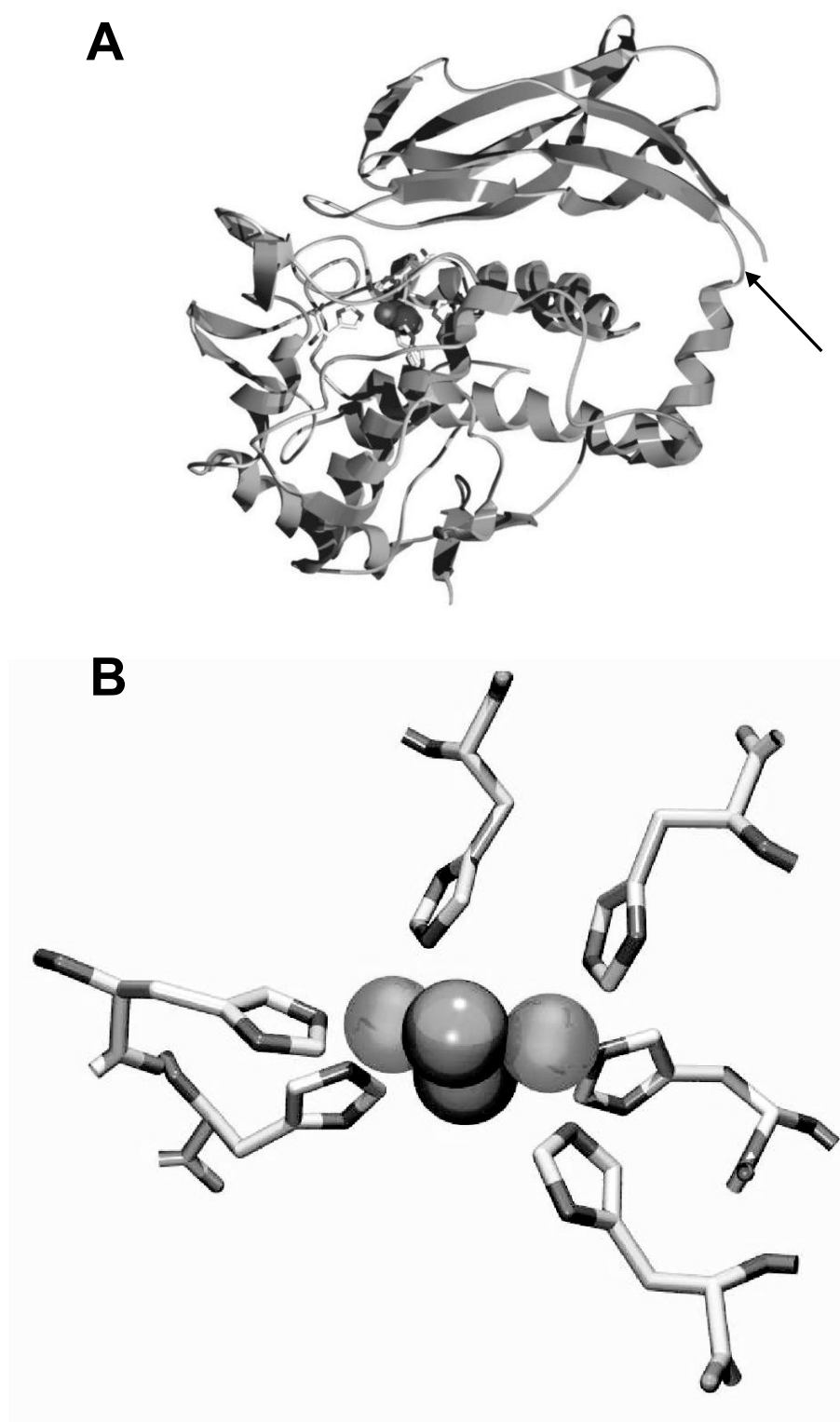
A

B

Figure 3.3: Structure (A) and active center (B) of the octopushemocyanin

Likewise an amino acid (aa) sequence for mushroom tyrosinase was described by Wichers et al. [25], but an active tyrosinase was not expressed in *Escherichia coli* (*E. coli*) until now. Only a homology search with this sequence *vs.* the protein sequence database resulted in the retrieval of many tyrosinases with highly significant similarity, strongly suggesting that the mushroom sequence represents tyrosinase. Furthermore, the protein was expressed in *E. coli* and was shown to crossreact with polyclonal antibodies against a 43kD tyrosinase isolated from mushroom powder [17].

Agaricus bisporus tyrosinase has, with a pI of around 5.0, the lowest isoelectric point, followed by *Neurospora crassa* tyrosinase, with a pI range of 6.0 – 8.0. For *S. antibioticus* tyrosinase the isoelectric point is very high, above 9.0. Unlike the differences in the isoelectric point the pH-optimum of all three tyrosinases is very similar, between a pH of 7.0 and a pH of 8.0. The *Agaricus bisporus* as well as the *Neurospora crassa* tyrosinase are hydrophilic proteins. The secondary structure of *S. antibioticus* tyrosinase obtained by computer analysis indicates that the enzyme does not display a distinctive hydrophobic or hydrophilic character. Nevertheless, the behaviour of the protein during purification suggests that hydrophobic domains are exposed on the external surface of the folded polypeptide [18]. The *Agaricus bisporus* as well as the *Neurospora crassa* tyrosinase are cytosolic, while that of *S. antibioticus* is secreted out of the cell.

Tyrosinase is active in aqueous solutions (buffer solutions) and also in many hydrophobic solvents like toluene, hexane, carbon tetrachloride and chloroform. On the other hand the enzyme is completely inactive in more hydrophilic organic solvents such as ethanol, butanol, acetone or acetonitrile [14].

Effects on tyrosinase activity can be measured when using conventional spectrophotometric methods by the detection of the substrate turnover at different wavelengths [27, 43, 44]. It is also possible to introduce a tracer into the assay [30, 32, 45–48]. Compounds reacting with the quinone to form a dye are introduced to increase the sensitivity of the assay. Most popular among them are Besthorn′s hydrazone [49] and proline [50]. Electrochemical methods are based on the measurement of oxygen consumption [51] or product formation. Here, a direct indication [52] or a coupled redox mediator based assay is used [53].

As it is illustrated in Figure 3.1 two activities are defined (cresolase and catecholase activity) into dependence of the used analyt (mono- or di-phenolic compound) in the activity test. But it should be noticed that tyrosinase does not really possess two separable activities. Both phenol and catechol are converted, but only the quinone is released from the enzyme, and not the di-phenol [54].

From mushroom tyrosinase it is also known that the subunits do not have catecholase or cresolase activity [16, 17]. Only tyrosinase activity was described for an enzyme with an apparent molecular weight (m.w.) of 69kD, which may then be L_2H (m.w.=69.8kD). The distribution of copper among the L and H subunits, and

the function, regulatory and/or catalytic of the association-dissociation phenomen remain to be determined [16].

The determination of the different activities is characterised by following experimental facts:

Tyrosinase activity, determined with mono-phenolic compounds (cresolase activity), shows a characteristic lag-phase and the time required to reach the steady state is dependent on the

- Enzyme source [55]

- Enzyme concentration (the higher, the shorter the lag-phase) [15, 56–58]

- Concentration of the mono-phenol (the smaller, the shorter the lag-phase) [56, 57]

- Presence of reducing agents, such as di-phenols, e.g. L-dopa or other reducing agents, such as ascorbic acid, NADH, NADPH (addition of reducing agents causes a shortening of the lag phase) [30, 48]

- Presence of catalytic amounts of transition metal ions (Zn^{2+}, Cd^{2+}, Ni^{2+} and Co^{2+}) have no influence on the lag period in the tyrosinase- catalysed oxidation of tyrosine, whereas with Cu^{2+} and Mn^{2+} a lengthening of the lag period was observed. Fe^{2+} addition led to a significant shortening of the lag period and Fe^{3+} ions have only a small and opposite influence) [59, 60]

The lag phase is attributed to an autocatalytic mechanism that depends on the formation of small amounts of L-dopa in the initial phase of the reaction pathway [54]. Two possible scenarios are discussed:

1. Allosteric activation of the enzyme by L-dopa or

2. Formation of *deoxy*tyrosinase by a two electron reduction of the active site with a reducing agent

Scenario number 2 is supported by the fact, that mono-phenolic compounds can only react with *oxy*tyrosinase (about 15% of purified tyrosinase) while di-phenolic compounds also react with *met*tyrosinase (about 85% of purified tyrosinase). But the presence of a reducing agent in the reaction medium results in the generation of *deoxy*tyrosinase which binds dioxygen immediately. Now the whole amount of purified tyrosinase is able to oxidise mono-phenolic compounds.

Tyrosinase activity, determined with di-phenolic compounds (catecholase activity), shows a lag-phase only at low pH if a cyclisable di-phenolic compound (e.g. L-dopa) is used. The lag-phase in this case is independent of the enzyme and
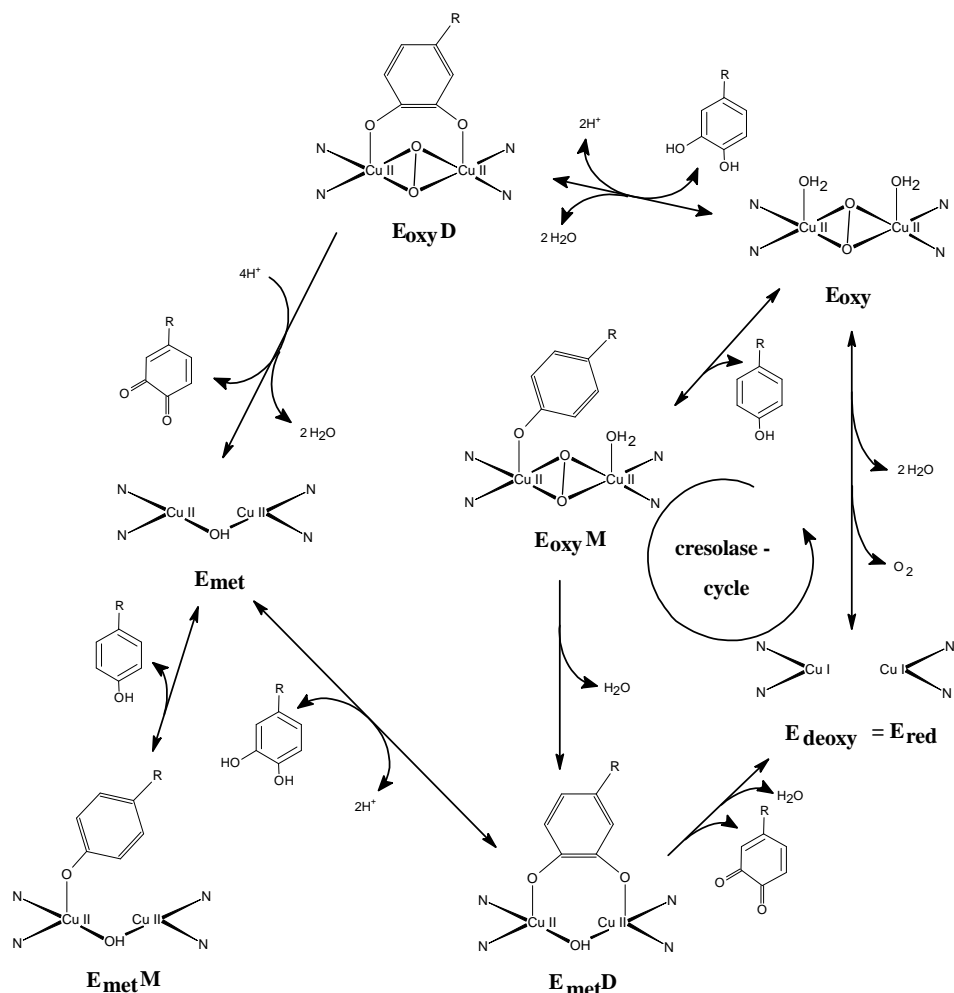
Figure 3.4: Catalytic cycle for the oxydation of mono-phenolic and di-phenolic compounds to o-quinones by tyrosinase in the presence of oxygen (adapted from [61])

substrate concentration used and indicates the presence of a chemical intermediate (o-dopaquinone-H$^+$) [61].

Numerous reports on the tyrosinase action mechanism have appeared to explain the characteristics of a cresolase and a catecholase activity, and in particular to clarify the presence of the lag-phase. E.g., during the last 40 years five different kinetic schemes were proposed by different authors; two of these take the non-enzymatic regeneration of L-dopa from the o-quinone into account [62, 63] and

three do not [64–66]. The catalytic cycle for the oxidation of mono-phenol and di-phenol substrates to o-quinone by tyrosinase in the presence of oxygen is represented by a simplified reaction scheme, illustrated in Figure 3.4 (adapted from reference [61]).

In brief, during catecholase activity, di-phenol binds both to E_{oxy} and E_{met} rendering $E_{oxy}D$ and $E_{met}D$ intermediates, which give rise to two o-quinones. These two o-quinones redox recycle to regenerate one o-di-phenol and one dopachrome. During the cresolase cycle, the binding of monophenol to the E_{oxy} form renders $E_{met}D$, as in the model of Wilcox et al. [66], but unlike this, the new model suggests that the binding of E_{met} to monophenol scavenges a portion of tyrosinase from the catalytic turnover as a dead-end complex in the steady state of monophenolase activity, as was first proposed by Vanneste and Zuberbühler [65]. One part, the mechanism of binding and activation of dioxygen by (binuclear) metalloproteins like tyrosinase is one of the fundamental questions in modern bioinorganic chemistry. Steady-state kinetic studies on mushroom tyrosinase have shown that the catecholase reaction is much faster than the cresolase reaction ($k_{catecholase}$ =$10^7 s^{-1}$, $k_{cresolase}$ =$10^3 s^{-1}$) [67].

Tyrosinase has been considered as an enzyme showing mechanism-based inhibition in aqueous solutions [68]. Inactivation caused by the relatively high concentration of phenol can be attributed to the covalent attachment of the substrate or product to the enzyme, as suggested for the reaction inactivation when tyrosine is used as substrate [69]. The suggested explanation entails the nucleophilic attack of the lysine amino groups of the enzyme on the quinone product yielding a cova-
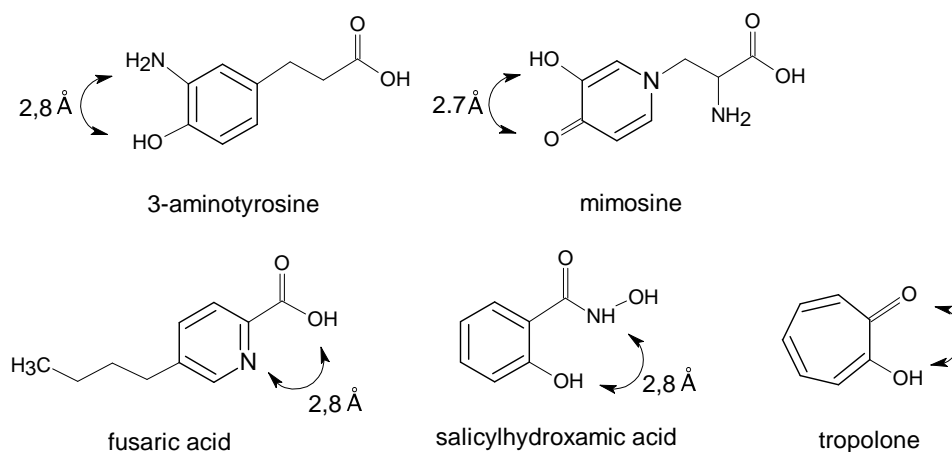

Figure 3.5: Some inhibitors of tyrosinase

lent adduct which blocks the active site [70]. Another possibility for autocatalytic inactivation could be a stepwise selective destruction of an essential group in a protein molecule [71], e.g., destruction of one histidine-ligand could lead to the loss of copper. It should also be noticed, that quinones suffer from high instability in water and they readily polymerise to polyaromatic compounds which have proved to inactivate the enzyme [70].

Various inhibitors of tyrosinase are known, e.g. aromatic carboxylic acids [66, 72–76], pyridinones [77], vanillyl compounds [78], karahanaenone and derivatives [79], cyclic peptides [80], flavonoids [81] and respiratory toxins such as azides and cyanids [82, 83]. The most efficient of these show either a nitrogen or an oxygen function in conjugation with another oxygen in a distance of about 2.7-2.8Å which corresponds to a distance of about 3Å of the copper atoms in the active site of the enzyme [84].

In Figure 3.5 the structure of some noteworthy examples are shown, e.g. tropolone [85], salicylhydroxamic acid [86], 3-aminotyrosine [87], ferulic acid [73], L-mimosine and fusaric acid [87]. Certain thiols which most likely form complexes with the copper atoms are also strong inhibitors of tyrosinase [88, 89]. But often the inhibition mechanism is unclear. Different authors discuss the copper-chelating properties of the tyrosinase inhibitors. They also focus on a possible reaction of the inhibitor with either the quinone or the enzyme to yield colorless compounds [90, 91].

Another family of tyrosinase inhibitors is based on kojic acid, examined by numerous authors within the last years [92–96]. This antibiotic compound has been used as an ingredient in cosmetics and as a colour stabilising agent for food [95]. It is synthesised by a variety of aerobic microorganisms utilising a wide range of carbon sources. The assay of kojic acid is therefore important for the monitoring of the fermentation processes [97].

Furthermore pesticides belong to the group of tyrosinase inhibitors, e.g. chloro-isopropyl carbamate [98] and diethyldithio carbamate [85]. The release of pesticides into the environment is of great concern because of their widespread use in agriculture and their role in drinking water pollution. Owing to their toxicity the pollution of ground, stream and drinking water with these contaminants is a health hazard. Therefore, their concentration in environmental samples, for example drinking water, surface or waste water, has to be controlled [99].

3.1.2   Glucose dehydrogenase

Soluble, periplasmic glucose dehydrogenase (s-GDH) containing pyrroloquinoline quinone (PQQ) (EC 1.1.99.17) shall now be described more thoroughly, since it was used for the development of different amperometric biosensors.

Table 3.2: Relative rate of substrate conversion of s-GDH

Reference **Substrate**	[100]	[101]	[102]	[103]
Mono-saccharides				
D-Glucose	100	100	100	100
D-Galactose	66	30	18	30
D-Allose			66	
2-Deoxy-D-Glucose	4.5		56	
D-Mannose	30		4	
D-Xylose	27	20	10	15
D-Ribose	7.5		1	8
D-Arabinose	1.6	35		
D-Fucose				28
Di-saccharides				
D-Arabinosedisaccharid			11	
D-Cellobiose		70	48	
D-Lactose		65	24	72
D-Maltose		90	60	93

S-GDH oxidises a wide range of mono- and di-saccharides to the corresponding lactones as it is illustrated in Figure 3.6.

The enzyme exhibits a relatively broad substrate specificity for monosaccharides including D-glucose (shown in Figure 3.6), D-fucose, D-galactose or D-xylose and in contrast to m-GDH it is capable to oxidise also disaccharides. In Table 3.2 substrates and the relative value of the specific activity of s-GDH in
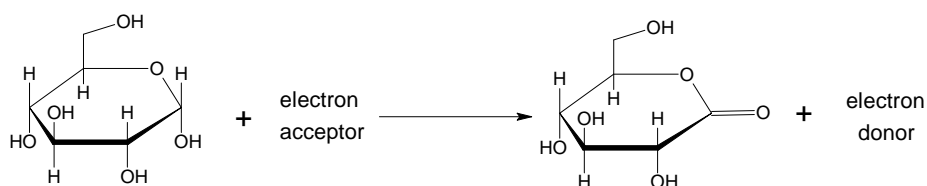

Figure 3.6: Illustration of the reaction of glucose dehydrogenase with glucose as substrate

solution are listed. It is obvious, that s-GDH has the highest activity if mono-saccharides are used, of it structur is close to glucose. Disaccharides which are oxidised with the highest activity have allways glucose as one component of the molecule, such as D-lactose and D-maltose or D-cellobiose.

The enzyme accepts artificial electron acceptors such as N,N,N',N'-tetramethyl-1,4-phenylenediamine (wursters blue) [104], 2,6-dichlorophenolindophenol [105], phenanzine methosulfate [104, 105], ferricyanide [100], methylene blue [100], ferrocene derivatives [106] di-phenolic compounds [107–109], as well as short-chain ubiquinone homologes (Q-1 and Q-2) [110] to reoxidise the reduced PQQ. But s-GDH is unable to react with long-chain ubiquinones (Q-6 and Q-9) [111], flavin adenine mononucleotide (FMN), flavin adenine dinucleotide (FAD), diphos-phopyridine nucleotide (DPN), triphosphopyridine nucleotide (TPN), triphenylte-trazolium chloride or oxygen [100]. There is a long-existing controversy with respect to the physiological electron acceptor of s-GDH. Dokter et al. [112] de-scribed that the s-GDH of *A. calcoaceticus* donates electrons to the respiratory chain via a cytochrome b_{562} as illustrated in Figure 3.7 adapted from Geerlof et al. [113].

The enzyme is active in aqueous solutions (buffer solutions) and has a broad pH-optimum [110]. (For example the enzyme has a pH-optimum of 9.0 in Tris/HCl buffers with wursters blue and 6.0 in potassium phosphate buffers with 2,6-di-chlorophenolindophenol as electron acceptor [101].) The enzyme is inactivated at temperatures above $35°C$ [114]. S-GDH is an alkaline enzyme and has an isoelec-tric point of 9.5 [101].

Figure 3.8 shows the 1.7Å crystal structure of the apo-form of s-GDH (adapted from [115]). S-GDH is a dimeric enzyme of identical sub-units [101]. Accord-ing to the MALDI mass-spectrum, made by Dr. S. Haebel (University of Pots-dam, Germany), one monomer has a size of 50.2kD (Figure 3.9) which is in good agreement with the molecular weight of 100kD (454 amino acid residues per monomer). One monomer binds one PQQ molecule and three calcium ions. One of the calcium ions is required for activation of the co-factor, the other two are needed for functional dimerisation of the protein [115, 116].

On the basis of structural information, biochemical and kinetic data for s-GDH reaction mechanisms have been proposed (Figure 3.10). In general, PQQ-dependent enzymes use a mechanism similar to that of nicotinamide- and flavin-dependent oxidoreductases. It involves a general base-catalysed proton abstrac-tion in concert with a hydride transfer to PQQ, and the subsequent tautomerisation to $PQQH_2$ [117].
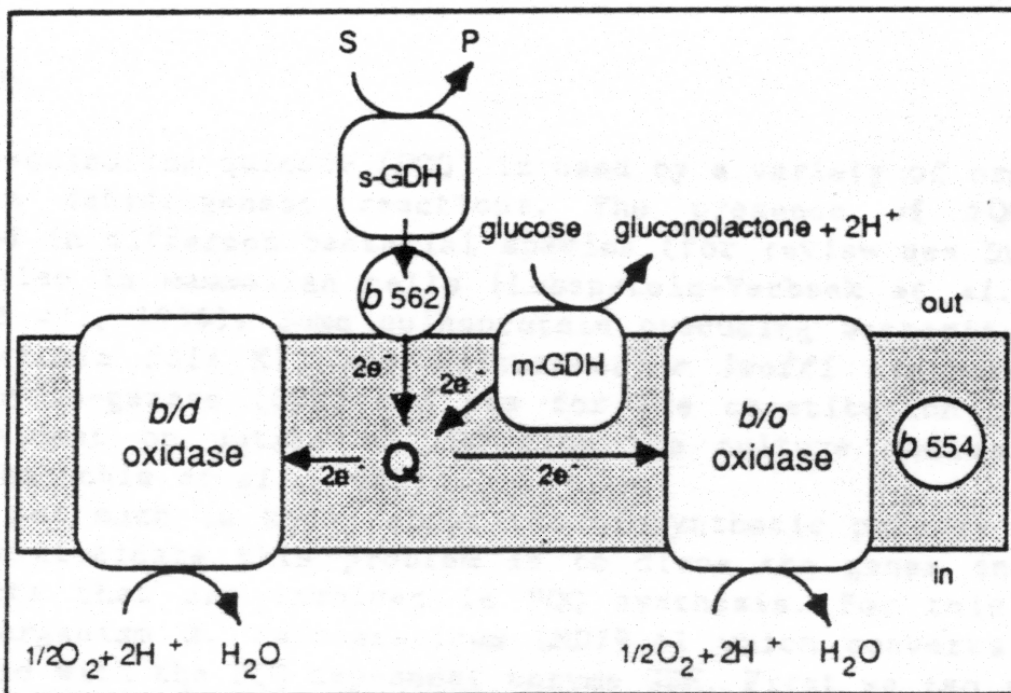
Figure 3.7: Linkage of GDH to the respiration chain of *A. calcoaceticus* (S = substrate, P = product, b562 = cytochrome b_{562}, b554 = cytochrome b_{554}, b/d oxidase = cytochrome b_{554}/cytochrome d-containing oxidase, b/o oxidase = cytochrome b_{554}/cytochrome o-containing oxidase) (adapted from [113])
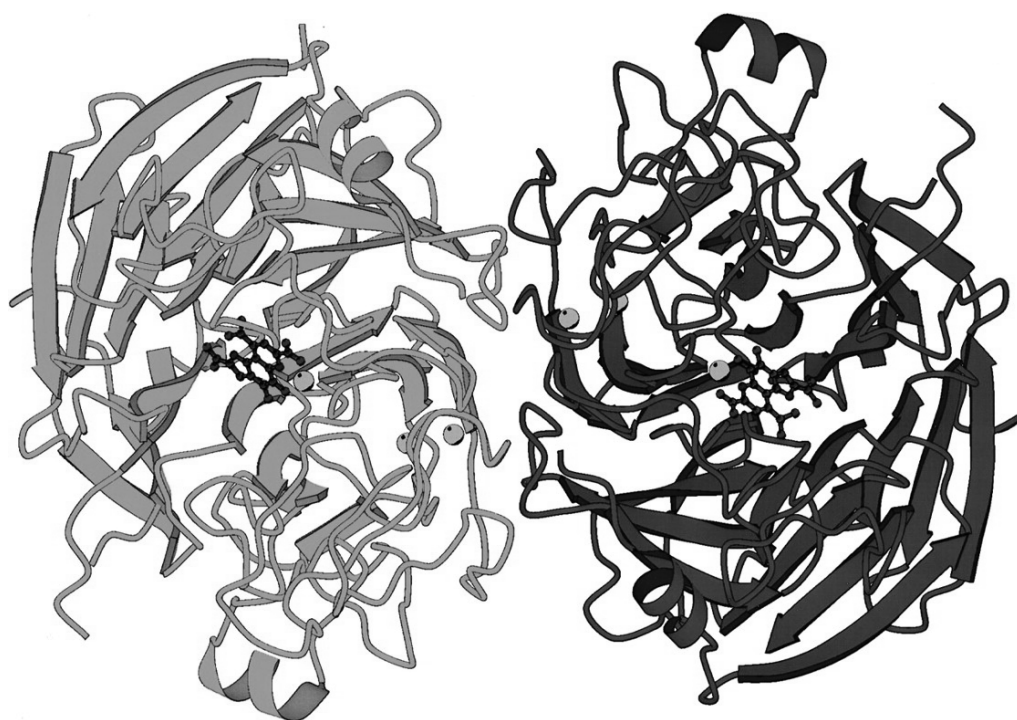
Figure 3.8: Crystal structure of the s-GDH at a reslution of 1.7Å (adapted from [115])
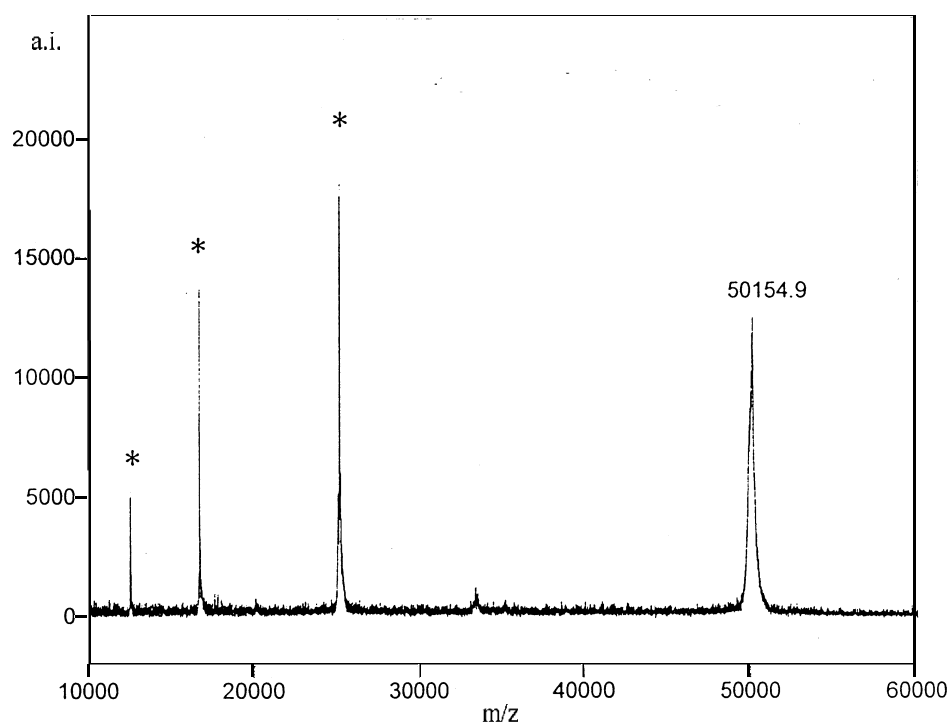
Figure 3.9: MALDI mass-spectrum of s-GDH
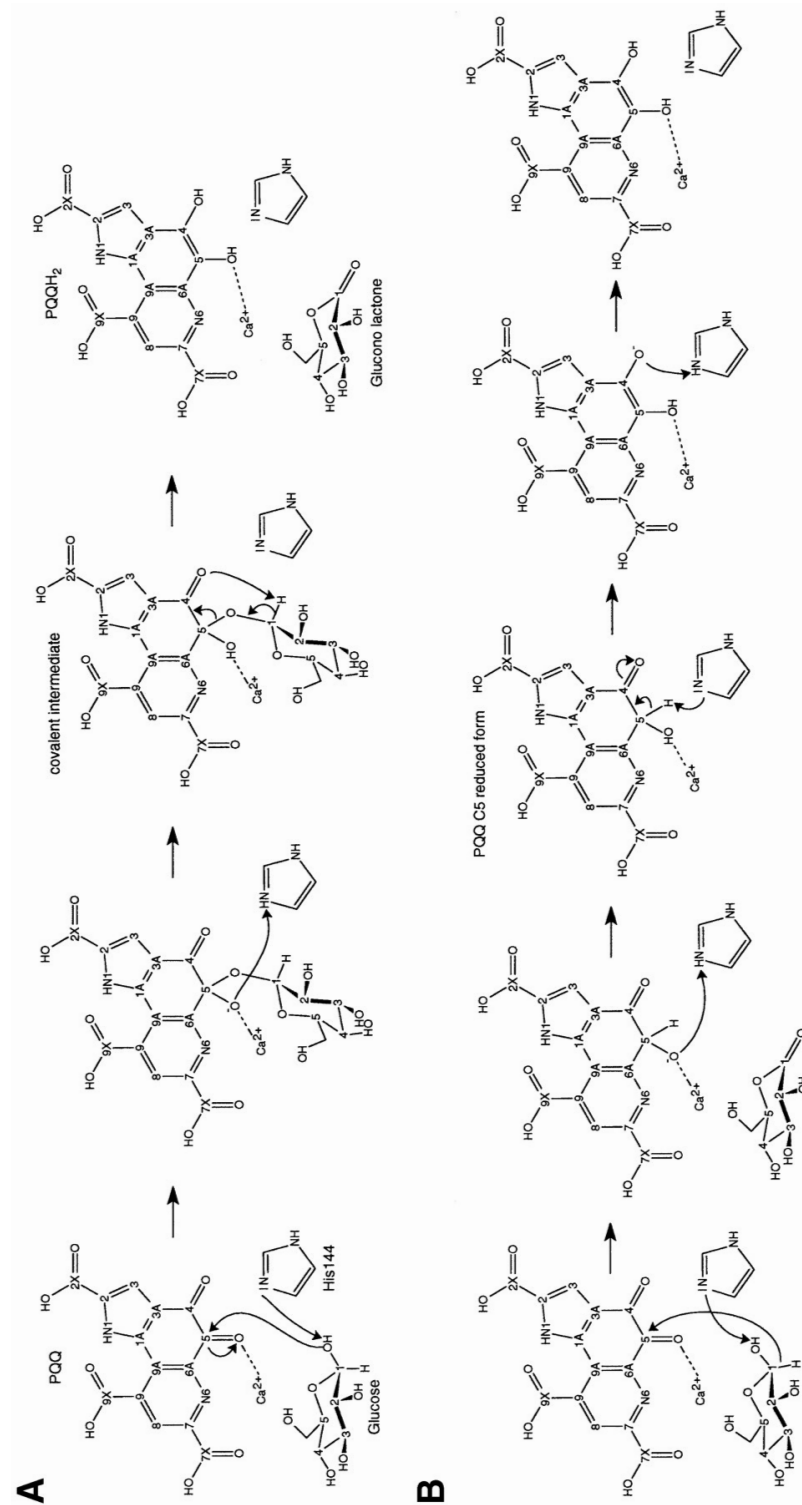
Figure 3.10: The two possible reaction mechanisms for s-GDH (adapted from [117])

3.2 Biosensors

A biosensor is created when the immobilised biological material is in close contact with a physical transducer. Here, the biological component translates the recognition of the analyte into a change of an easily measurable physicochemical parameter. This change is converted into an electrical signal by the transducer, amplified, processed, and displayed in a suitable form. Figure 3.11 illustrates the general structure.

The specific recognition is not only provided by enzymes. Other immobilised biological material can be employed, such as cells, organelles and tissues. They are usable for quantification of biologically related parameters, such as taste, odour, fatigue substances, mutagenicity and nutritive value. Furthermore, binding assays can be performed with receptors, nucleic acids, antibodies and antigens.

The most frequently used transducers are electrochemical, optical and thermal detectors, but piezoelectric and surface acoustic wave methods may also be used [3, 8, 118–122].

Enzyme electrodes are the first type of biosensors to have been proposed [5] and work with this electrodes is at present the best established branch of biosensor research. In amperometric biosensors, the function of the enzyme is to generate or consume a redox-active compound in the specific catalytic conversion of the target analyte (substrate). The redox-active compound is oxidised or reduced at the electrode poised at an appropriate potential. The generated current can be correlated to the analyte concentration.

In the following paragraph 3.2.1 the measurement principle of amperometry is explained first followed by a description of the single components of amperometric biosensors in paragraph 3.2.2 and paragraph 3.2.3 and of the ensemble

Figure 3.11: Schematic illustration of a biosensor (adapted from [4])

acting of the single components in amperometric biosensors in paragraph 3.2.4. This is completed by paragraph 3.3, which gives a summary of ways to improve the biosensor performance, e.g., in this paragraph possibilities are described to enhance t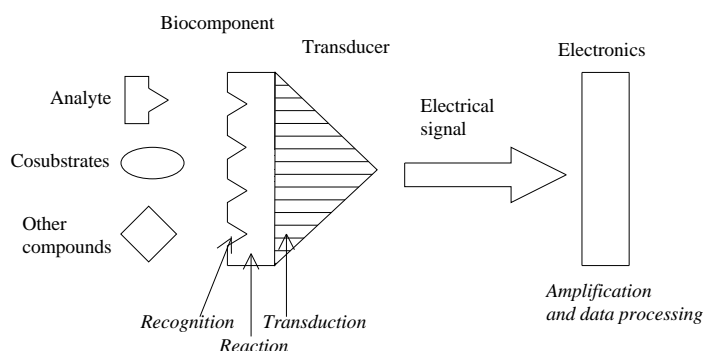he sensitivity of amperometric biosensors. Finally in paragraph 3.4 a comparison of tyrosinase sensors developed within the last years with respect to their stability and sensitivity is given and different immobilisation methods were compared.

3.2.1   Amperometry

Amperometry is the measurement of the diffusion boundary current at a constant potential between a polarised working electrode and a reference electrode. The working electrode is the electrode where the reaction of interest takes place. It is typically made of an inert material, e.g. platinum, gold or carbon. Typical reference electrodes are silver/silver chloride (Ag/AgCl/KCl) and saturated calomel ($Hg/Hg_2Cl_2/KCl_{sat}$). If the working potential is sufficiently high to achieve maximum conversions rate (diffusion boundary current) than the current, measured by the working electrode, is linearly dependent on the concentration of the electroactive compound in the solution.

In most cases of amperometric biosensor development all the required parameters were already obtained with this simple two electrode set-up. Otherwise a three electrode set-up can be used, consisting of a working-, a reference- and a counter electrode. In this case the counter electrode provides the current path in an electrochemical cell.

3.2.2   Amperometric electrodes

Electrodes based on platinum materials, especially the Clark type oxygen electrodes (COE), belong to the most used transducers for the combination with oxidases and mono-oxygenases. Many bi- and multi-enzyme systems are based on this kind of combination as well [2]. Electrodes based on carbon materials are cheep and offer a wide potential range and a high electric conductivity [123].

Clark type oxygen electrodes (COE)   The COE is a membrane-covered electrode, where the electrolyte (KCl solution) will be retained behind the membrane and where the gas-permeable membrane (polyethylene or teflon) barrier prevents electroactive or surface-active impurities from the sample giving an erroneous signal or poisoning the electrode.

The COE was developed in 1962 [5] and is a two electrode set-up consisting of a platinum cathode and a Ag/AgCl reference electrode. Figure 3.12 shows a
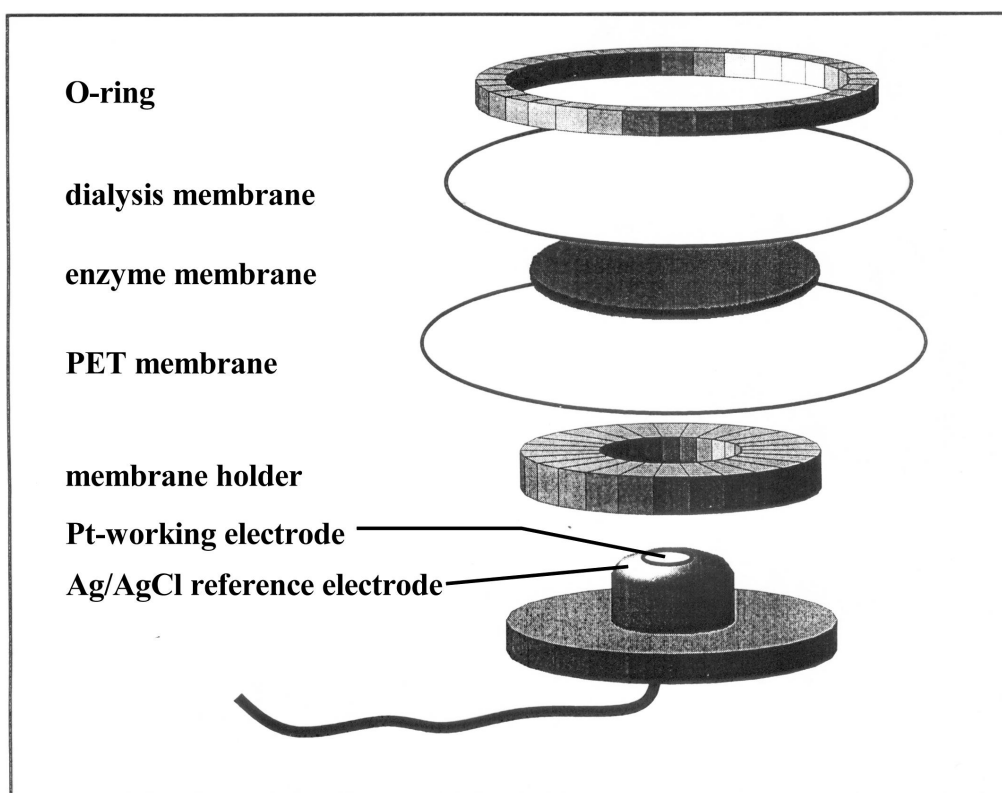
Figure 3.12: Illustration of a biosensor consisting of a Clark type oxygen electrode (COE) with an additional enzyme membrane as it was used in this studies (adapted from [124])

scheme of a COE. The cathodical O_2 reduction current, described in the scheme below, is measured when the potential of the platinum cathode is -600mV.

$$\text{cathodical } O_2 \text{ reduction: } \tfrac{1}{2}\, O_2 + H_2O + 2\, e^- \longrightarrow 2\, OH^-$$
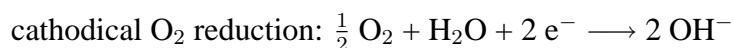
Carbon paste electrodes (CPE)   Electrodes based on carbon materials are produced by mixing of graphite powder with a hydrophobic (paraffin-oil, teflon) or a hydrophilic (sol gel, polyacrylamide) binder. The electrode surface can be replaced again simply by polishing.

Screen printed electrodes (SPE)   Screen printing techniques are used to produce the complete electrochemical measuring chain (e.g. WE, RE and CE) on one chip. Any material which can be printed can be used. In this studies screen
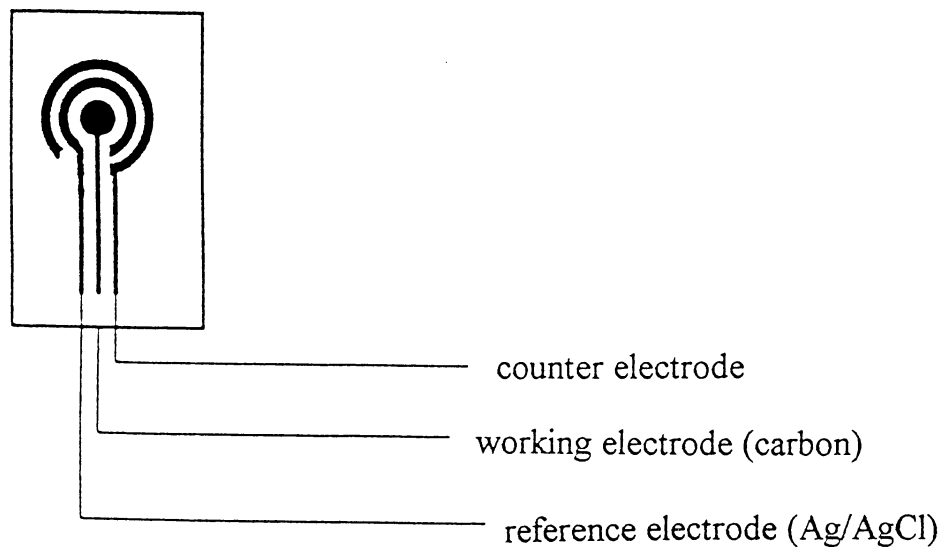
Figure 3.13: Illustration of a screen printed electrode (SPE)

printed electrodes made from carbon paste, a silver/silverchloride reference electrode and a carbon counter electrode are used (Krejci, Czech Rep.). Typically the size of the sensor chip is about 1cm x 2cm. Figure 3.13 shows a scheme of such a screen printed electrode.

3.2.3   Enzyme immobilisation in amperometric electrodes

In order to be able to use enzymes repeatedly, methods for their attachment on a support (immobilisation techniques) have been developed. The enzymes are better handable due to the immobilisation and usually the stability of the enzyme is increased. In Figure 3.14 a division of immobilisation techniques is illustrated [125].

Immobilisation can be achieved by either coupling or embedding of an enzyme. The binding of an enzyme with a support, due to adsorptive or ionic interactions, covalent binding or crosslinking, all belong to techniques of coupling.

Physically adsorbing an enzyme on to a matrix is the oldest immobilisation technique. It is characterised by its simplicity and by the fact, that undesirable chemical effects are avoided, since adsorption is usually a gentle procedure. By this sort of immobilisation neither the enzyme activity changes nor catalytic characteristics of the enzyme [126]. Possible supports for the adsorptive or ionic bind-
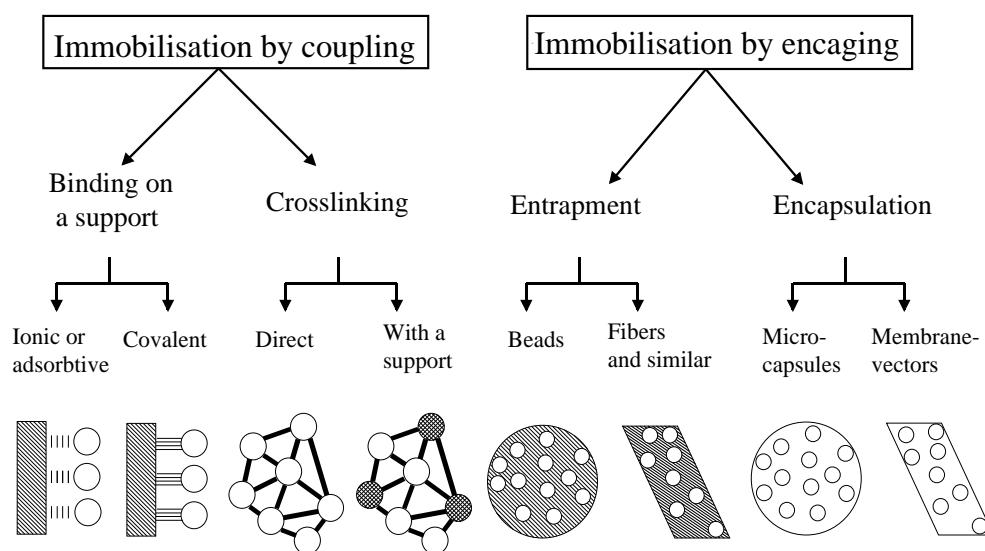
Figure 3.14: Immobilisation methods for enzymes (adapted from [125])

ing of enzymes are for example anionic or cationic resins, active charcoal, silica gel, clay, aluminium oxide and porous glass [126–129]. Since the attraction forces between such supports and the enzymes are often rather weak, and since the bonds are largely dependent on the environment (pH, ionic strength or solvent), enzyme leakage may appear.

For covalent binding on a support, an irreversible technique, a lot of functionalised supports can be used (extensive information according to covalent binding and functionalised supports are given in the review of Scouten [128]). A major disadvantage is the potential inactivation of an enzyme since essential catalytical groups may be covalently modified during the coupling.

The crosslinking of enzymes by bi- or multi-functional reagents with and without support normally results in gelatinous precipitates and often a considerable loss of enzyme activity is observed. Reactive groups of an enzyme that can be targeted using a cross-linker include primary amines, sulfhydryls, carbonyls, carbohydrates and carboxylic acids. In addition, any reactive group can be coupled nonselective using a photoreactive crosslinker. The method of crosslinking is simply to be handled and the formation of a three-dimensional network of connected enzymes is advisable.

On the other hand entrapment and encapsulation methods are available. Entrapment methods are based on the encaging of enzymes within a polymer network. The enzyme is added to a monomer solution before polymerisation is ini-

tiated. With this methods a gentle immobilisation is possible which is generally quite easy to perform [2]. The most important matrices used for the entrapment of enzymes are gelatin, polyacrylamid and pre-polymers crosslinked by addition of water (e.g. polyurethanes) or light (e.g. polyvinylalcohol). Disadvantages are the mechanical, chemical and thermal instability of the most polymers as well as the inactivation of the enzyme during the polymerisation procedure.

The encapsulation method, which is related to the entrapment method, involves the localisation of the enzymes within various forms of semipermeable membranes (e.g. polyethylene, polypropylene or regenerated cellulose membranes). A very high enzyme/protein concentrations per unit volume of these microcapsules can be obtained. Herein lies the advantage of this method.

3.2.4   Amperometric biosensors

As it is already mentioned at the beginning of this paragraph 3.2, first, a biosensor is created when the immobilised biological material is in close contact with a physical transducer and second, immobilised enzymes are effected by the surroundings in which they operate. The characteristics of an amperometric biosensor are influenced by different effects:

- changes in the conformation of the enzyme by the immobilisation process generally leads to a reduction of the affinity to the substrate (increase of K_M) and an inactivation of a part of the or the whole enzyme (decrease of v_{max})

- effects imposed by the matrix (i.e. effects of charge, hydrophobicity and matrix structure) can also lead to a change of K_M or v_{max}

- diffusion effects will result in concentration differences within the enzyme matrix (internal diffusion restriction) as well as within the boundary layer bulk solution/biosensor and a semi-permeable membrane (external diffusion restriction)

Dependent on the construction of a biosensor (electrode material, amount of immobilised enzyme, etc.) different correlation between substrate concentration and generated current are observed. If the process of current generation is limited by diffusion, e.g. high enzyme loading, then the current generated is:

$$I = n \cdot A \cdot F \frac{D \cdot S}{d} \tag{3.1}$$

With I the generated current, n the number of electrons, A the area, F the Faraday constant, D the diffusion coefficient, S the substrate concentration and d the thickness of the enzyme layer.

Under kinetic control the current generated is:

$$I = n \cdot A \cdot F \frac{v_{max} \cdot S}{K_M} \qquad (3.2)$$

With I the generated current, n the number of electrons, A the area, F the Faraday constant, v_{max} the maximal velocity of the enzyme, S the substrate concentration and K_M the Michaelis Menten constant of the enzyme. In addition to the measurement of substrates this type of biosensor can also be used for the detection of inhibitors and effectors of the enzyme.

3.3 Amplification systems

Electroanalytical techniques are fairly sensitive and currents as low as 10^{-10}A can be recorded by commercial devices. But the introduction of a layer incorporating the enzyme over the surface of the electrode decreases the sensitivity of the electrode by one or two orders of magnitude, due to the additional diffusion resistance. Therefore, for the measurement of analyte concentrations in the nanomolar range an increase of sensitivity of the enzyme electrode is required. One way to solve this problem is the continuous regeneration of the analyte in cyclic reactions.

The combination of the electrochemical detection principle and the recycling of the analyte can be performed in a number of ways (see Figure 3.15, adapted from Wollenberger et al., 1995 [130]):

- the electrochemical (analyte regeneration between two electrodes)

- the bioelectrocatalytic (analyte regeneration between an electrode and an enzyme) and

- the biocatalytic recycling (analyte regeneration between two enzymes).

3.3.1 Electrochemical recycling

The increase in sensitivity is based on redox recycling of the analyte between two electrodes. Therefore the analyte itself has to be electroactive and the current will be generated during the recycling. The signal enhancement by redox recycling has been studied for a number of reversible species at integrated gold and platinum electrodes with 1μm spacing [130]. An amplification of the signal of one order of magnitude has been achieved.
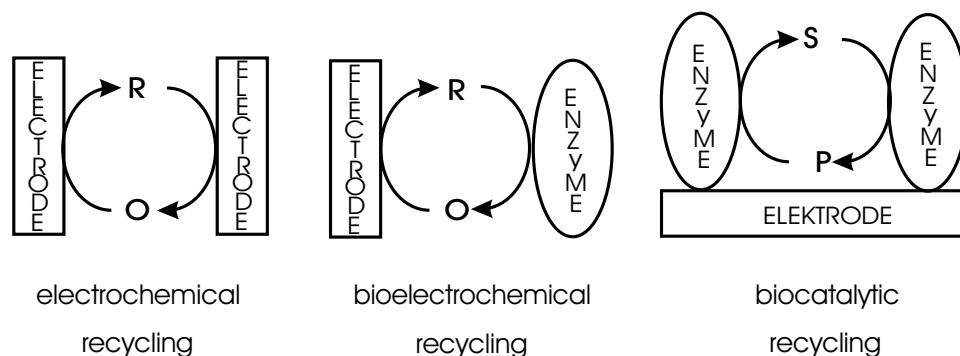
Figure 3.15: Illustration of the analyte recycling schemes (R = reduced redox species, O = oxidised redox species, S = substrate, P = product) (adapted from [130])

3.3.2   Bioelectrocatalytic recycling

In the bioelectrocatalytic approach the target analyte is recycled between the electrode and the redox centre of the enzyme, thus mediating the charge transfer to the electrode. Therefore the enzyme product has to be essentially electroactive. In ideal cases sufficient (co)substrate of the enzyme is present, the potential required for the regeneration is low, and the analyte is stable in both redox states. Vital for a rapid heterogeneous electron transfer is the close contact of enzyme and electrode material. Furthermore a requisite for a high sensitivity is a high conversion rate of both redox partners. A number of enzymes have been investigated and biosensors using tyrosinase for the determination of phenolic compounds are listed in Table 3.3 (paragraph 3.4.3). Furthermore tyrosinase electrodes have been developed using mediated bioelectrocatalytic recycling for amplification. They are also described in paragraph 3.4.3.

3.3.3   Biocatalytic recycling

In the bienzymatic approach, the sensitivity enhancement is provided by shuttling the analyte between enzymes acting in a cyclic series of reactions accompanied by a co-substrate consumption and an accumulation of by-products. The target analyte can be a substrate or co-enzyme of the appropriate enzyme. Assuming a sufficiently high activity of enzyme E_1 in the presence of its co-substrate C_1 and an analyte at a concentration far below its Michaelis Menten constant, an amplification is achieved by turning-on the second enzyme (E_2) by addition of its

co-substrate C_2.

By measuring the concentration change of one of these co-reactants directly or in an additional analytical step, the recycling system is used as a biochemical amplifier for the analyte ($S = S_1$ or S_2). Theoretical considerations have been made for the case of linear recycling by a pair of enzymes. According to theory [131, 132] the amplification factor, G, is under steady state conditions and with a high enzyme load:

$$G = \frac{L^2 \cdot k_1 \cdot k_2}{2 \cdot D \cdot (k_1 + k_2)} \tag{3.3}$$

Where k_i is the first order rate constant, L the membrane thickness, and D the diffusion coefficient. At high activities of both enzymes which are immobilised into the enzyme layer with high characteristic diffusion time (L^2 / D), the possible amplification is very large.

If one molecule of product is formed per substrate molecule the total concentration of intermediate substrates ($S_1 + S_2$) remains constant and the concentrations of the co-reactants increase or decrease linearly with time. Then the number of cycles in which the substrate is turned over in a given time is a function of the substrate concentration. This concept of linear enzymatic signal amplification has been realised by coupling dehydrogenases with oxidases or transaminases, or by coupling kinases with each other. If oxidases are coupled with their respective dehydrogenases, electrode detectable species are included in the reaction system. Therefore, the change of co-reactant concentration can be measured directly at the electrode onto which the recycling enzyme pair is immobilised. In most cases a consumption of oxygen has followed. In paragraph 4.3 tyrosinase electrodes are described in combination with glucose dehydrogenase.

3.4   Tyrosinase electrodes in the comparison

Among the water producing oxidases, tyrosinase is the most frequently applied enzyme for the construction of amperometric biosensors. Tyrosinase possesses many attractive properties such as:

- It is commercial available

- Within the enzymatic and the electrochemical procedures an amplification of the signal can be observed and

- The enzyme offers rather broad specificity

.

As mentioned in paragraph 3.1.1 tyrosinase catalyses the oxidation of phenolic compounds to the corresponding o-quinones, whereby the enzyme is oxidised back to its native form by molecular oxygen. Based on the enzyme reaction for electrode development different principles of detection are used.

Primarily tyrosinase produces o-quinones, which are electrochemically active. They can be reduced back to form catechol directly at low applied potentials (-50mV *vs* Ag/AgCl) or indirectly *vs* a mediator which can be in solution or immobilised.

On the other hand tyrosinase consumes oxygen upon application of an analyte, which leads to a measurable decrease of current (oxygen reduction) at a COE.

Following, a comparison of tyrosinase electrodes with respect to tyrosinase immobilisation procedures, stability and sensitivity is given.

3.4.1   Immobilisation procedures

The immobilisation procedure is an important parameter when constructing a tyrosinase electrode. Parameters, such as selectivity, temperature stability and long-term stability, are dependent on the fixation of tyrosinase to the electrode.

Depending on the electrode different immobilisation methods (bases were described in paragraph 3.2.3) were used.

The most used electrode materials for construction of tyrosinase electrodes is based on carbon materials, e.g. carbon paste electrodes (CPE), glassy carbon electrodes (GCE), glassy carbon disk electrodes (GCDE), solid graphite electrodes (SGE), graphite disk electrodes (GDE), screen printed carbon electrodes (SPCE). These electrodes are cheep and they offer possibilities for the use of easy and gentle immobilisation methods.

One of the fastest and simplest possibilities is drying the tyrosinase on the top of the electrode (GDE: [133–136], SGE: [137]). Also tyrosinase electrodes are described where after the drying procedure the surface was additionally protected with:

- A dialysis membrane (SGE: [138, 139], GCE: [139])

- An ion exchange polymer membrane, e.g. Eastman AQ (commercial name of a group of poly-ester sulfonic acid cation exchangers) (GCE: [140–143], GCDE: [144], SGE:[145])

- Nafion (a linear copolymer derived from tetrafluoroethylene and perfluoro-sulphonic acid monomers) (GCE: [146], SGE:[145]).

An other possibility was the entrapment of tyrosinase in a polymer network, e.g.:

- Poly-hydroxylcellulose (GCE: [147, 148])

- Poly-vinylalcohol (SGE: [149])

- Poly-tyramine gel (RVCE: [150])

- Poly-carbamoyl sulfonat hydrogel (SPCE: [151])

- Poly-vinyl pyridine hydrogel (SGE:[152])

- Sol-gel (GCE: [153, 154])

This tyrosinase polymer network was than placed on the surface of the electrode. Additionally the electropolymerisation of a pyrrole amphiphilic monomer tyrosinase mixture pre-adsorbed on the electrode surface is described (GCE: [155–159]).

If CPE were used than often tyrosinase was dissolved into a buffer solution and added to graphite powder. This mixture was dried and used (CPE: [137, 145], SPCE: [160]) or in some cases paraffin oil [137, 161–166] or paraffin wax [167] was added. But also tyrosinase-CPEs are described where tyrosinase was dried on the top of the electrode [137, 139, 168] and sometime protected with a polymer network, e.g. sol-gel [169] or nafion [170]. Tyrosinase has also been co-immobilised with different additives to examine the effects on the stability and the sensitivity of the electrode (for explanation see paragraph 3.4.2 and 3.4.3).

Some authors have also described the activation of graphite via carbodiimide in CPEs before use for immobilisation of tyrosinase [137] and in some cases the activated graphite contains also glutaraldehyd (GA) (SGE: [137, 171], GCE: [172], CPE: [137]) or bovine serum albumin (BSA) (SGE and CPE: [137]). Also metallised CPEs were used for immobilisation of tyrosinase [173].

Briefly described, if electrodes were used, which were made from carbon material, then fast and easy immobilisation techniques are usable, like drying the tyrosinase on the top of the electrode or mixing of a tyrosinase solution with the carbon material with or without additives. Efforts were made to improve the stability as well as the sensitivity of this electrodes. These efforts will be described in the following two paragraphs 3.4.2 and 3.4.3.

If COE were used, than tyrosinase was normally sandwiched between an oxygen permeable membrane (mostly polyethylene) and a dialysis membrane (mostly cellulose). This was carried out by encapsulation of tyrosinase [174–178] as well as by entrapment in a polymer network, e.g.:

- Gelatin [88, 179]

- Triacetate [180, 181]

- Kappa-carrageenan gel [181–183]

- Poly-acrylamide [88, 184]

- Poly-vinylalcohol [33, 179, 185, 186]

Additionally covalent binding via carbodiimide on the carboxylic groups of a nylon membrane [176, 180], crosslinking via glutaraldehyde on a polyamide mesh [88] or on a commercial available preactivated membrane [187] were used.

Also one tyrosinase sensor based on pH-sensitive field-effect transistor (pH-FET) was descibed [188]. Here the biologically active membranes were formed on the pH-FET surface by crosslinking of tyrosinase with bovine serum albunin in a saturated glutaraldehyde vapour.

Briefly described, if COE were used, than encapsulation of tyrosinase is an easy immobilisation method but the loss of activity of tyrosinase in solution may be the main reason for the restricted lifetime of this kind of tyrosinase electrodes. Other immobilisation methods like covalent immobilisation via carbodiimide or entrapment in poly-acrylamide use health harmful chemicals during the immobilisation procedure. Tyrosinase electrodes made by entrapment in poly-vinylalcohol are part of the tyrosinase electrodes which are the most promising.

In summary, tyrosinase electrodes were intensively studied during the last years, because the possibilities for an analytical application are numerous. But it is an unstable enzyme and efforts were made to find immobilisation methods which lead to a stabilisation of the enzyme and with that to a higher life time of the electrode. But also the sensitivity is of big interest for an analytical approach. The next two paragraphs (3.4.2 and 3.4.3) will give a summary of the most current research results of the last 5 years obtained on developments in the stability and sensitivity.

3.4.2 Stability

A general problem for many tyrosinase electrodes is the lack of the operational and storage stability needed for commercial exploitation. This is currently the major obstacle to be solved in the biosensor area. Possible reasons for the restricted life time of tyrosinase electrodes are:

- Quinones suffer from high instability in water and they readily polymerise to polyaromatic compounds (e.g., melanin) which have been proved to inactivate the enzyme and may foul the electrode [70, 88].

- The formation of intermediate radicals in the enzymatic and electrochemical reaction may have the same consequences [145, 189].

Several papers describe the addition of various additives and modifications of tyrosinase electrodes (based on carbon material) to influence both their stability and sensitivity. Polymers (e.g. polyethylenimine [151, 161, 190], poly(pyrrole-lactobionamide) [156], poly(amphiphilic pyrrole) [158]), proteins (e.g. bovine serum albumin [137, 161]) and also small molecules (e.g. lactitol [156, 161], cationic anitbiotics [161]) belong to the group of stabilising agents. Improved operational stability was also observed for composite electrodes such as epoxy/graphit [191–193] and teflon/graphit [194].

Another possibility to improve the stability of tyrosinase electrodes and to avoid these problems of polymerisation was the application of the enzyme electrodes in organic solvents. The reason, suggested by Kazandijan and Klibanov [14] as well as Yang and Robb [195], could be that the organic solvent allows the o-quinone to escape from the aqueous phase which surrounds the enzyme and thereby prevents inactivation of the enzyme.

The ability of tyrosinase to function in non aqueous media has led to the development of numerous biosensors, which were used in organic solvents. Campanella and coworkers ([175–177, 181–183]) described an organic tyrosinase biosensor based on a clark oxygen electrode with the tyrosinase in phosphate buffer or immobilised in kappa-carrageenan-gel and separated from the solvent by a dialysis membrane. Several authors, particularly within the last years like Wang et al. ([140–142]), have published papers in this field [144, 147, 149, 174, 196, 197]. But hydrophilic organic solvents can moreover remove the essential water which surrounds the enzyme and in its absence tyrosinase looses its biological activity [156, 158, 197, 198]

Another possible approach, applied by different authors, was the replacment of purified tyrosinases with the source from which they were isolated (tissue). These relatively cheap tissue electrodes usually have a higher stability because the natural environment in the tissue provides the enzyme with a better protection from deactivation. On the other hand most tissues contain many other enzymes which would adversively affect the selectivity and usefulness of the biosensor. Tyrosinase rich tissue from animal [199] and vegetable, e.g. mushroom [139, 164, 200–204], potato [200, 202–207], egg-plant [200, 208], spinach [209], banana [201, 203, 204] and apple powder [203, 210] have been applied to oxygen electrodes. Vegetable crude extracts have also been succesfully employed [211–213].

Other authors go into a similar direction. They use thermophilic micro organisms (also here tyrosinase can stay in the natural environment) for the construction of a biosensor, because thermophilic micro organisms are stable under extreme conditions (pH, temperature, organic solvents, etc.). Rella et al., e.g., described in 1996 a high-temperature operating biosensor for the determination of phenol and related compounds [214]. Even microbial cells of Pseudomonas [215] and Rhodococcus [216] were used in combination with Clark type oxygen electrodes.

3.4.3 Sensitivity

Determination of phenolic compounds Tyrosinase electrodes described in literature are often developed for their application in environmental control, where the determination of substituted phenols is necessary [217–219] or for their application in clinical diagnostic to determine, e.g. salicylic acid [166, 220] and catecholamines [167, 179, 203, 204, 207, 210]. Tyrosinase has also been considered for the task of indirect food moisture monitoring, because of its strong action in non-aqueous media. The quantification of polyphenols in olive oils and other fats has been described by Capannesi et al. [187] and Campanella et al. [181, 183]. Beside the use of tyrosinase electrodes for substrate quantification the electrode has also been used in combination with immunoassays (alkaline phosphatase quantification) [165, 221].

Considerable attention has been given to the improvement of sensitivity because already small quantities of phenols can have a toxic effect on animals and plants. Therefore the concentrations which have to be proved are small. If a measuring instrument should be developed, which can be used directly, without sample preparation, than it is absolutely necessary that the biosensor in the measuring instrument is able to measure corresponding to the admissible individual concentration. The European Community directive (80/778/EEC), e.g., sets the maximum concentration permitted for all phenols in aquatic environments at 5nM and at 1nM for individual phenols.

Mono-enzyme electrodes without any amplification Mono-enzyme electrodes using oxygen reduction at a potential of -600mV can be used for detection of concentrations on a micromolar level. Schubert et al., e.g., described a tyrosinase electrode with a nonlinear calibration line up to 5mM and a detection limit of 100μM [174]. But the use of mono-enzyme electrodes without an amplification step is often connected with certain disadvantages, e.g., gradual fouling of the surface due to adsorption of reaction products and limited flexibility in their design.

Highest sensitivities have been obtained with electrodes where a cyclic amplification method is employed. Here the detection limit could be improved 10-1000 fold. Different methods are used for tyrosinase electrodes, e.g.:

Bioelectrocatalytic recycling Bioelectrocatalytic recycling, as depicted in paragraph 3.3.2 is one of the most applied amplification principle in the development of high sensitive tyrosinase electrodes. The use of the electrochemical reduction of generated o-quinones as detection reaction for the quantification of phenols gives at least two advantages:

- The reaction inactivation by polymerisation is hindered by the electrochemical removal of quinone

- The low applied potential minimises the influence of different sample-matrix interferences

To illustrate the achievements in the field of improvement of sensitivity, the measuring range and the detection limits of tyrosinase electrodes are presented in Table 3.3. Only electrodes are listed which were published during the last five years and in which the principle of bioelectrocatalytic recycling was used.

Obviously, in the reported cases carbonaceous electrode material has been employed. This material facilitates fast redox conversion of quinones. Therefore, these types of substances could be detected in the nanomolar concentration range [145, 147, 149, 153, 154, 157, 165, 169–171]. Particularly within the last years electrodes were developed, which are able to measure very sensitive. Especially two groups have extensively studied the interaction of tyrosinase with a carbon electrode, e.g., Gorton and coworkers [137, 145, 161–163, 171, 192, 222] and Wang and coworkers [140, 141, 146, 153, 154, 173, 191, 201, 223].

As described above in paragraph 3.4.2 one of the most important analytical problem that appears in the case of tyrosinase-modified electrodes is their low operational stability, especially for detecting o-di-phenols [137, 168]. One way to improve the operational stability was the addition of various additives. As an alternative to additives and preparation techniques cited in literature Dantoni et al. have developed a carbon paste electrode containing a tyrosinase-DNA-mixture. They described a response decay of ca. 50% after every 3 to 4 days of use (with dry storage at 4°C overnight), but the sensitivity of this electrode is only in the micromolar range which is not enough for an application.

Table 3.3: List of bioelectrocatalytic recycling tyrosinase electrodes developed in the last five years

Elec-trode	Enzyme immobilisation	Mode	Measuring potential	Analyte	Linearity of the ca-libration curve	Detection limit / G	Ref.
CPE	TYR mixed with graphite powder, carbon paste and different pasting liquid binder	S-S + FI-S	-50mV *vs.* Ag/AgCl	Phenol Catechol	1-10μM 10-75μM	n.d. 6nM	[223]
GCE	Electropolymerisa-tion of a pyrrole amphiphilic monomer-tyrosinase mixture previously adsorbed on the electrode surface	S-S	-200mV *vs.* SCE	Phenol	0.01-10μM	10nM	[157]
CPE + SGE	(1) TYR mixed with graphit powder (2) + (3) TYR dried on the top of the electrode before Eastman AQ 29D(2) or Nafion (3) was added	FI-S	-50mV *vs.* Ag/AgCl	Different MDC Catechol Catechol	0.05-150μM 0.05-150μM	30nM 15nM	[145]
GCE	TYR mixed with poly (vinyl alcohol) / poly (hydroxyl cellulose) hydrogel	FI-S	-200mV *vs.* Ag/AgCl	Catechol Phenol p-Cresol and other MDC	100nM-100μM 1-100μM 0.5-50μM	20nM 10nM 20nM	[148]
SPCE	Electropolymerisa-tion of a pyrrole amphiphilic monomer-tyrosinase mixture previously adsorbed on the electrode surface	FI-S	-200mV *vs.* Ag/AgCl	Catechol	0.025-33μM	n.d.	[159]

continued form previous page

Elec-trode	Enzyme immobilisation	Mode	Measuring potential	Analyte	Linearity of the calibration curve	Detection limit / G	Ref.
CPE	TYR mixed with graphite powder, paraffin oil and octadecan	FI-S	-50mV *vs.* SCE	Phenol p-Cresol and other MDC	n.d. n.d.	26nM 40nM	[222]
CPE	TYR mixed with graphite powder and paraffin oil	S-S	0mV *vs.* Ag/AgCl	Phenol	n.d.	35nM	[165]
GCE	TYR immobilised in sol-gel thin film, than dried on the top of the electrode	S-S	0mV *vs.* Ag/AgCl	Catechol Phenol p-Cresol and other MDC	0.1-100μM 0.2-160μM 0.1-230μM	40nM 100nM 50nM	[153]
CPE	TYR dried on the top of the electrode before silica sol-gel was added	S-S	0mV *vs.* Ag/Agl	Catechol and other MDC	0.2-26μM	120nM	[169]
GCE	TYR immobilised in sol-gel thin film, than dried on the top of the electrode	S-S	-200mV *vs.* Ag/AgCl	Catechol Phenol p-Cresol and other MDC	1-60μM 5-120μM 6-190μM	200nM 400nM 500nM	[154]
RVCE	TYR bound on RVC activated with carbodiimide	FI-S	-200mV *vs.* Ag/Agl	Phenol and other MDC	5-100μM	300nM	[224]
SGE	TYR mixed with poly(hydroxyl cellulose) hydrogel	S-S	-200mV *vs.* Ag/AgCl	Catechol Phenol p-Cresol and other MDC	0.2-4μM	n.d.	[149]

continued form previous page

Elec-trode	Enzyme immobilisation	Mode	Measuring potential	Analyte	Linearity of the ca-libration curve	Detection limit / G	Ref.
CPE	TYR mixed with graphite powder and Nafion	S-S	0mV *vs.* Ag/AgCl	Phenol p-Cresol and other MDC	500nM-100μM 50μM-5mM	500nM	[170]
CPE	TYR mixed with graphite powder and silicon oils or mineral oils or paraffin waxes	FI-S	-200mV *vs.* Ag/AgCl	Phenol Catechol	1-200μM 1-200μM	n.d.	[225]
CPE	TYR-DNA mixture incorporated into carbon paste	FI-S	-150mV *vs.* Ag/AgCl	Catechol and other MDC	1-50μM	1μM	[226]
GCE	Electropolymerisa-tion of a pyrrole amphiphilic monomer-tyrosinase mixture previously adsorbed on the electrode surface	S-S	-200mV *vs.* SCE	Phenol	n.d.	n.d.	[227]
CPE	SH/TYR/GDH admixed with graphite powder, NADH and paraffin oil and covered with a dialysis membrane	FI-S	-100mV *vs.* Ag/AgCl	Salicylate	3.5-250μM	3.5μM	[220]
CPE	TYR mixed with graphite powder and paraffin oil	S-S	-150mV *vs.* Ag/AgCl	Gentisic acid Salicylic acid and other	50-200μM	50μM	[166]
CPE	SH/TYR/PADH admixed with graphite powder paraffin oil	S-S	-50mV *vs.* Ag/AgCl	L-Phenylalanine	20-150μM	5μM	[228]

continued form previous page

Elec- trode	Enzyme immobilisation	Mode	Measuring potential	Analyte	Linearity of the ca- libration curve	Detection limit / G	Ref.
CPE	TYR mixed with graphite powder and mineral oil	S-S	-200mV -185mV *vs.* Ag/AgCl	AOH AME	1.9-100μM 39-250μM	1.9μM 7.5μM	[164]

CPE = carbon paste electrode, SGE = solid graphite electrode, GCE = glassy carbon electrode, SCE = saturated calomel electrode, RVCE = reticulated vitreous carbon electrode, RVC = reticulated vitreous carbon, G = amplification factor, FI-S = flow injection system, S-S = stationary system, TYR = tyrosinase, GDH = glucose dehydrogenase, SH = salicylate hydroxylase, PADH = L-phenylalanine dehydrogenase, NADH = nicotinamide adenine dinucleotide reduced form, Eastman AQ 29D = registered trademark of Eastman Kodak (Kingsport, Tennessee, USA) for a polyester-sulphonic acid cation exchanger, MDC = mono- and di-phenolic compounds, Nafion = registered trademark of E. I. du Pont de Nemours and Company (Wilmington, Dellaware, USA) for a perfluorinated-sulphonated cation exchanger, DNA = deoxyribonucleic acid, AOH = alternariol, AME = alternariol monomethyl ether, n.d. = not described

Pedano et al. [166] described the application of their tyrosinase electrodes for gentisic acid quantification, in which salicylic acid and other derivatives could not be detected. More interesting for application in medical diagnostic as well as in environmental control (E.coli density) is the determination of salicylic acid or L-phenylalanine. Martin et al. [220] combined tyrosinase with salicylate hydroxylase, forming catechol from salicylate, and a determination of salicylic acid in the micromolar range was proved. Huang et a. [228] combined the bioelectrocatalytic recycling between tyrosinase and a carbon paste electrode with the enzymatic reactions of salicylate hydroxylase and L-phenylalanine dehydrogenase to determine L-phenylalanine. This multienzyme sensor was able to quantify L-phenylalanine with a linear range of 20-150μM and a detection limit of 5μM.

Recently Moressi et al. [164] have used a tyrosinase electrode for quantification of *Alternaria mycotoxins* and have shown that both alternariol and alternariol monomethyl ether are substrates of tyrosinase.

Mediated bioelectrocatalytic recycling

Furthermore tyrosinase electrodes have been developed using mediated bioelectrocatalytic recycling for enhancing the sensitivity. Reducing agents which were used as mediators in order to shuttle electrons from the enzyme to the electrode surface,are, e.g., L-ascorbic acid [184, 206], hexacyanoferrate [229, 230], N-methylimidazol [231], 5-methylphenazonium cation [151] and tetracyanochinodimethane (TCNQ) [138]. The main problem associated with the approach of

mediators is the leaching of them into the bulk solution. For this reason redox polymers were used with non-diffusional mediators, such as an osmium complexed phenanthroline dione [152, 163, 232] or a conducting poly(1-vinylimidazole)-based osmium polymer [197, 233].

Biocatalytic recycling Another approach for improving sensitivity is the principle of biocatalytic recycling, where the target analyte is recycled between tyrosinase and another enzyme (for explanation see paragraph 3.3.3). According to the best of my knowledge up till now tyrosinase has only been used in combination with glucose dehydrogenase [179]. Lisdat et al. have quantified with this bienzyme sensor dopamine and other neurotransmitter with a detection limit of 25nM. Alternative to the biocatalytic recycling a tyrosinase based chemically amplified biosensor is described based on a substrate recycling of polyphenolic compounds driven by tyrosinase catalysed oxidation and chemical reduction of o-quinones by ascorbic acid [184].

Biocatalytic pre-concentration The sensitivity of electroanalytical measurements can also be enhanced by accumulating the electrochemically active species on the electrode surface. This principle can readily be adapted to enzyme-membrane electrodes based on sequentially acting enzymes. Such sensors combine biocatalytic pre-concentration of an intermediate with an enzymatic indicator system to measure the accumulated intermediate. Campanella and co-worker have used this principle for the development of tyrosinase electrodes [176, 177, 180–183].

Another way of biocatalytic pre-concentration was shown by Wang and Chen [146]. By allowing the enzymatic reaction to proceed for different time periods (under open-circuit conditions) it is possible to accumulate the quinone product near the transducer surface.

Investigation and determination of inhibitors of tyrosinase   Inhibitor enzyme electrodes make it possible to detect directly dangerous pollutants (i.e. cyanids, pesticides) without any preconcentration or sample treatment. The list of species detectable by tyrosinase is very long. Tyrosinase electrodes are used for the quantification of aromatic carboxylic acids [53, 97, 135, 160], thio compounds [88, 97, 135, 160, 178], respiratory toxins such as azides [82, 234, 235], cyanids [83, 98, 230] and pesticides [98, 172]. Even a number of organic substrate analogues are detected such as kojic acid and derivatives [97].

A multitude of tyrosinase-based electrodes, used for the investigation and determination of inhibitors of tyrosinase (inhibitors are described in paragraph 3.1.1), has been developed in the past few years. Stancik et al. has developed the only mono-enzyme electrode, a tyrosinase electrode using oxygen reduction for the determination of thiourea derivatives with detection limits in the range of

Table 3.4: List of mediated bioelectrocatalytic recycling tyrosinase electrodes developed in the last five years

Electrode	Enzyme immobilisation	Mode	Measuring potential	Analyte	Linearity of the calibration curve	Detection limit / G	Ref.
SGE	Covalently cross-linked TYR on carbodiimide-activated graphite and TYR coimmobilised with osmium compexed phenanthroline dione in a hydrogel	FI-S	-90mV *vs.* SCE	Phenol	n.d.	6nM	[152]
CPE	TYR mixed with graphite powder and an osmium compexed phenanthroline dione	FI-S	-50mV *vs.* Ag/AgCl	Catechol Phenol and other MDC	2.5-15μM 2.5-13μM	10nM 10nM	[232]
GCE	TYR immobilised in a conducting poly(1-vinylimidazole)-based osmium polymer, than dried on the electrode surface	FI-S	-200mV *vs.* SCE	Phenol p-Cresol and other MDC	n.d. n.d.	58nM 4nM	[233]
CPE GCE	TYR mixed with graphite powder or glassy carbon powder, paraffin oil and an osmium compexed phenanthroline dione	FI-S	-50mV *vs.* Ag/AgCl	Catechol Phenol and other MDC	n.d.	n.d.	[163]

CPE = carbon paste electrode, SGE = solid graphite electrode, GCE = glassy carbon electrodes, SCE = saturated calomel electrode, G = amplification factor, FI-S = flow injection system, S-S = stationary system, MDC = mono- and di-phenolic compounds, TYR = tyrosinase, n.d. = not described

Table 3.5: List of biocatalytic recycling and biocatalytic preconcentration tyrosinase electrodes developed in the last years

Electrode	Enzyme immobilisation	Mode	Measuring potential	Analyte	Linearity of the calibration curve	Detection limit / G	Ref.
Biocatalytic recycling							
COE	TYR/GDH mixture entrapped in gelatine	S-S + FI-S	500mV *vs.* Ag/AgCl	Dopamin and other NT	0.025- 1μM	25nM	[179]
Biocatalytic preconcentration							
COE	TYR entrapped in κ-carrageenan gel and fixed on the top of the electrode between a gas permeable and a dialysis membrane	S-S	-600mV *vs.* Ag/AgCl	Phenol	1-37μM	200nM	[182] [181] [183]

COE = Clark-oxygen electrode, G = amplification factor, FI-S = flow injection system, S-S = stationary system, NT = neurotransmitter, TYR = tyrosinase, GDH = glucose dehydrogenase

13-181nM [178].

As described above in paragraph 3.3, mediated or non-mediated electrochemical substrate regeneration (or bioelectrocatalytic recycling) are powerful methods which increase the sensitivity of an enzymatic assay. Beside the improvement of subtrate detectors, cyclic amplification methods have also been used for the investigation of inhibitors and will be described in the following. If a substrate analogue should be measured the amplification step will be interrupted and a very sensitive determination of this substances will be possible. Different devices for monitoring benzoic acid, pesticides and herbizides, e.g. single-use devices by Wang et al. [143, 160], or cyanide, chlorophenols, atrazine and pesticides by Besombes et al. [98], offered convenient quantification of micromolar levels of these pollutants. Reversed micelles in biosensors have been used also for monitoring inhibitors of tyrosinase such as benzoic acid, thiourea or propyl gallate [134] or different pesticides [136].

Furthermore tyrosinase electrodes have been developed for inhibitor determination using mediators, e.g. ferrocyanid [230], hydrazine [88], 1,2naphthquinone 4-sulfonate (NQS) [53, 172]. The Os-polymer, [Os(bpy)$_2$(PVI)$_{10}$Cl]Cl (bpy = 2,2$'$-bipyridyl, PVP = poly(4-vinylimidazol)) has also been used to form reagentless biosensors with tyrosinase, which have been applied for quantification of sodium azide [82, 234, 235].

Moreover Hasebe et al. described a tyrosinase electrode based on a substrate recycling of polyphenolic compounds driven by tyrosinase catalysed oxidation and chemical reduction of o-quinones by L-ascorbic acid [97].

In summary, several tyrosinase electrodes for the determination of tyrosinase inhibitors are described, developed on the basis of different attempts (a mono-enzyme electrode, electrodes based on bioelectrocatalytic recycling, on mediated bioelectrocatalytic recycling and a recycling between tyrosinase and ascorbic acid.). Most of them can measure millimolar or micromolar concentrations of hazardous compounds. A particular interesting application involves water quality control, because methods generally used to measure cyanids, pesticides or herbizides, are HPLC or GC/MS involving extraction of large volumes of water, extensive purification and often derivatisation. Furthermore experienced technicians and expensive equipments are required. As a consequence attention has been directed to newer methods. But the threshold concentration for individual compounds is $0.1\mu g/l$ in Germany (drinking water ordinance paragraph 2). The electrodes must therefore be able to measure nanomolare concentrations of the health harmful substances.

In Table 3.6 a list of inhibitor measurement using tyrosinase and developed in the last 5 years is given. Only two tyrosinase electrodes are able to measure inhibitors in a nanomolar concentration range. Everett and Rechnitz have used mediated bioelectrocatalytic amplification to measure organophosphorus pesticides with a tyrosinase-based oxygen biosensor, but only dichlorvos was determined with a detection limit of 75nM. The second tyrosinase electrode with a sensitivity which permits measurements in the nanomolar concentration range is based on bioelectrocatalytic recycling [136]. According to the best of my knowledge no tyrosinase electrode based on biocatalytic recycling is used up till now for inhibitor quantification, although with this method the detection limit of biosensors can be lowered by several orders of magnitude [4].

Table 3.6: Inhibitor measurement using tyrosinase electrodes with different amplification methods developed in the last five years

Elec-trode	Enzyme immobilisation	Mode	Measuring potential	Analyte	Linearity of the calibration curve	Detection limit / G	Ref.
Bioelectrocatalytic recycling							
SPCE	TYR mixed with carbon ink was printed onto a alumina ceramic plate and covered with a insulator layer	S-S	-200mV *vs.* Ag/AgCl	Pesticides Herbicides Benzoic acid	n.d.	2-10μM / 100μM	[160]
GDE	TYR adsorbed on the electrode surface	S-S	-200mV *vs.* Ag/AgCl	Pesticides	in the micromolar range	70nM-1.7μM	[136]
Mediated bioelectrocatalytic recycling							
GCE	TYR coimmobilised with an osmium redox mediator in a hydrogel	S-S	0mV *vs.* Ag/AgCl	Sodium azide	n.d.	10μM	[234, 235]
GCE	Covalently cross-linked TYR with glutaraldehyde on the surface of the electrode and covered with a dialysis membrane	S-S	-150mV *vs.* Ag/AgCl	Diazinon Dichlorvos	5-100μM n.d.	5μM 75nM	[172]

GCE = glassy carbon electrodes, SPCE = screen printed carbon electrode, GDE = graphite disk electrode, G = amplification factor, S-S = stationary system, TYR = tyrosinase, n.d. = not described

4 Results

4.1 Investigation of mushroom tyrosinase and tyrosinase from *S. antibioticus*

4.1.1 Purification of mushroom tyrosinase and isolation of *S. antibioticus* tyrosinase

Mushroom tyrosinase   The enzyme has been purified by Makower et al. [236] from a commercial lyophilised powder prepared from the mushroom *Agaricus bispora*. The purified tyrosinase was analysed using MALDI mass-spectroscopy (see Figure 4.1), the activity was measured (see paragraph 4.1.2) and the stability was investigated (see paragraph 4.1.3). But during the purification procedure about 60
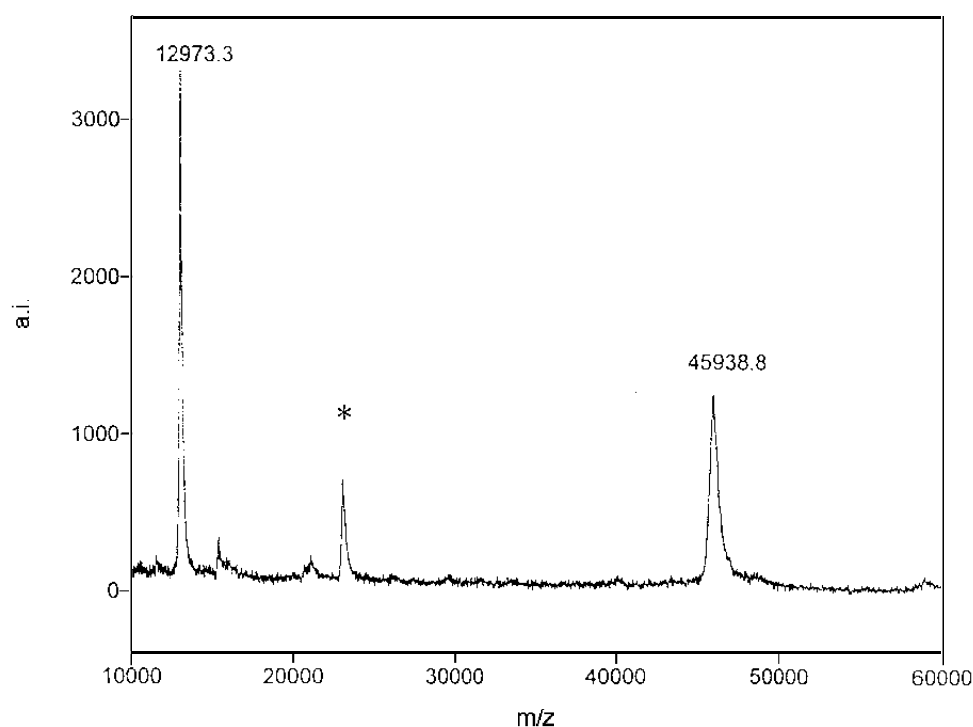

Figure 4.1: MALDI mass-spectroscopy of purified mushroom tyrosinase with peaks at around 13kD and 46kD which corresponds to the molecular weight of the L− and the H−subunit and a peak at around 23kD which is exactly the half of the molecular weight of the H−subunit

per cent of enzyme activity got lost [236] and purified tyrosinase had a similar stability as unpurified tyrosinase. For this reason all studies were performed with the unpurified enzyme.

According to the MALDI mass-spectroscopy, made by Dr. S. Haebel [237], the subunits of the purified protein have a size of 13kD and 46kD (Figure 4.1) which is in good agreement with the molecular weight of 13kD and 43kD as estimated through the SDS-PAGE [16].

***S. antibioticus* tyrosinase**   Tyrosinase as produced by *S. antibioticus* is excreted into the medium. The main task for the purification of the tyrosinase was the removal of melanin, a product of tyrosinase. This could be achieved by utilising the large difference between the isoelectric point of tyrosinase (above 9 [1]) and the electrochemical characteristics of the melanins (melanins are hetorogeneous negatively charged polymers). The bacterial mycelium was removed from the growth medium by vacuum filtration using a glass filter (type P2) funnel containing glass wool. Efficient and selective binding of tyrosinase from the growth medium is achieved by diluting the medium ten-fold with water and bringing the pH of the solution to 6.25. The dilution step results in a decrease in the ionic strength of the medium, which otherwise would be too high for the protein to bind to carboxymethylsepharose (in the following called CM). After dilution and changing pH, the CM (equilibrated with 10mM phosphate buffer at pH=6.0) was added to the medium where the total amount added typical constituted 0.5 to 1.0 % of the total volume of the diluted medium. After the initial binding step, the CM appears dark-gray indicating the binding of melanins as well.

Then the enzyme was eluted with a linear phosphate gradient (10mM phosphate pH=6.0 to 100mM phosphate pH=7.2, 500ml of each). After concentration of collected fractions (fractions between 58min and 142min), there is still some melanin present, requiring a second chromatography step. To lower the ionic-strength in the pooled fractions, the pool is washed with 10mM phosphate buffer with pH=7.2 by Amicon filtration prior the binding to the second CM column. This time the enzyme was eluted with a linear phosphate gradient (10mM phosphate pH=7.2 to 100mM phosphate pH=7.2, 500ml of each). After chromatography step two, all fractions between 12min and 100min were pooled, concentrated, a buffer exchange to 40mM phosphate buffer (pH=7.2) was executed by Amicon filtration and 20% of glycerol were added. In Figure 4.2 the elution profiles of the two chromatography steps detected by absorption at 280nm are shown. Two overlapping peaks are visible, the first is melanin and the second tyrosinase. But in the elution profile of chromatography step two (Figure 4.2**B**) the peak, indicating melanin, is clearly narrower. The general purification protocol is adapted from [1] and more clearly described in paragraph 7.3.1.

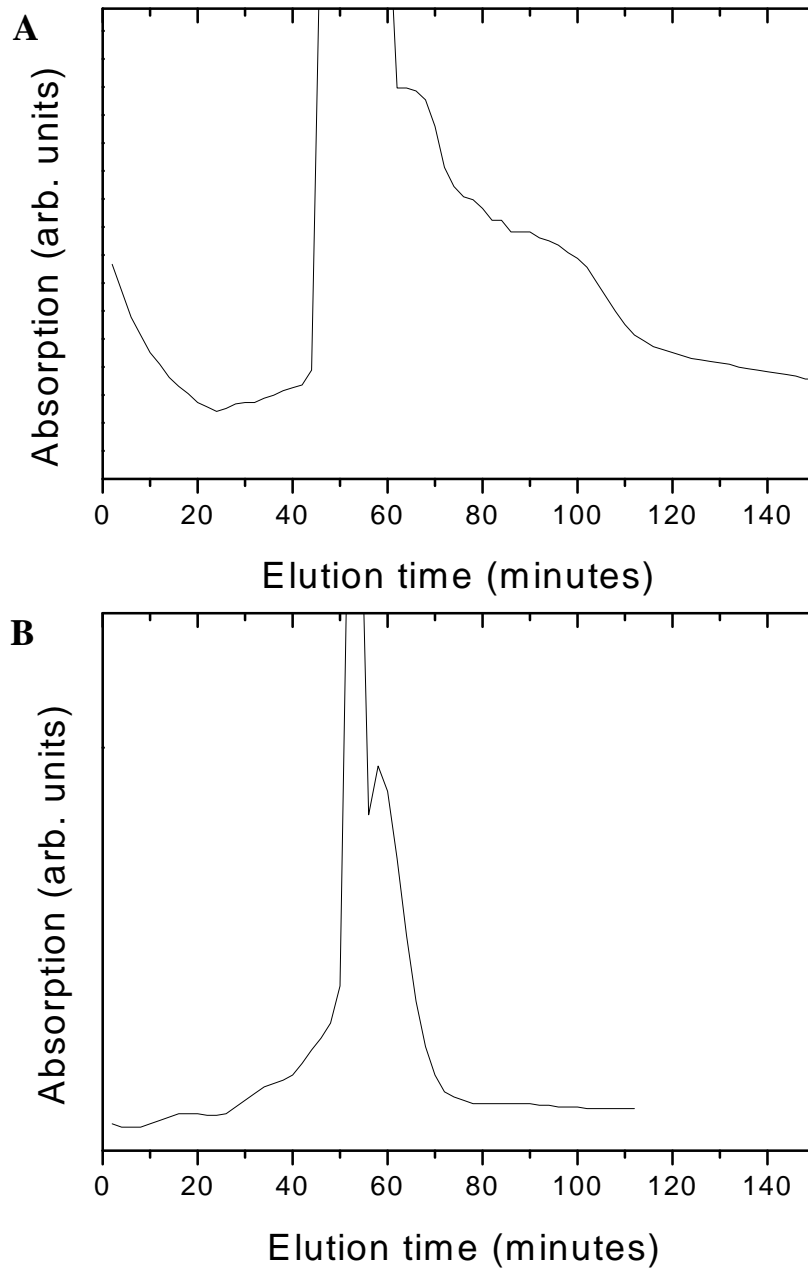Figure 4.2: Elution profile of the first chromatography (**A**) (column material: CM; elution gradient: linear, 10mM phosphate pH=6.0 to 100mM phosphate pH=7.2, 500ml of each) and the second chromatography (**B**) (column material: CM; elution gradient: linear, 10mM phosphate pH=7.2 to 100mM phosphate pH=7.2, 500ml of each) of *S. antibioticus* tyrosinase purification detected by absorption at 280nm
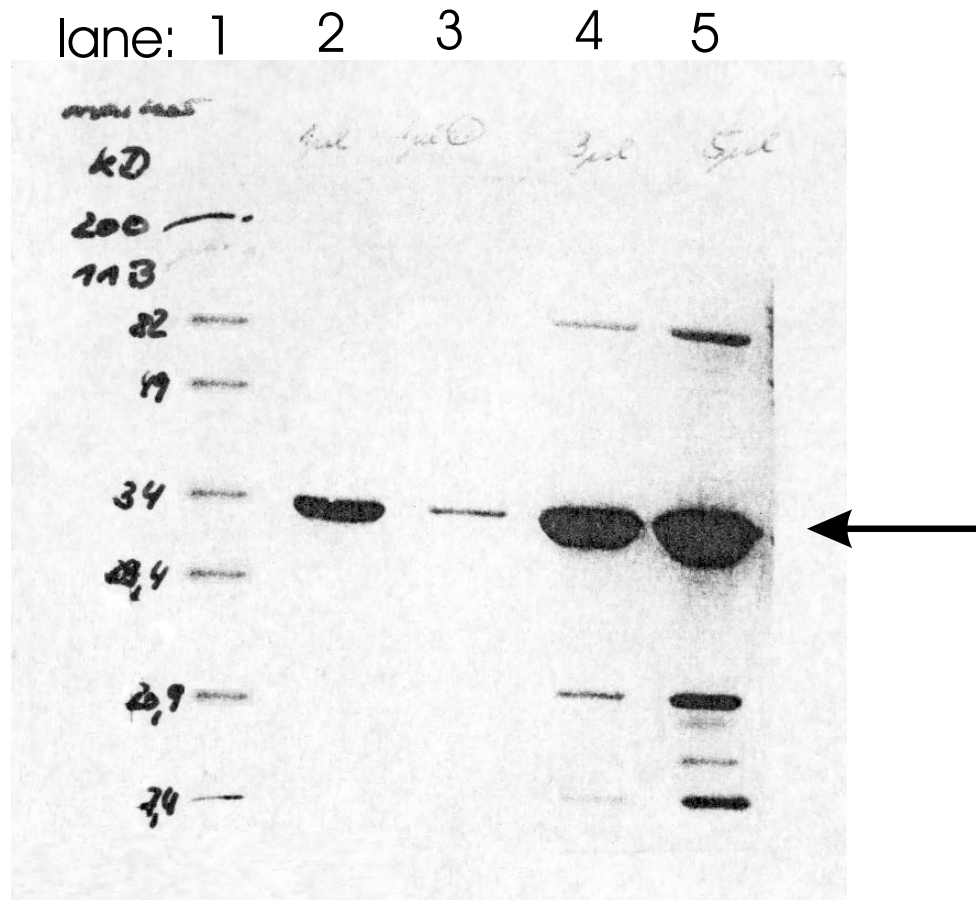
Figure 4.3: Analytical SDS-polyacrylamide gel of $1\mu l$ (lane 2), $0.1\mu l$ (lane 3), $3\mu l$ (lane 4) and $5\mu l$ (lane 5) of the final solution of *S. antibioticus* tyrosinase after purification. The arrow marks the line of *S. antibioticus* tyrosinase. The lines of the marker (lane 1) have been highlighted and the numbers written with the hand correspond to the molecular weight of the proteins of the marker (listed in kD).

In Figure 4.3 an analytical SDS-polyacrylamide gel of different amounts of the final solution of *S. antibioticus* tyrosinase is shown. As long as a moderate protein concentrations are used for the SDS-PAGE (maximum $5\mu g$/lane like in lane 1 to 3) only two very thin lines additionally to the line at about 31kD are visible, which demonstrates the very high purity of the final tyrosinase solution. Furthermore it should be pointed out that preparations from different isolation experiments had a consistently high degree of purity. According to the MALDI mass-spectroscopy [237] the isolated protein has a size of 30.6 kD (Figure 4.4)
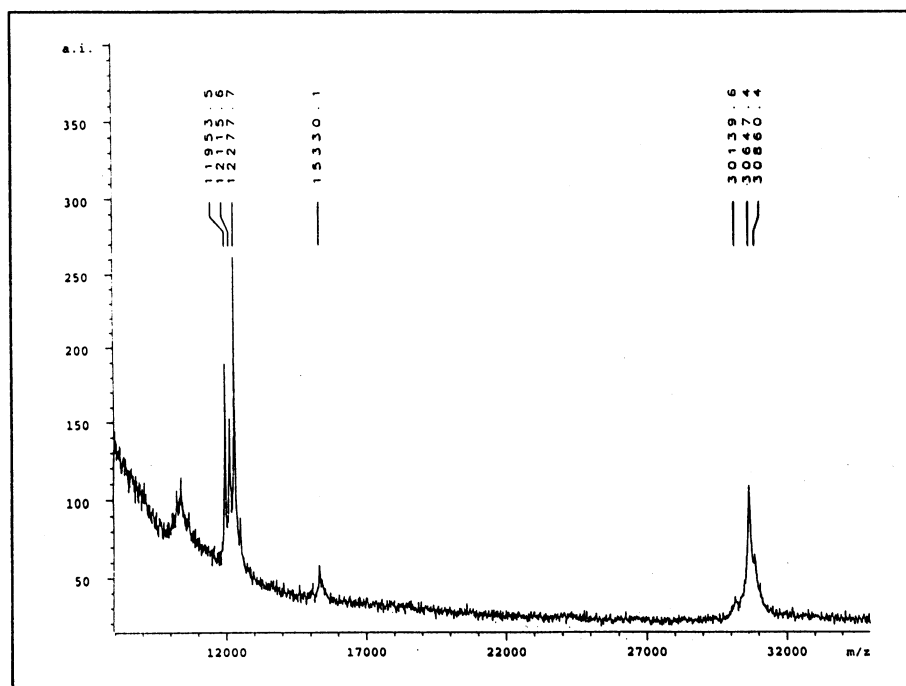
Figure 4.4: MALDI mass-spectroscopy of the eluate obtained after the second chromatography with a peak at around 30.6kD which corresponds to the molecular weight of *S. antibioticus* tyrosinase and a peak at around 15.3kD which is exactly half the molecular weight of tyrosinase. The identities of the peaks around 12.1kD are not known.

which is in good agreement with the molecular weight of 29.5 kD as estimated through the SDS-PAGE and 30.6kD as predicted through the sequence [18].

During the purification procedure hardly any enzyme activity was lost because of the special technique of the purification (described in paragraph 7.3.1). The yield was always over 90%.

Some information about the characteristics of the two tyrosinases is given in the following paragraphs (paragraph 4.1.2 and paragraph 4.1.3).

4.1.2 Characterisation of mushroom tyrosinase and *S. antibioticus* tyrosinase

To compare the activities of the two tyrosinases, used in this studies, two spectrophotometric methods were applied because the substrate spectrum differs substantially:
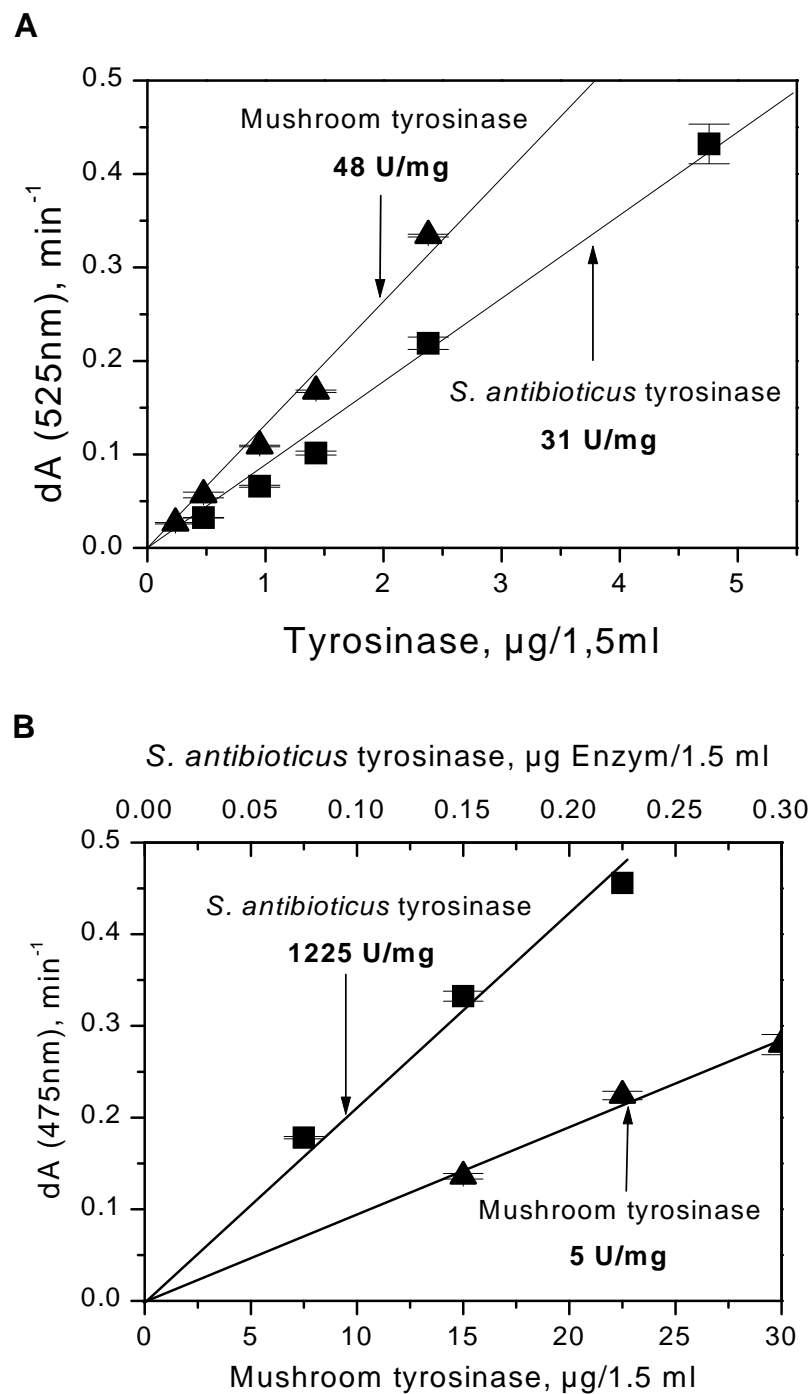
Figure 4.5: Differential absorption (dA) dependence of the quinone formation at 525nm (**A**) and of the dopachrome appearance at 475nm (**B**) on the concentration of *S. antibioticus* tyrosinase (■) and mushroom tyrosinase (▲)

Method 1 is based on the coupling reaction between L-proline and o-quinone, product of the enzymatic oxidation of catechol. The chromogenic product of the assay, 4-*N*-prolyl-o-quinone, was stable over the course of reaction (see proline assay in paragraph 7.3.3). It is a very user-friendly method and allows to determine the tyrosinase activity with a very good reproducibility.

Method 2 (see dopachrome assay in paragraph 7.3.3) was chosen because L-dopa, a physiologically interesting substrate, is used. Here the rate of dopachrome appearance is measured (Dopachrome is an oxidation product of dopaquinone.).

In Figure 4.5 the results of the two methods are illustrated. Using Method 1 the two enzymes show similar activities, with 31U/mg protein as the specific activity of *S. antibioticus* tyrosinase and 48U/mg for the lyophilisate of mushroom tyrosinase. However, with L-dopa as substrate (Method 2) the activities differ significantly. An activity of 1225U/mg protein was obtained for *S. antibioticus* tyrosinase, but the mushroom tyrosinase had only an activity of 5.2U/mg lyophilisate. This difference in the activity is measured with a L-dopa concentration of 5mM, which corresponds to approximately ten times K_M in the case of mushroom tyrosinase (K_M=380μM [66], 480μM [85]) and to approximately the half of K_M in the case of *S. antibioticus* tyrosinase (K_M=8.9mM [1]). Therefore about the maximum speed of mushroom tyrosinase and about the half maximum speed of the *S. antibioticus* tyrosinase was measured.

Figure 4.6 shows the enzyme activity (normalised with respect to the highest activity) as a function of pH when an o-diphenol (catechol for mushroom tyrosinase and L-dopa in the case of *S. antibioticus* tyrosinase) is used as substrate. As it is illustrated for mushroom tyrosinase the reaction was optimal at pH 7.5 but the enzyme still exhibited more than 75% of maximum activity over a range of 5.0−8.0 (Figure 4.6) [30]. The activity optimum of *S. antibioticus* tyrosinase is around pH=7.0 close to 6.8, the pH-optimum of *Streptomyces glaucescens* tyrosinase [238].

Effect of inhibitors in solution   Spectrophotometric assays in solution were based on the reaction of proline and o-quinone in accordance with the Rzepecki and Waite procedure [50]. For the measurement of inhibition a cuvette was filled with various volumes of inhibitor solution, 30μl proline (1M) and 15μl catechol (10mM) and made up to 1.44ml with phosphate buffer (100mM, pH=6.5 containing 1M sodium chloride). The solutions were mixed in the cuvette for 2min. To start the assay, 15μl tyrosinase solution (300μg/ml) was added and mixed again. After 10sec, the differential absorption at 525nm was measured. This way the effects of benzoic acid and derivatives, kojic acid and derivatives as well as thiourea and derivatives in solution were investigated.

In solution, mushroom tyrosinase was 70% inhibited by benzoic acid (100μM).
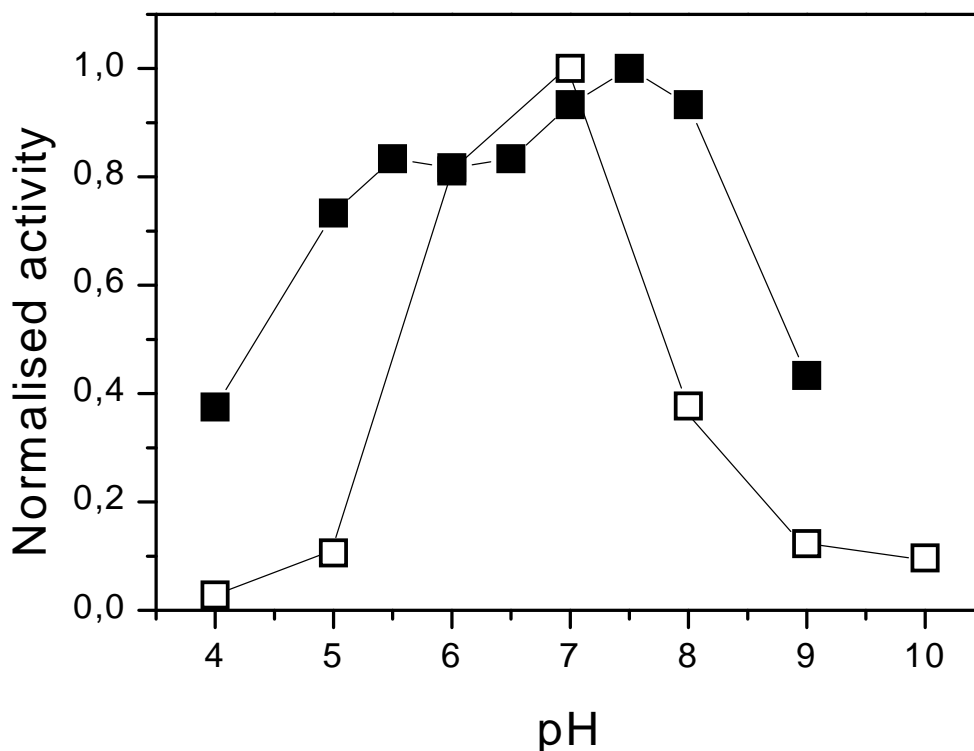
Figure 4.6: Dependence of *S. antibioticus* tyrosinase (□) and mushroom tyrosinase (■) activity on pH (The dependence of mushroom tyrosinase on pH is adapted from Brown et al. [30].)

Kahn and Andrawis [85] reported a I_{50}-value of $300\mu M$ using L-tyrosine as the substrate and detection of dopachrome.

For synthesis of kojic acid derivatives mostly the two hydroxylgroups, one at position 5 and the other at position 7, were used. For a better understanding the chemical names according to IUPAC were reduced to a shorter name. This name is started with kojic acid in front of the name, than the position of the hydroxylgroup used for synthesis is given followed by the name of the compound which was used for synthesis. In Figure 4.7 the structure of kojic acid and of its derivatives, marked by their shorter name and their IUPAC name in parenthesis, is given.

The Rzepecki and Waite assay procedure has also been used by Kobayashi et al. [95, 96] who investigated the inhibition of tyrosinase by kojic acid and some of its derivatives.They found that derivatives of kojic acid, where an additional group was added via an ester coupling with the hydroxylgroup at position 7 of kojic acid
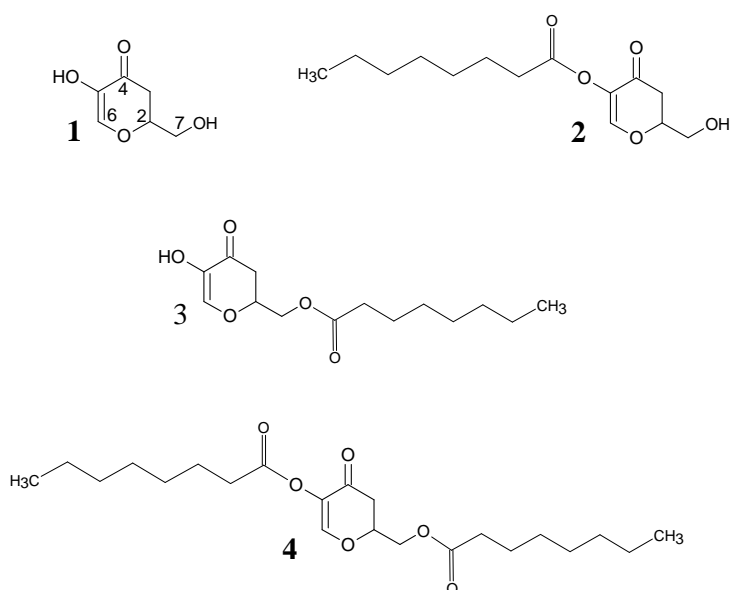
Figure 4.7: Kojic acid (**1** = 5-hydroxy-2-hydroxymethyl-4*H*-4-pyrone), kojic acid 5-*O*-capryloate (**2** = octanoic acid 2-hydroxymethyl-4-oxo-4*H*-pyran-5-yl ester), kojic acid 7-*O*-capryloate (**3** = octanoic acid 5-hydroxy-4-oxo-4*H*-pyran-2-yl)-methyl ester) and kojic acid 5,7-di-*O*-di-capryloate (**4** = octanoic acid 4-oxo-2-(1-oxooctyloxymethyl)-4*H*-pyran-5-yl ester)

(7-*O*-acyl derivatives), were similar or slightly stronger inhibitors than kojic acid (I_{50}=23μM).

This is similar to the data described here and summarised in Table 4.1. About 70% inhibition were determined with 100μM kojic acid. So far, inhibiton of tyrosinase by 5-*O*-acyl kojic acid derivatives has not been reported. A free hydroxy group at position 5 should be necessary for inhibiton. This consideration is confirmed by the much weaker inhibition of tyrosinase by kojic acid 5-*O*-capryloate (about 50% inhibition at 100μM). The di-ester showed no inhibition of the catecholase activity even at concentrations up to 100μM (Table 4.1). This is in some contrast to the results of Nagai and Izumi [239] who described an inhibition of skin tyrosinase and melanocytes by fatty acid di-esters of kojic acid.

Thiourea derivatives are among the strongest inhibitors of catecholase activity. All thiourea derivatives investigated were detected in the lower micromolar range. 1-Phenyl-2-thiourea was the most effective inhibitor, diminishing the catecholase activity when it is present in nanomolar concentration, followed by 1-allyl-2-thiourea. An inhibition of 7% with 10μM 1-allyl-2-thiourea was found. *N,N'*-diphenylthiourea and thiourea inhibited tyrosinase in the same order of mag-

Table 4.1: Inhibition of tyrosinase in solution by different classes of inhibitors. (measured with the proline assay, which is described in paragraph 7.3.3)

Compound	Concentration, μM	Inhibition, %
Benzoic acid and derivatives		
Benzoic acid	100	70
Kojic acid and derivatives		
Kojic acid[a]	100	68
kojic acid 5-*O-capryloate*[a]	100	47
kojic acid 7-*O-capryloate*[a]	100	83
kojic acid 5,7-di-*O-di-capryloate*[a]	100	0
Thiourea and derivatives		
Thiourea	100	71
N,N′-Diphenylthiourea	10	7
	100	80
1-Allyl-2-thiourea	10	76

[a] For the IUPAC name and the structure see Figure 4.7.

nitude. A reduction in activity of 70-80% was observed with 100μM of these inhibitors.

4.1.3   Stability of mushroom tyrosinase and *S. antibioticus* tyrosinase

Maintaining high activity levels even after long-term storage is an important feature for a successful sensor. Therefore, the stabilty of the tyrosinases used in this thesis was investigated by measuring the activity as a function of the time upon storage under different conditions.

Mushroom tyrosinase   The activity of lyophilised non-purified and purified mushroom tyrosinase was determined as a function of storage time at a temperature of -18°C. In Figure 4.8 the normalised activity is shown to make a comparison between both purification states possible. No loss of activity could be measured for
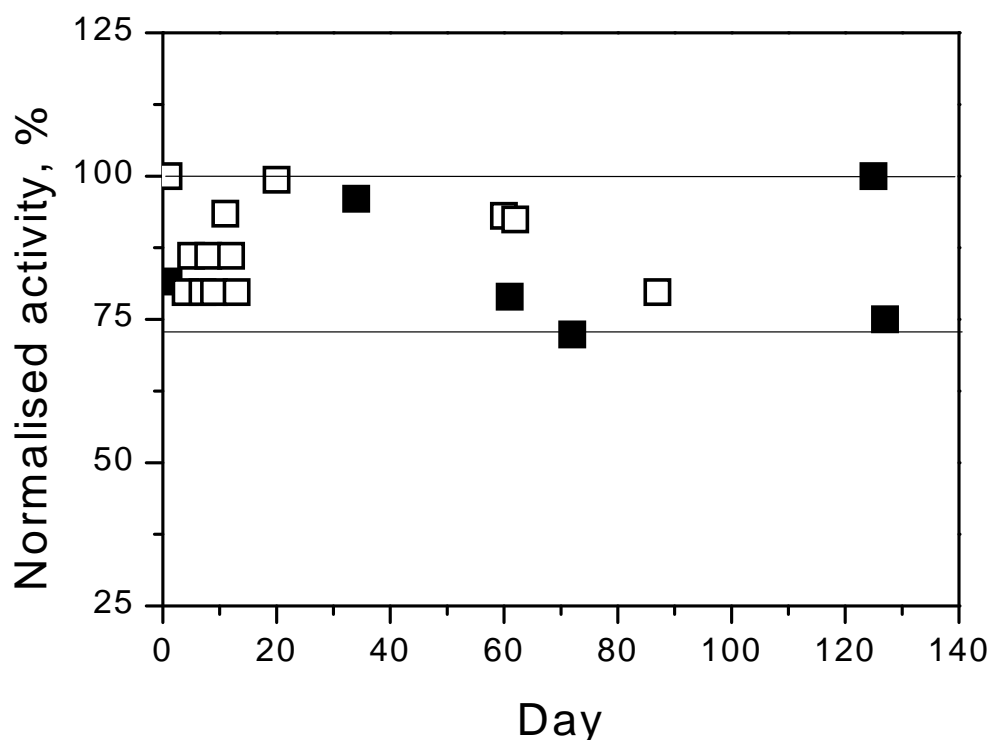
Figure 4.8: Storage stability of lyophilised purified (□) and non-purified mushroom tyrosinase (■) at a temperature of -18°C. The normalised activity as a function of time is shown. (The investigation of purified mushroom tyrosinase was made by Makower et al. [236].)

lyophilisised purified as well as non-purified mushroom tyrosinase during more than four months. But if mushroom tyrosinase was stored in buffer solution at temperatures of -18°C or 4°C, then about 80 per cent of enzyme activity was lost within four days [236].

***S. antibioticus* tyrosinase** The activity of *S. antibioticus* tyrosinase was determined as a function of the storage time. For this tyrosinase was solved in 40mM phosphate buffer pH 7.2 with and without glycerol and stored at four different temperatures (-80°C, -18°C, +4°C and +37°C). Also dried tyrosinase was stored at these four different temperatures. The enzyme activity was reduced by only 30% after 50days storage at 4°C, while storage of the enzyme at -18°C or +37°C led to an almost complete loss of activity within the first few days (see Figure 4.9**A**). The addition of glycerol resulted in a stabilisation. In the presence of 20%

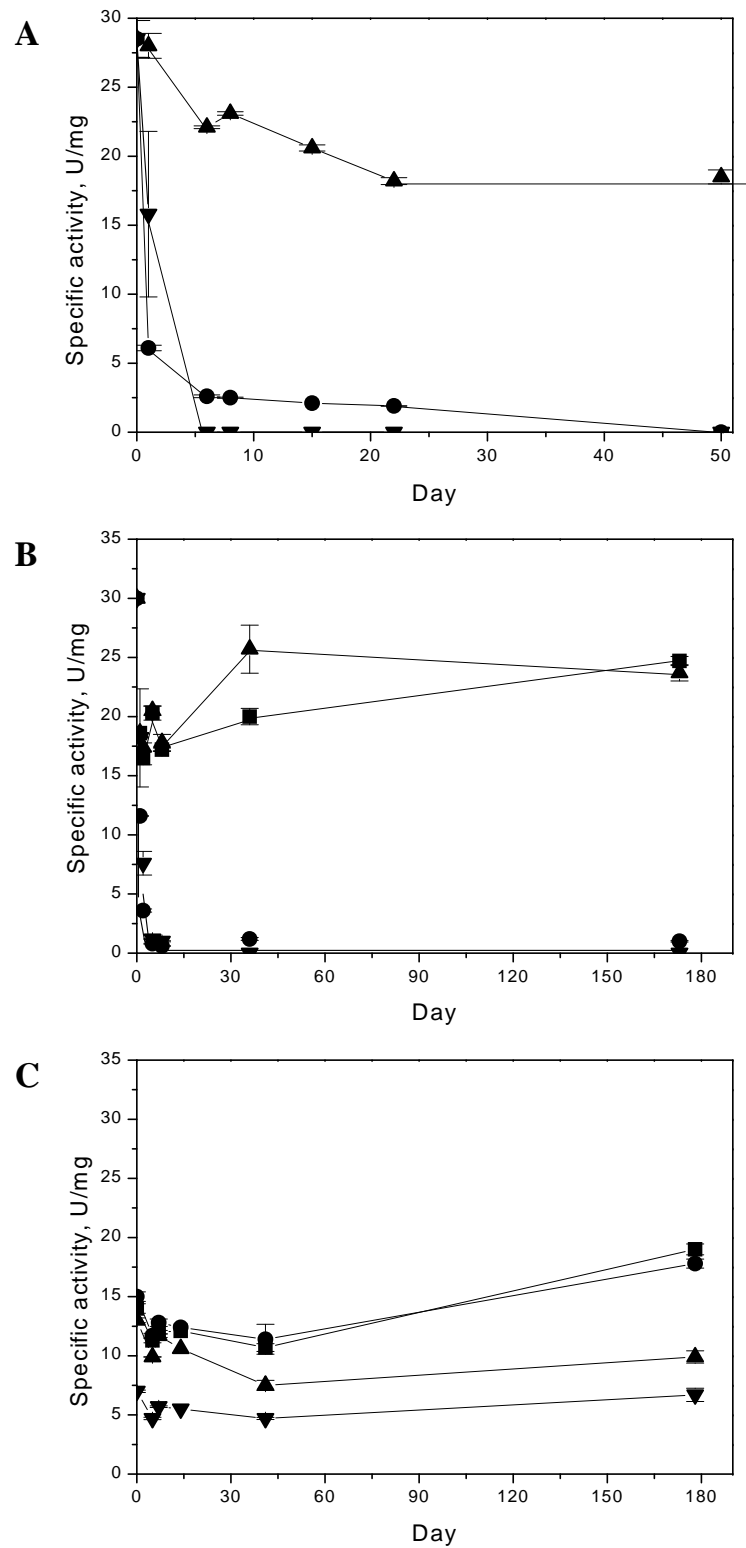Figure 4.9: Storage stability of *S. antibioticus* tyrosinase in A: phosphate buffer, 40mM, pH=7.2, B: phosphate buffer, 40mM, pH =7.2 containing 20% glycerol and C: the dried enzyme at different temperatures: -80°C: ■, -18°C: ●, +4°C: ▲, +37°C: ▼.

glycerol no loss of activity was observed after 170days of storage at 4°C and -80°C. But even in the presence of 20% glycerol the activity drop already within the first days was significant at -18°C and +37°C (Figure 4.9**B**). The loss of enzyme activity at -18°C is due to the storage conditions since enzyme solutions which initially were stored at -80°C showed a loss of activity with further storage at -18°C. Tyrosinase solution stored at -80°C followed by a period of storage at +4°C maintained full activity. In addition, the storage of *S. antibioticus* tyrosinase as a dried sample was investigated. In this case storage at temperatures below zero, -18°C and -80°C, turned out to be the best condition. Samples have been stored for at least 6months without any loss of activity at these temperatures (Figure 4.9**C**).

Streptomyces glaucescens tyrosinase which is quite similar to tyrosinase from *S. antibioticus* has been reported to retain its activity after two months storage at -30°C in the presence of 20% glycerol [238]. This is in good agreement with our data for *S. antibioticus* tyrosinase.
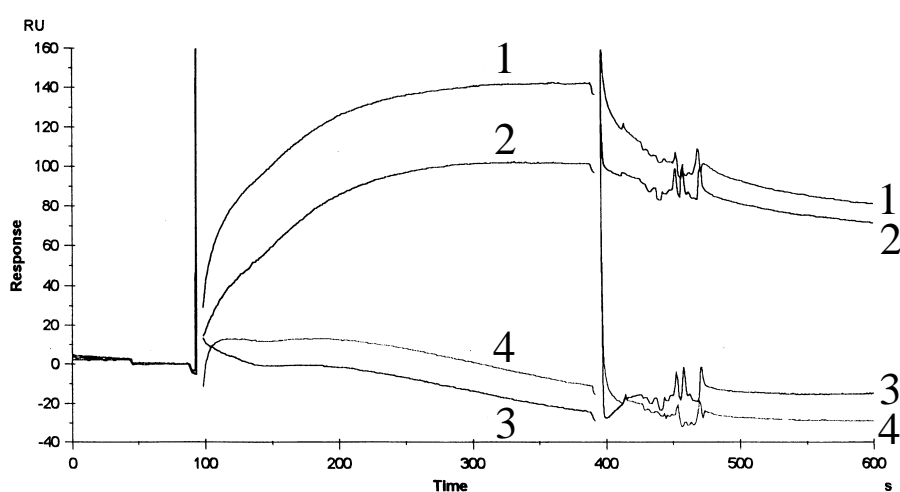
Figure 4.10: Sensorgrams of interactions of *S. antibioticus* tyrosinase and bovine serum albumin (BSA) with immobilised kojic acid and immobilised ethanolamine measured with a surface plasmon resonance (SPR)-based interaction analysis technique. The curves illustrate the differences in association and dissoziation rates of *S. antibioticus* tyrosinase to immobilised kojic acid (sensorgram 1) and immobilised ethanolamine (sensorgram 2) and BSA to immobilised kojic acid (sensorgram 3) and immobilised ethanolamine (sensorgram 4).

4.1.4   Interactions of mushroom and *S. antibioticus* tyrosinase with immobilised kojic acid

Kojic acid is an reversible inhibitor of tyrosinase and therefore kojic acid can be potentially used to enrich tyrosinase at a surface. Surface plasmon resonance was used for observation of molecular interactions between tyrosinase and immobilised kojic acid. In paragraph 7.2.1 the preparation of the sensor surface and the protocol used for investigation of the binding and dissociation of tyrosinase have been described. At first different enzyme concentrations were tested and it was found that a concentration of 2mg/ml lyophilised mushroom tyrosinase and 0.2mg/ml *S. antibioticus* tyrosinase were optimal for the investigation of binding and dissoziation processes to kojic acid.

A specific binding of both tyrosinases to a surface modified with kojic acid could be observed. In Figure 4.10 the sensorgrams for binding of *S. antibioticus* tyrosinase in comparison to binding of bovine serum albumin (BSA) is shown. It can be easily seen that the binding of tyrosinase to immobilised kojic acid (sensorgram 1 in Figure 4.10) is significantly better than the binding to immobilised ethanolamine (sensorgram 2 in Figure 4.10). No binding was obtained for BSA to both, immobilised kojic acid (sensorgram 3 in Figure 4.10) and immobilised ethanolamine (sensorgram 4 in Figure 4.10) . If one now subtracts the binding of *S. antibioticus* tyrosinase to ethanolamine (sensorgram 2 in Figure 4.10) from the
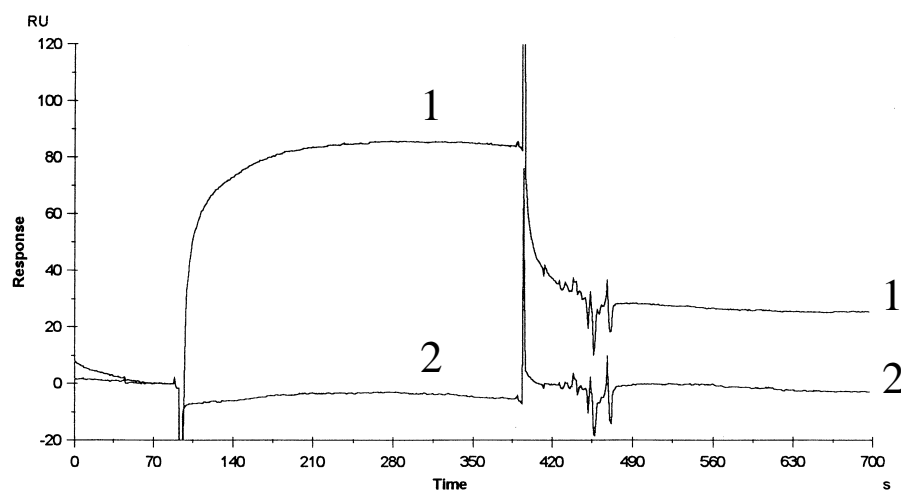

Figure 4.11: Illustration of the difference between sensorgram 1 and 2 from Figure 4.10 (line 1) to show clearly the specific interactions of *S. antibioticus* tyrosinase and kojic acid in comparison to BSA (line 2). (Line 2 is the illustration of the difference between sensorgram 3 and 4 from Figure 4.10.)

binding of *S. antibioticus* tyrosinase to kojic acid (sensorgram 1 in Figure 4.10), then only the specific part of the binding of *S. antibioticus* tyrosinase remains (for comparison see line 1 in Figure 4.11).

Also the inhibition of binding of mushroom tyrosinase by tropolone was investigated. Tropolone is one of the strongest inhibitors of tyrosinase. Therefore an inhibition of kojic acid binding to tyrosinase should be visible if tropolone is added to the tyrosinase solution. Such an inhibiton of tyrosinase binding of around 12% was obtained. This inhibition effect was measured at three different temperatures (10°C, 20°C and 30°C) and no dependence from temperature could be found.

4.2   Monoenzyme electrodes

4.2.1   Mushroom tyrosinase electrodes

As discussed above in the previous paragraph (see paragraph 3.1.1), tyrosinase converts monophenol into o-diphenol by a hydroxylation step. The produced o-diphenol is further oxidised by a second enzymatic step into o-quinone. During these two steps oxygen is consumed. Therefore, for the construction of the tyrosinase electrodes two measuring principles were used:

- The reduction of the produced o-quinone and

- The reduction of oxygen.

If the reduction of o-quinone is measured than a recycling principle can be used for detection, the bioelectrocatalytic recycling (see also paragraph 3.3.2). In this case quinone produced by tyrosinase is reduced back to the o-diphenol by the electrode, which is than oxidised again by tyrosinase and so on. For the quantification of o-quinones electrodes based on carbon materials are preferentially used and the reduction takes place at a potential of -50mV versus Ag/AgCl. In this work screen printed electrodes (SPE) made from carbon paste were choosed (see paragraph 3.2.2). Here mushroom tyrosinase has been immobilised in a polymeric netwerk (nafion and polyurethane) on the surface of the graphite SPE. Mushroom tyrosinase electrodes where tyrosinase was immobilised in nafion shall be named SPE_MT_N and where tyrosinase was immobilised in polyurethan shall be named SPE_MT_PU.

The other possibility was the measurement of oxygen reduction at -600mV versus Ag/AgCl. Here membrane-covered Clark type oxygen electrodes (COE) were used (for explanation see paragraph 3.2.2). In this case oxygen consumed by tyrosinase can be detected as a loss of measuring signal. To fixe the enzyme on

the electrode surface, mushroom tyrosinase has been immobilised in polyvinyl-alcohol membranes. In the following this mushroom tyrosinase electrodes shall be named COE_MT_PVA.

At first the conditions for the tyrosinase electrode reactions have been optimised. The maximum activity was obtained for electrode SPE_MT_N at a pH between 6.0 to 7.0, for electrode SPE_MT_PU at a pH between 5.0 to 5.5 and for electrode COE_MT_PVA at a pH between 6.5 to 7.5 if catechol was used as the substrate for tyrosinase. The detection limit for catechol of electrode COE_MT_PVA (1μM) is four to five times higher than that of electrode SPE_MT_PU (250nM) or electrode SPE_MT_N (200nM). The electrodes allow detection of phenolic compounds in the lower micromolar range. The measuring range of electrodes COE_MT_PVA and SPE_MT_N is comparable. Only with electrode SPE_MT_PU a broad measuring range is obtained. The fixation of tyrosinase, already immobilised in a polyvinyl-alcohol membrane, onto a Clark type oxygen electrode led to a short response time of only 40sec in contrast to 3.5min (electrode SPE_MT_N) and 4min (electrode SPE_MT_PU). Regarding the application it is important to mention, that a storage of the enzyme-membranes, used for electrode COE_MT_PVA, is possible for several months at 4°C. A summary of the sensor-characteristics of the obtained electrodes is given in Table 4.2.

Figure 4.12 shows the current-time response of a tyrosinase polyvinyl-alcohol membrane electrode on successive catechol injections measured with the stationary system (**A**). The Figure below represents the corresponding calibration graph for catechol up to 70μM (**B**).

From Figure 4.12**A** it is easily to be seen that the time which is necessary to obtain the steady state response is very short. For concentrations of about 10μM after only 40sec 95% of the steady state signal are reached. Catechol can be determined down to a concentration of 1μM and the calibration graph is linear between 10 to 40μM.

Figure 4.13 shows the calibration graph for catechol, L-dopa, phenol and p-cresol up to 25μM, which reflects the tyrosinase catalysed oxidation of the respective substrate.

The concentration dependence for phenol and p-cresol exhibits a curvature, whereas for catechol and L-dopa the electrode response increases linearly over the entire range examined (sensitivity for catechol: 93 ± 2nA/M, for L-dopa: 35.0 ± 0.4nA/M). The sensitivity order of the electrode is: p-cresol > phenol > catechol > L-dopa, which was similar to that described by Kotte et al. [151] for a mediator-modified tyrosinase electrode.
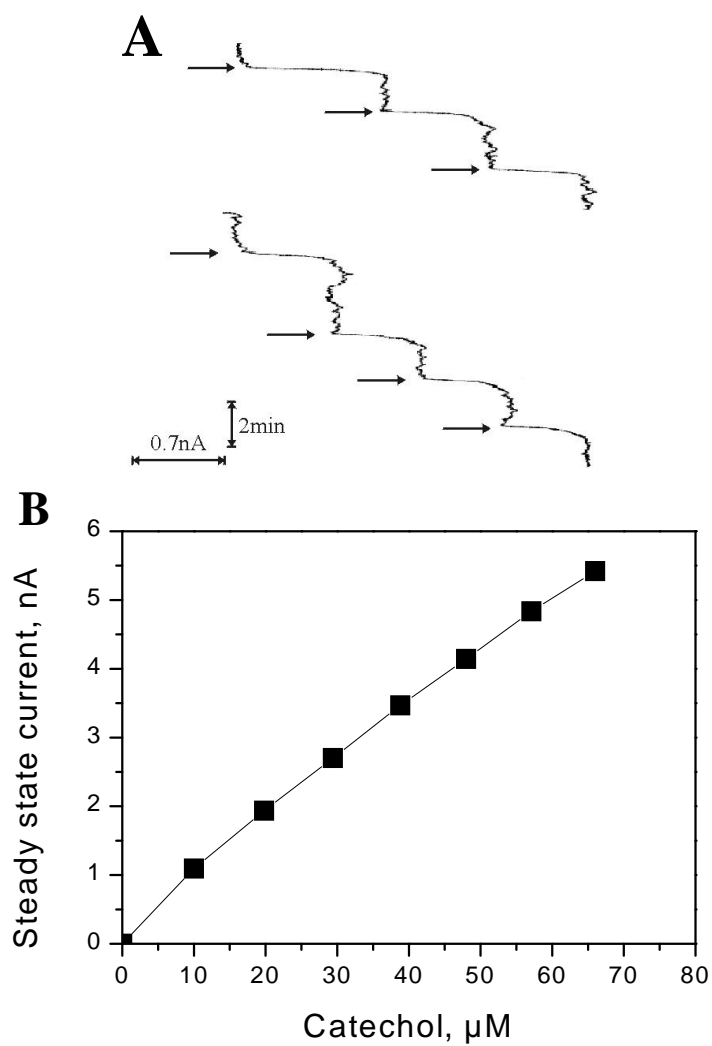
Figure 4.12: Current-time response of electrode COE_MT_PVA on successive catechol injections measured with the stationary system (**A**) and the corresponding calibration graph (**B**)

Table 4.2: Sensor characteristics of mushroom tyrosinase sensors

tyrosinase electrode	COE_MT_PVA	SPE_MT_N	SPE_MT_PU
Tyrosinase immobilised in	Polyvinyl alcohol(PVA)	Nafion (N)	Polyurethane (PU)
Electrode	Clark type oxygen electrode (COE)	Screen printed electrode (SPE)	Screen printed electrode (SPE)
Potential	-600mV vs. Ag/AgCl	-50mV vs. Ag/AgCl	-50mV vs. Ag/AgCl
pH-Optimum for catechol	6.5 - 7.5	6.0 - 7.0	5 - 5.5
Detection limit for catechol	$1\mu M$	200nM	250nM
Measuring range for catechol	1 - 70μM	0.2 - 16μM	0.25 - 630μM
Response time for catechol	40sec (10μM)	3.5min (2μM)	4min (10μM)
Reproducibility for catechol	n.d.	2.5% (n=14)	1.2% (n=15)
Storage stability	Several months at 4°C	n.d.	n.d.

4.2.2   *S. antibioticus* tyrosinase electrode

S. antibioticus tyrosinase has been immobilised in a polyvinyl-alcohol membrane which was then fixed onto a Clark type oxygen electrode (COE) (paragraph 7.2.1). This *S. antibioticus* tyrosinase electrodes shall be named COE_ST_PVA. As it is described above for the membrane-covered COE made with immobilised mushroom tyrosinase (electrode: COE_MT_PVA) oxygen reduction at -600mV versus Ag/AgCl is measured. Moreover, also this membrane can be stored several months at 4°C.

Phosphate buffer, with a concentration of 50mM and a pH of 6.5, was used for quantification of phenolic compounds. Catechol can be determined with this electrodes in the micromolar range, starting from 0.5μM up to 25μM.In Figure 4.14**A** the current time response of the electrode on successive catechol injections measured with the stationary system is shown. The Figure below (4.14**B**) represents the corresponding calibration graph. The response time of the electrode is fast (40sec), but three minutes are necessary, before steady state is reached and the next sample can be added.
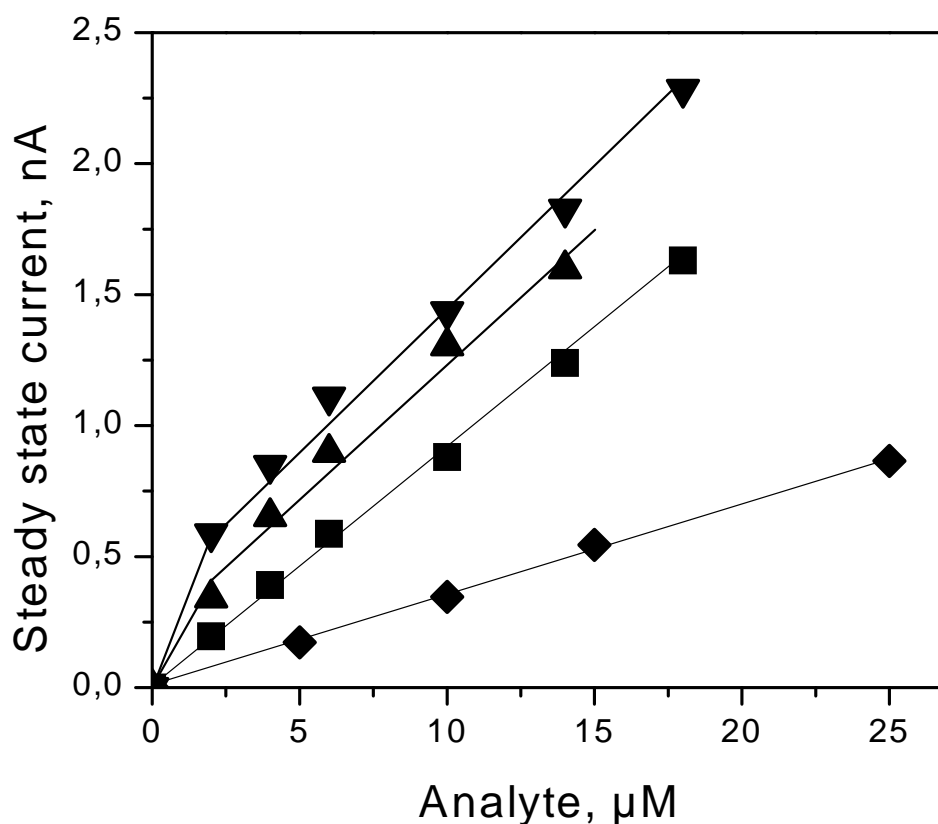
Figure 4.13: Calibration graph for ■: catechol, ♦: L-dopa, ▲: phenol and ▼: p-cresol of the Clark type oxygen electrode with tyrosinase immobilised in a polyvinyl-alcohol membrane (COE_MT_PVA) measured with the stationary system

Also different phenolic compounds were detected and a quantification of them in the lower micromolar range is possible. However, the different phenolic compounds were measured with different sensitivities. The sequence started with p-cresol as the analyte measurable with the highest sensitivity ($0.4nA/\mu M$). It was followed by phenol and catechol which could be quantified with a sensitivity of about $0.15nA/\mu M$. L-dopa was the analyte which could be quantified with the lowest sensitivity ($0.06nA/\mu M$) but also within a measuring range starting from $2\mu M$ up to $25\mu M$. These results of the *S. antibioticus* tyrosinase electrode with respect to the micromolar measuring range and the different sensiitvities for the various phenolic compounds were comparable with electrode COE_MT_PVA (described above in paragraph 4.2.1).

4.3   Bienzyme electrodes

The construction of bienzyme electrodes is a continuation of the development of the monoenzyme electrodes COE_MT_PVA and COE_ST_PVA. In order to achieve a high sensitivity a second enzyme (the quinoprotein glucose dehydrogenase, in the following called GDH) was additionally immobilised to tyrosinase in the membrane to create an analyte recycling system. Figure 4.15 illustrates the substrate regeneration in which repeated oxidation of a diphenolic compound by tyrosinase and reduction of quinone by GDH takes place. The substrate S of tyrosinase, is identical to the product P of GDH and S of GDH equals P of tyrosinase. If a monophenolic compound is the substrate of tyrosinase, then the first reaction would be the orthohydroxylation of it by tyrosinase. After that the sub-
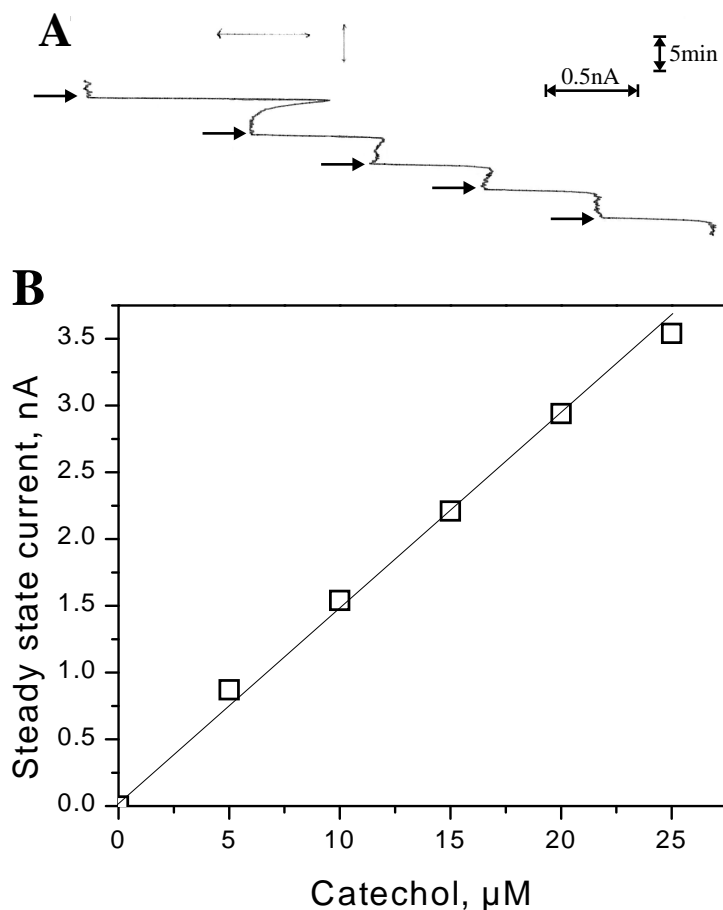
Figure 4.14: Current-time response of electrode COE_ST_PVA on successive catechol injections measured with the stationary system (**A**) and the corresponding calibration graph (**B**)
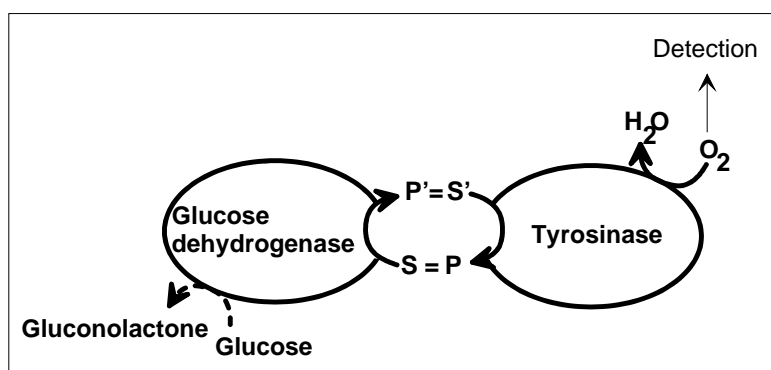
Figure 4.15: Schematic representation of the enzymatic substrate recycling between tyrosinase and quinoprotein glucose dehydrogenase (GDH)

strate regeneration can start. The reduction of oxygen is measured at a potential of -600mV vs. Ag/AgCl with Clark type oxygen electrodes (COE).
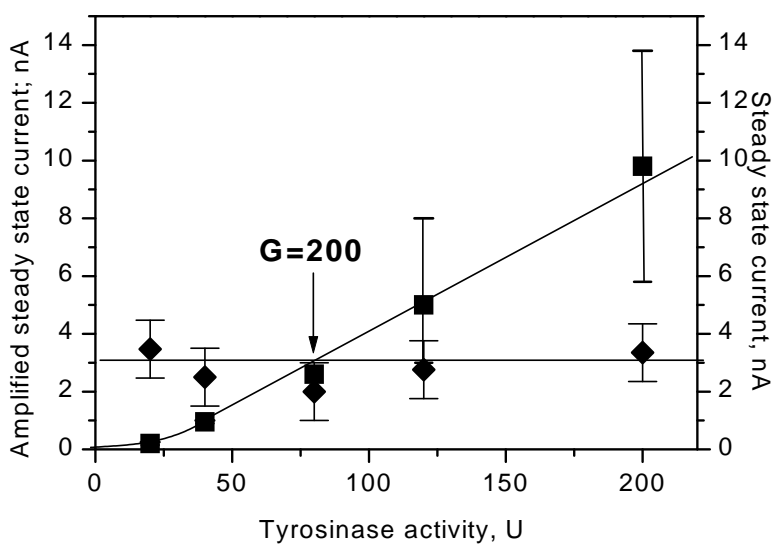
Figure 4.16: Dependence of the response of the bienzyme electrodes on tyrosinase activity for 100nM catechol (■) if 10mM glucose is added and GDH is active as well as for $20\mu M$ catechol (♦) with only the tyrosinase active, because the 50mM phosphate buffer contained no glucose

4.3.1   Mushroom tyrosinase/glucose dehydrogenase electrode

Determination of phenolic compounds   At first the conditions for the tyrosinase/glucose dehydrogenase (GDH) substrate recycling reaction in the mushroom tyrosinase/GDH electrode (MT/GDH-sensor) have been optimised. This was started with the variation of the ratio between GDH and tyrosinase. For these studies allways 40μl buffer solution were prepared, containing the two enzymes, PQQ, BSA when required and PVA. The amount of GDH (350U/mg) remained constant (1.3mg per 40μl solution) and the amount of mushroom tyrosinase (2400U/mg) was varied (0.16-1.7mg per 40μl solution). From these 40μl enzyme-PVA-solution membranes were prepared, allways 2μl solution for one membrane. 20 membranes altogether were got per attempt, to prepare with them the bienzyme electrodes and these were then tested. Alltogehter 100 bienzyme electrodes (20 with 20U tyrosinase, 20 with 40U tyrosinase, 20 with 80U tyrosinase, 20 with 120U tyrosinase and 20 with 200U tyrosinase) were tested and statistically evaluated, which is illustrated in Figure 4.16.
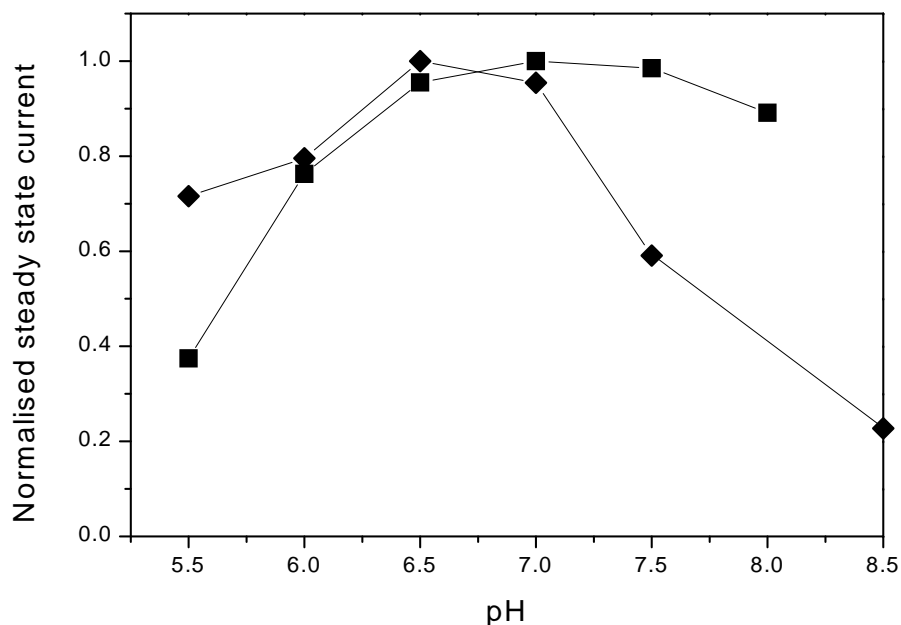
Figure 4.17: pH-dependence of the MT/GDH-sensor response for 250nM catechol (■) and 1μM L-tyrosine (♦) in 50mM phosphate buffer containing 10mM glucose

The response of the bienzyme electrodes increases linearly from 20U to 200U of tyrosinase activity per membrane. Obviously, the variation coefficient increases with increasing tyrosinase activity. Therefore, it should be noted, that the biosensor responses with a higher coefficient of variation (standart deviation smaller than 5%) were observed at a tyrosinase activity range of 20-80U. Thus the following experiments were carried out with the MT/GDH-sensor containing 80U mushroom tyrosinase per membrane. For this MT/GDH-sensor an amplification factor G of 200 was determined (an explanation and the definition of G can be found in paragraph 3.3.3).

Figure 4.17 illustrates variations in the sensitivity (normalised regarding to the highest sensitivity) as a function of pH when either L-tyrosine or catechol were measured.

For catechol response a relatively broad pH-optimum between 6.5 up to 8.0 was observed. In contrast, for L-tyrosine the pH-optimum ranges only from 6.5 to 7.0. This is comparable with the pH-optimum of mushroom tyrosinase in solution which is around 7.5 if catechol is used as a substrate [30]. Consequently the highest sensitivity of the bienzyme electrode will be obtained in a pH-range of 6.5 to 7.0; thus a pH of 6.5 was chosen for further investigations.

Figure 4.18 shows the current-time response of the bienzyme electrode on successive catechol injections measured with the stationary system (**A**). In addition, the corresponding calibration graph for catechol up to 700nM (**B**) is depicted.

From Figure 4.18**A** it is easily to be seen that the time which is necessary to obtain the steady state response is very short. For concentrations of about 100nM after only 2min 95% of the steady state signal are reached. Also the noise of the signal is very low. This opens a way for the application of the bienzyme electrode for online monitoring, e.g. of phenolic compounds in see, river or urban waste water. Catechol can be determined down to a concentration of 0.6nM and the calibration graph is linear up to 600nM. This is a linear measurement range over four orders of magnitude.

The sensor respond not only to catechol but also a broad range of phenolic compounds. In Table 4.3 the specificity of the bienzyme electrode is summarised. Most of them can be measured up to a subnanomolar level, like phenol(detection limit: 0.9nM). Catechol, phenol, p-cresol and p-chlorophenol will be detected in almost the same order of magnitude. The highest sensitivity is shown for p-cresol, followed by catechol and phenol. All of them have a linear calibration line up to 600nM. Consequently this bienzyme electrode can be used not only for the determination of the content of phenolic compounds in seeping water (limit 10μg/l or 100nM according to the Holländische Liste, 1984) or in waste water (limit 200μg/l or 2μM according to the Abwasserverordnung, 1987), it can also be used in drinking water analysis, because the limit in drinking water is 0.5μg/l or 5nM according to the EU- Trinkwasserverordnung, 2001.

A

B

Figure 4.18: Current-time response of the MT/GDH-sensor on successive cate-chol injections measured with the stationary system (**A**) and the corresponding calibration graph (**B**)

Table 4.3: Relative response of the MT/GDH-sensor for 100nM of different phenolic compounds. The response is related to catechol. A comparison to a published tyrosinase electrode is included.

	Relative response related to 100nM Catechol, %	Relative response related to 100nM Catechol, % [151]
Mono-phenolic compounds		
Phenol	100	100
p-Aminophenol	12	25
Hydroquinone	8	1
p-Chlorophenol	60	225
p-Cresol	130	185
L-Tyrosine	5	1
p-Nitrophenol	0.5[a]	0.0
Di-phenolic compounds		
Catechol	100	100
L-Dopa	3[a]	4.5
Dopamine	8	12
Noradrenaline	0.55[a]	n.d.
Adrenaline	1.15[a]	n.d.
4-Metylcatechol	134	n.d.
4-Nitrocatechol	0.95[a]	n.d.

[a] The relative response marked was calculated (simply by division through 10) from the signal measured with 1μM of the compound and than related to 100nM catechol.
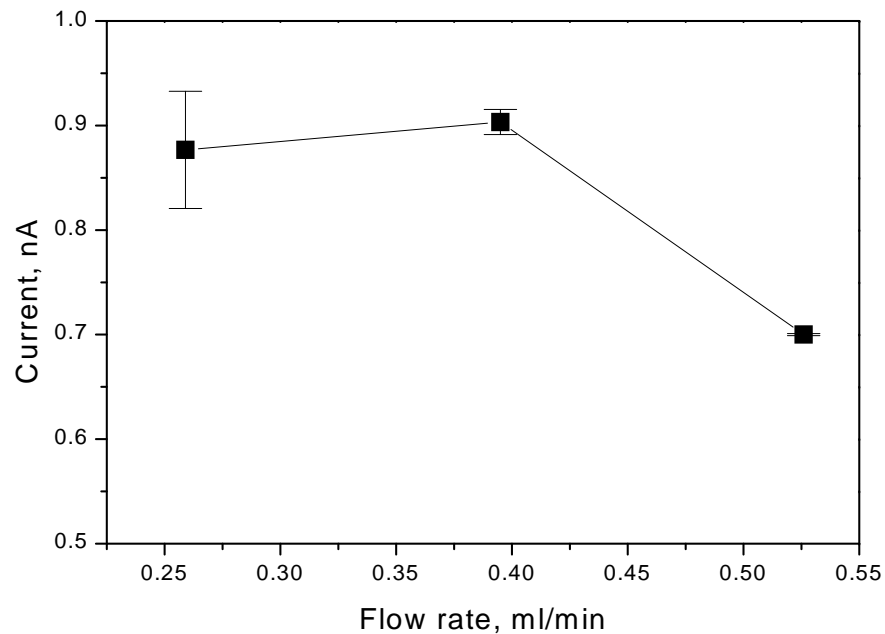
Figure 4.19: Current-flow rate response of the MT/GDH-sensor used in the flow-through set-up on successive catechol injections

Analytes with importance for the medical area, e.g. the catecholamines dopamine, adrenaline or noradrenaline, will be detected in the lower micromolar range. The detection limit for dopamine is about 25nM. Adrenaline is detected approximately five times less sensitive. This concentration range is relevant in determining the catecholamine content of certain cells or tissues as well as the analysis for urine.

The bienzyme electrode was also used in a flow-through set-up (for explanation see Figure 7.3 in paragraph 7.2.2). In Figure 4.19 the dependency of the electrode response to the flow-rate is illustrated and it is demonstrated that the highest sensitivities were measured with low flow rates. The electrode responses at flow rates of 0.25ml/min and at 0.4ml/min are almost the same, but a decrease is observed above that value. 0.4ml/min was chosen as the ideal flow-rate because of the high sensitivity of the electrode connected with a low noise of the electrode response.
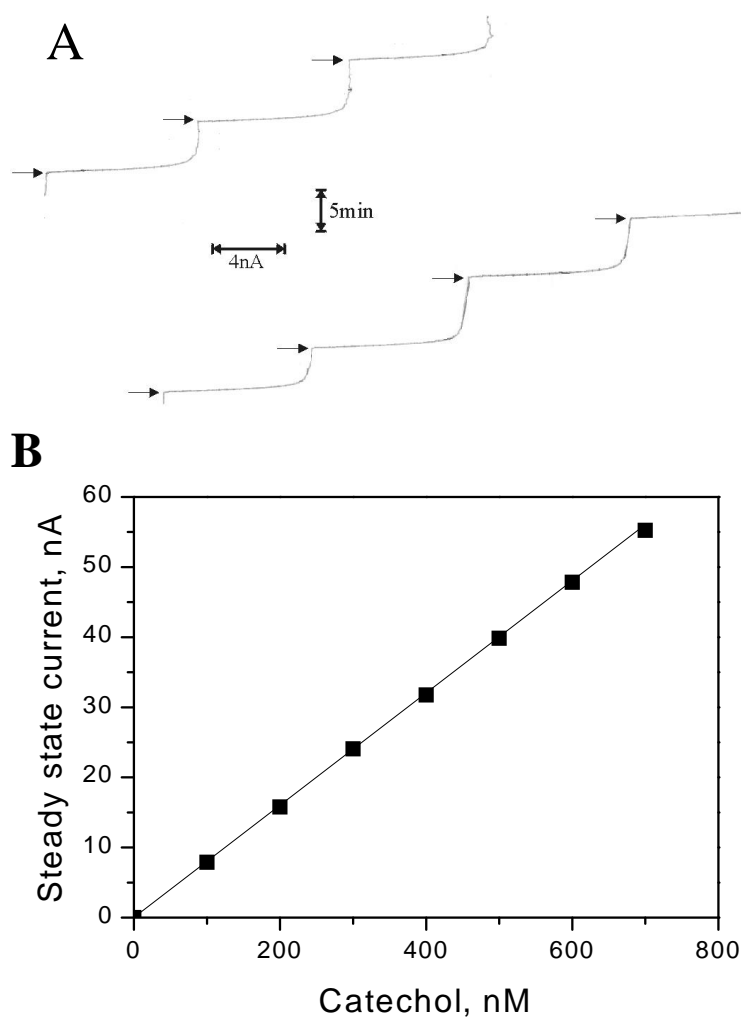
A

B
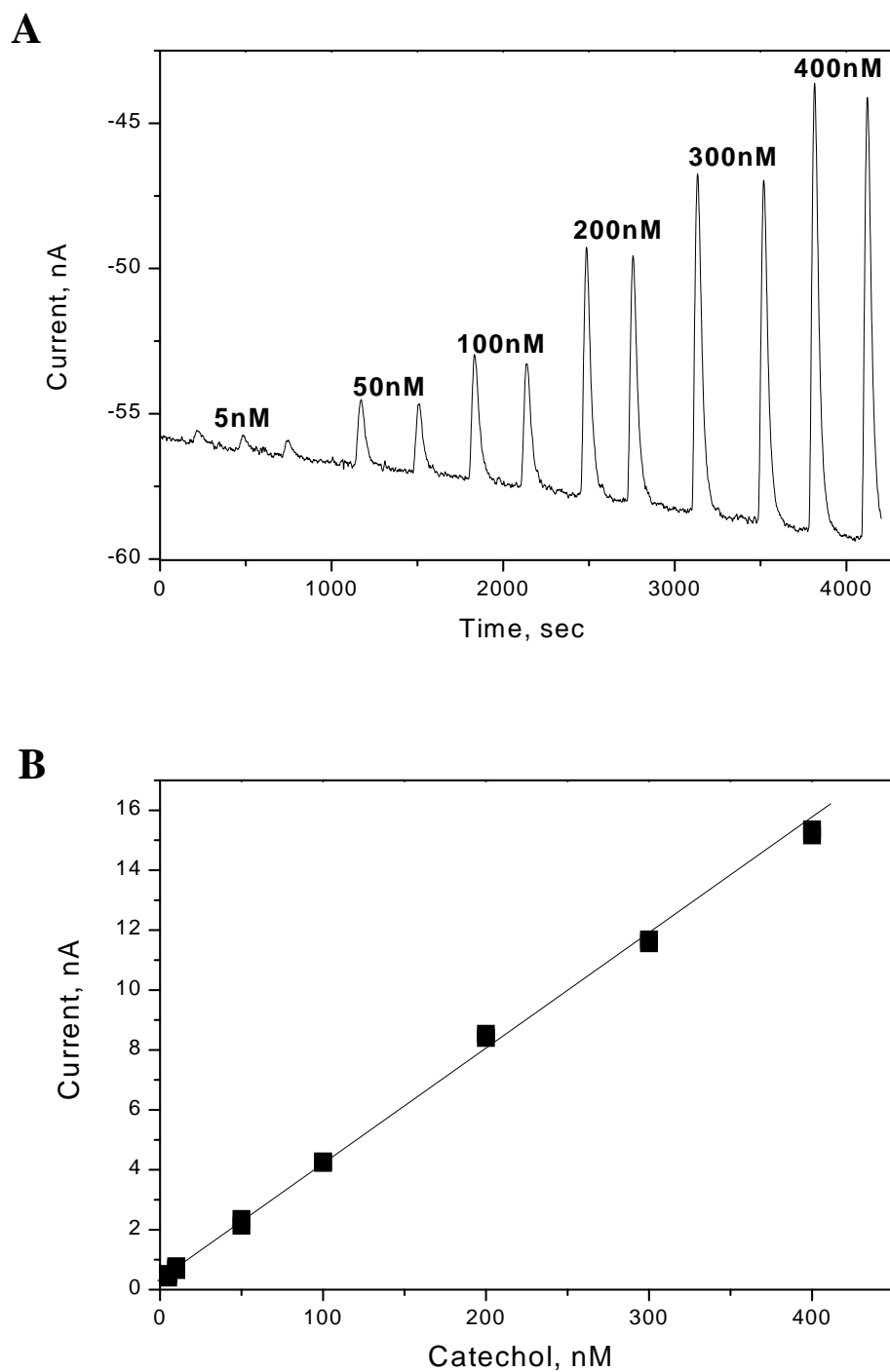

Figure 4.20: Current-time response of the MT/GDH-sensor on successive cate-chol injections measured with the flow-through set-up (**A**) and the corresponding calibration graph (**B**)

Table 4.4: Sensor characteristic of the MT/GDH-sensor

Application:	Stationary system	Flow-through set-up
Detection limit for catechol:	0.6nM	5nM
Measurement range:	0.6 - 600nM	5nM - 1μM
Response time (100nM catechol):	2min	30sec
Coefficient of variations:	5% (n=8)	1.8% (n=11)
Storage stability:	several months at 4°C	several months at 4°C

In Figure 4.20 a typical current-time response of the bienzyme electrode on repeated catechol injections (Figure 4.20**A**) and the corresponding calibration graph up to 400nM (Figure 4.20**B**) is shown. With this set-up the maximal response is obtained already after 30sec and not more than four minutes are needed to start the next measurement. Therefore, a sample frequency of 12 samples/hour is possible accompanied with a very good coefficient of variation of the electrode response of 1.8%.

A summary of the sensor-characteristics in the stationary system as well as in the flow-through set-up is given in Table 4.4. The detection limit for catechol of bienzyme electrode used in the flow-through set-up is one order of magnitude higher than that of the bienzyme electrode in the stationary system. But with the flow-through set-up the sample frequency is much higher than with the stationary system because of the necessary regeneration time of the membrane in the stationary system. The linear measurement range is comparable in both systems. The flow-through set-up impresses with the very short response time of only 30sec and with the good coefficient of variations of 1.8% in comparison to 5% for the stationary system. The main reason for this is the measurement time. To determine the coefficient of variations repetitive measurements of one catechol concentration were performed (eight times with the stationary system and eleven times with the flow-through set-up). These repeated measurements with the MT/GDH-sensor in the stationary system were very time consuming. For the detection of one concentration eight times, more than eight ours were necessary, but the integration of the MT/GDH-sensor in the flow-through set-up permits the quantification of repeated measurements in less than one hour and the changes in the membrane are smaller within an hour than within a day. Regarding the application it is important to mention, that a storage of the bienzyme membranes is possible for several months at 4°C.

Application The bienzyme electrode has been applied for water analysis. Various water samples were analysed, e.g. urban waste water, river water and see water. The results were compared with the traditionally used Standard Method DIN 38409-H16-1, a 4-aminoantipyrine (4-AAP) colorimetric procedure 7.3.4. The results of both measurement principles (bienzyme electrode and colorimetric procedure) were exypressed as 'total phenol'. Analysts in environmental laboratories still apply this colorimetric procedure because of its simplicity, although it is well known that 4-AAP does not react with nitro- and para-substituted phenols. However, the MT/GDH-sensor does not have any problems with the quantification of these phenolic compounds.

Furthermore, with the colorimetric procedure a time consuming and expensive sample preparation is required before a result will be obtained. This is also not required for the MT/GDH-sensor. Only one dilution step is necessary and the measurement can start. The reason for the dilution step can be found in the measurement principle of the sensor, because all measurments were carried out on the basis of oxygen measurement and it has to be taken into account that the solubility of oxygen differs in buffers with different ionic strengths. For this reason before the measurement of a sample it is very important to dilute the sample with a buffer of higher concentration than the sample has almost the same ionic strength as the stream of the carrier solution. Also other sources of possible matrix effects, like the influence of the sample addition to the dilution of the glucose or to the change in pH were tested. None of them had an influence to the bienzyme electrode response.

Figure 4.21 illustrates the biosensor response for phenolic standard solutions and for waste water spiked with $10 \mu l$ of the phenolic standard solutions. The inetercept of the second curve corresponds to a final concentration of 24nmol/l in the waste water sample. If the content of phenolic compounds was determined with the Standard Method DIN 38409-H16-1 then 20nmol/l were obetained. Therefore, the content of phenolic compounds was determined with both measuring methods (bienzyme electrode and colorimetric procedure) in the same order of magnitude.

In addition I have participated in the first European Technical Meeting Biosensors for Environmental Monitoring in Berlin with the GDH/MT-sensor integrated in a flow-through set-up (see 7.2.2). During this meeting the content of phenolic compounds in different water samples (see water from Stölpchensee, Pohlesee, small and big Wannsee, Jungfernsee, Glienicker See and Griebnitzsee, as well as river water from the river Havel from different stations in Berlin (Kleinmachnow, Böckmann Brücke, Kladow, Pfaueninsel) and urban waste water from the sewage plant Berlin-Ruhleben) were determined.

Phenolic compounds were detected only in the sample obtained directly at the station in Kleinmachnow. The total phenol content was quantified to be $8 \mu g/l$. All other samples contained phenolics below the detection limit for field experi-
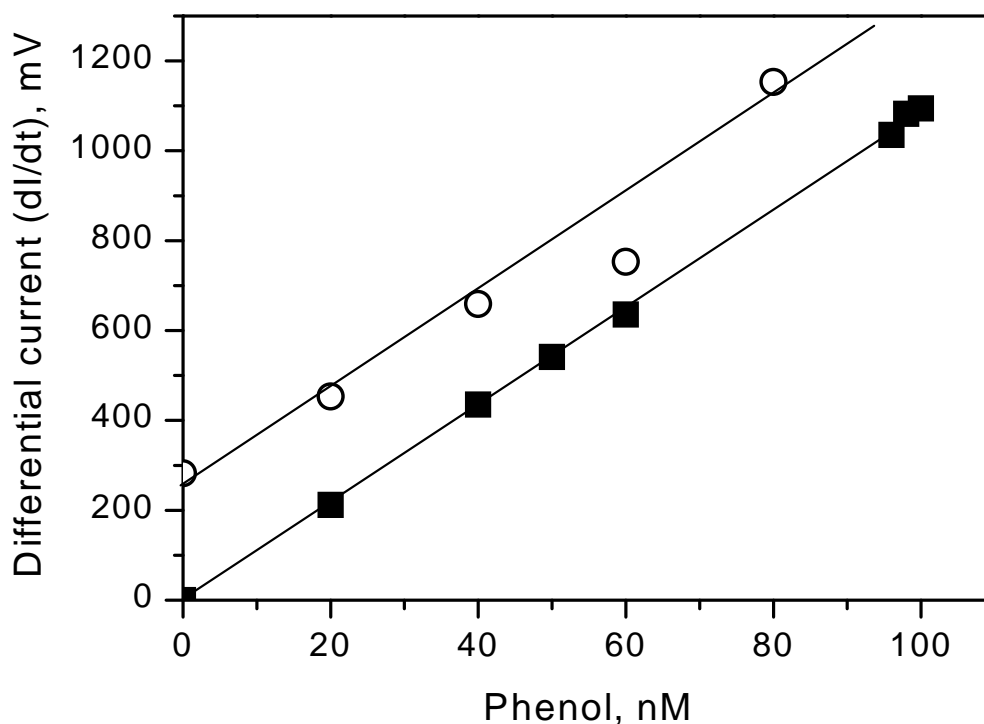
Figure 4.21: Calibration lines of the differential current-time curve (dI/dt) for phenolic standard solutions (■) and for urban waste water samples spiked with 10μl of the phenolic standard solutions (○).

ments. The content of total phenol was additionally determined with the Standard Method DIN 38409-H16-1 and again only in one sample, the sample obtained directly at the station in Kleinmachnow, the total phenol could be determined and 10μg/l were obtained. A comparison of both results show that both methods have quantified phenolic compounds in different water samples in the same order of magnitude.

Investigation and determination of inhibitors of tyrosinase   The MT/GDH-sensor has also been used for the investigation of tyrosinase inhibitors. According to the best of my knowledge for the first time the principle of biocatalytic recycling has been applied as an amplification system for inhibitor studies. Inhibitors, e.g. benzoic acid and derivatives, kojic acid and derivatives, inorganic ions as well as thiourea and derivatives were investigated. Two alternatives for the measurement protocol were studied.

First, the inhibitor (kojic acid) was introduced after a steady state signal for

catechol was obtained (Method 1, section (7.2.2)). The measuring signal is obtained from the decrease of the current output in relation to the uninhibited reaction (I_{max}) expressed as a percentage of signal intensity. A typical current response of the bienzyme electrode obtained with this Method with the addition of kojic acid as the inhibitor is shown in Figure 4.22. After the addition of glucose (solution 1) and 100nM catechol (solution 2) dissolved in phosphate buffer, catechol is converted by tyrosinase to quinone consuming oxygen. This quinone is reconverted to catechol by GDH, resulting in a steady-state current response of the bienzyme electrode, based on the reduction current of the remaining oxygen dissolved. After the introduction of 10μM kojic acid (solution 3) for 30sec, this current response is diminished. This current response was recovered completely when the sensor was again incubated with phosphate buffer containing glucose and catechol (Method1). As can be seen kojic acid concentrations above 10μM can be measured.

To characterise the sensor performance, benzoic acid was chosen as a model compound. Benzoic acid is a widely used preservative. Like other carboxylic acids, it is difficult to detect with conventional methods. Several groups have measured benzoic acid [53, 88, 97, 143, 160]. A low detection limit (700nmol/l) has been obtained with a very sensitive chemically amplified tyrosinase-based biosensor [97].

In the second approach, the dependence of catechol concentration on the inhibitory effect was evaluated according to Method 2 (section 7.2.2). In the presence of 10mM glucose in phosphate buffer, a steady-state current was obtained. The addition of different concentrations of catechol for 30sec resulted in current peaks. In the presence of benzoic acid the response was reduced for catechol concentrations between 0.01 and 1μM. Figure 4.23 shows a typical calibration curve for catechol without inhibitor in comparison to the calibration curves measured with different concentrations of benzoic acid. Due to the longer response and regeneration time for higher catechol concentrations, a concentration of 100nM catechol was used as standard for further studies.

In Figure 4.24 the decrease of the current output in relation to the uninhibited reaction (I_{max}) expressed as a percentage of signal intensity, is shown, if benzoic acid was introduced after a steady state signal for catechol was obtained (Method 1, section (7.2.2)). A maximum inhibition of about 80% was obtained for 100μM benzoic acid. After the incubation with benzoic acid, the catechol response of an uninhibited tyrosinase was completely recovered when the sensor had been incubated for 2-4min with a phosphate buffer. The comparison of both methods showed similar results on the dependence of benzoic acid concentration (see Figure 4.24). Since Method 2 (section 7.2.2) took more time, Method 1 (section 7.2.2) was used for further studies. From the data of Figure 4.24 an I_{50}-value of $20\pm2\mu$M was calculated.

During a measurement period over eight hours the sensors retained ca. 50% of
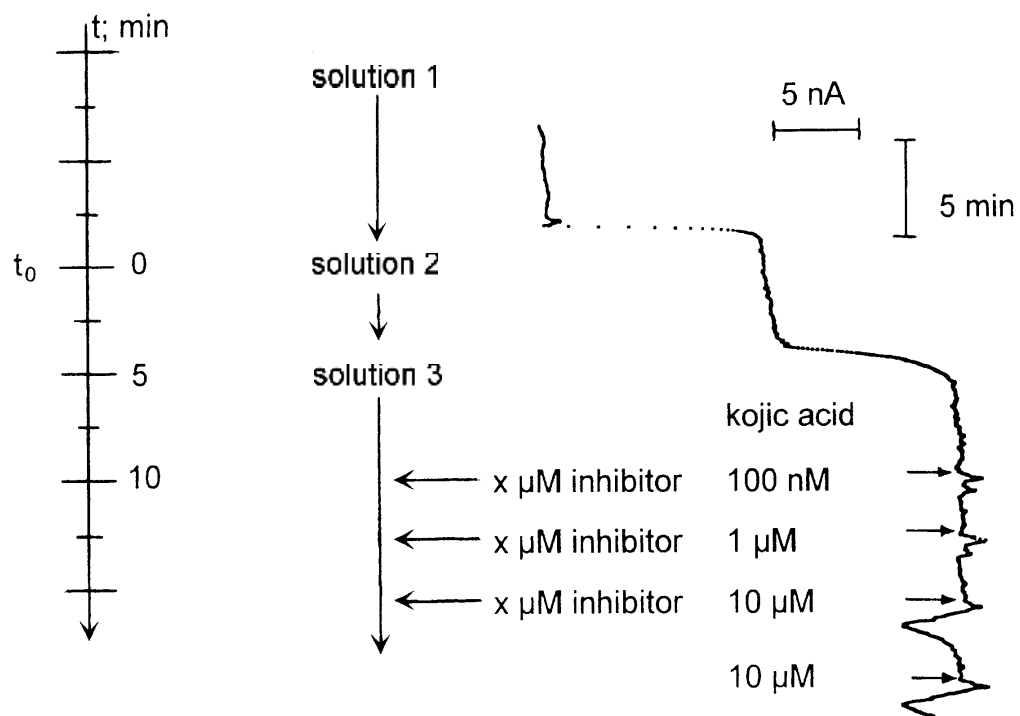
Figure 4.22: Scheme representing the steps of the measuring procedure of Method 1 and a typical current response of the MT/GDH-sensor obtained after addition of kojic acid. After the MT/GDH-sensor was incubated in solution 1, the addition of 10mM glucose (solution 2) and 100nM catechol (solution 3) to the phosphate buffer led to a steady-state current response of the bienzyme electrode. After addition of an inhibitor for 30sec (solution 4), this steady-state current was diminished but recovered completely when the sensor was incubated with solution 3. (Solution 1: phosphate buffer; solution 2: phosphate buffer + 10mM glucose; solution 3: phosphate buffer + 10mM glucose + 100nM catechol and solution 4: phosphate buffer + 10mM glucose + 100nM catechol + different concentrations of inhibitor).

the initial response to catechol. During this time, at least 100 successive injections were carried out. From a comparison of ten different sensors which were prepared with the same batch of bienzyme membranes an inhibition of 31±3% of the response of 100nM catechol by 10μM benzoic acid was obtained. A relative error of 10% was calculated as the mean value for all sensors. For the measurement of 10μM benzoic acid with one sensor, a relative error of the mean at 3.6% and that of a single value at 9% were calculated. In most cases, the sensors were stable and measurements of benzoic or kojic acid derivatives with lower errors were possible

for individual sensors. In contrast, the measurements of thioureas at high concentrations produced a lower working stability and higher errors. It appears that some inhibitors affected not only the enzyme but also the membrane including GDH. Obviously, the stability and reliability of the sensor depends strongly on its history.

The main advantage of this flow-through procedure is the short time required for an inhibition assay. Inhibition occurs within 1 min and the measurements can be repeated every 3 to 5 min.

The recognition of other inhibitors studied are summarised in 4.5. The inhibi-
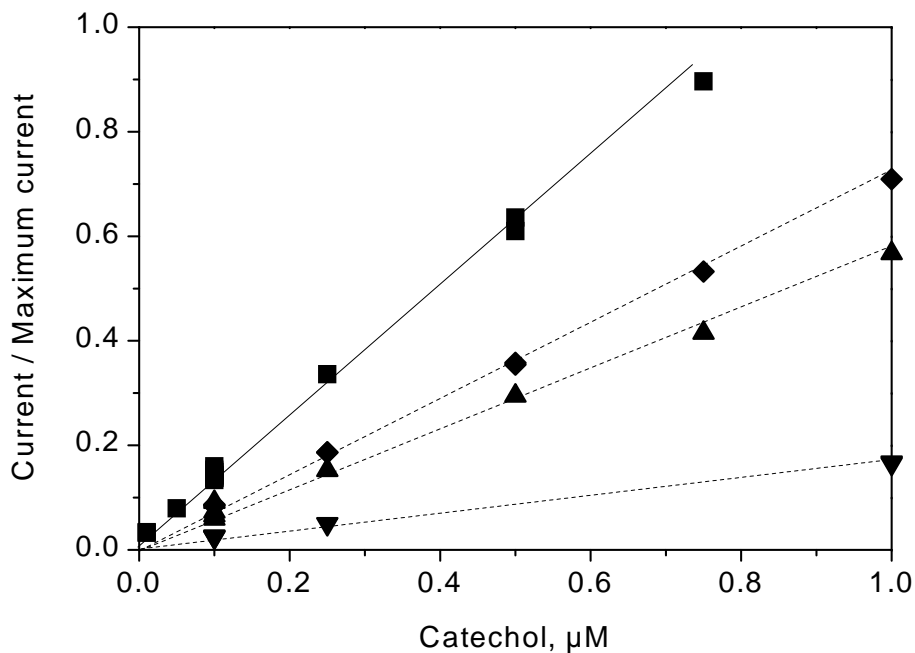
Figure 4.23: Calibration graph for catechol measured in 50mM phosphate buffer, pH=6.5 without benzoic acid (■) and with benzoic acid of different concentrations (10μM (♦), 20μM (▲) and 100μM (▼)). Note, the increasing inhibition at higher benzoic acid concentrations. The maximum current is the current obtained at excess of catechol over inhibitor. Steady state current instead of a transient response was obtained.

Table 4.5: Inhibition of tyrosinase immobilised in the MT/GDH-sensor

Compound	Concentration, μM	Inhibition, %
Benzoic acid and derivatives		
Benzoic acid	10	25
	100	80
2-Chlorobenzoic acid	10	42
4-Chlorobenzoic acid	10	22
Methyl 4-hydroxy benzoate	1000	8
Propyl 4-hydroxy benzoate	1000	4
Kojic acid and derivatives		
Kojic acid[a]	10	15
	100	68
kojic acid 5-*O-capryloate*[a]	100	55
kojic acid 7-*O-capryloate*[a]	100	20
kojic acid 5,7-di-*O-di-capryloate*[a]	100	0
Inorganic ions		
Azide	10	23
Fluoride	100	5
Thiourea and derivatives		
Thiourea	10	6
	100	22
	1000	63
1-Phenyl-2-thiourea	0.1	3
N,N'-Diphenylthiourea	10	8
	100	8
	1000	13
1-Allyl-2-thiourea	0.1	3
	1	10
	10	63

[a] For the IUPAC name and the structure see Figure 4.7 in paragraph 4.1.2
    on page 53.
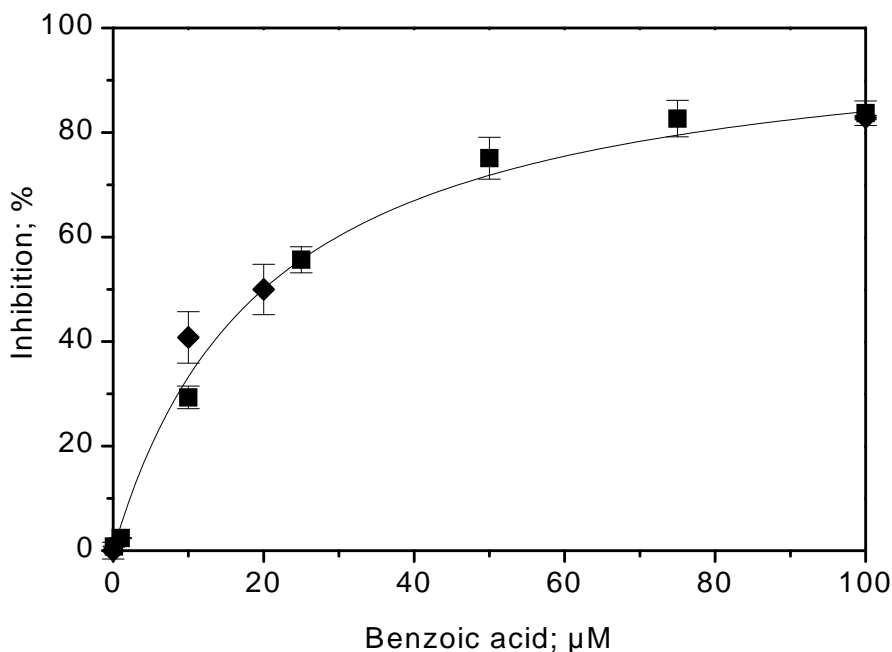
Figure 4.24: Relative inhibition of the catechol signal by different benzoic acid concentrations measured with Method 1 (■) and Method 2 (♦). The solid line is modelled after Michaelis-Menten kinetics, assuming a competitive inhibition type. The I_{50}-value has been calculated at $20\pm2\mu$M.

tion of tyrosinase by benzoic acid is comparable to that of 4-chlorobenzoic acid and lower than that of the 2-chloro derivative. The presence of an ester group affects the chelating properties and results in very weak inhibitors as shown with the preservatives methyl- and propyl-4-hydroxybenzoate.

Another family of tyrosinase inhibitors is based on kojic acid (structures of kojic acid and derivatives were illustrated in Figure 4.7 in paragraph 4.1.2). This antibiotic compound has been used as an ingredient in cosmetics and as a color stabilising agent for food [95]. It is synthesized by a variety of aerobic microorganisms utilising a wide range of carbon sources. The assay of kojic acid is therefore important for monitoring of fermentation processes [97]. Here kojic acid and some derivatives, such as kojic acid 5-*O*-capryloate, kojic acid 7-*O*-capryloate as well as the corresponding kojic acid 5,7-di-*O*-di-capryloate have been investigated. No inhibition of the catecholase activity was observed with the di-ester at

concentrations up to 100μM (for comparison see Table 4.5). The 5-octanoate and kojic acid inhibited the activity to almost the same degree, whereas the effect of the 2-octanoate was significantly lower. Thus kojic acid and its derivatives were measured in the lower micromolar range. Kojic acid and its derivatives therefore are weaker inhibitors of tyrosinase than benzoic acid.

The inorganic ions, azide and fluoride, were detected in the lower micromolar range. Azides were identified as non-competitive inhibitors for substrates of tyrosinase, such as L-tyrosine or L-dopa as well as for oxygen [66]. A sensitive assay for azide is of practical interest because its utilisation in explosives and as an environmental toxin. Fluoride should be controlled in drinking water.

Finally, thiourea and some derivatives were investigated (see also Table 4.5). Some of those compounds have been described as inhibitors of tyrosinase in an enzyme electrode by Stancik et al. [178]. Thiourea is generated in the environment by degradation of dithiocarbamate pesticides [160]. The strongest inhibition with a detection limit of 100nM was observed with 1-phenyl- and 1-allyl-2-thiourea whereas the detection limit with thiourea and N,N-diphenylthiourea was 10μM. Stancik et al. [178] reported that 1-allyl-, 1-phenyl-2-thiourea and N,N$'$-diphenylthiourea inhibited mushroom tyrosinase that was immobilised on a Clark type oxygen electrode of an amperometric biosensor to nearly the same extent.

4.3.2   *S. antibioticus* tyrosinase/glucose dehydrogenase electrode

Determination of phenolic compounds   For the application of *S. antibioticus* tyrosinase in a sensor, the enzyme was co-immobilised with GDH as described above for the MT/GDH-sensor. First the efficiency of the tyrosinase/GDH substrate recycling in the *S. antibioticus* tyrosinase/GDH electrode (ST/GDH-sensor) as a function of the pH was determined. Figure 4.25 illustrates the change in activity (normalised with respect to the highest activity) when either L-dopa or catechol were used as substrates for tyrosinase. For catechol a relatively broad pH-optimum, from 6.5 to 8.0 was observed. In contrast, the pH-optimum for the L-dopa conversion extends only from 6.5 to 7.0, which is similar to that of *S. antibioticus* tyrosinase in solution. Consequently, the highest sensitivity for both substrates is obtained in the pH-range from 6.5 to 7.0. Therefore, all further studies were carried out in phosphate buffer at pH 6.5.

The ST/GDH-sensor gives a linear response for catechol up to 700nM, shown in Figure 4.26(**B**). In the Figure above (Figure 4.26(**A**)) the current-time response of the bienzyme electrode on successive catechol injections measured with the stationary system is depicted. It is easily to be seen that the time which is necessary to obtain the steady state response is very short. For concentrations of about 100nM 95% of the steady state signal are reached after only 2min. Catechol can be determined down to a concentration of 10nM.

In Table 4.6 the characteristics of the bienzyme electrode for catechol in comparison to L-dopa quantification is summarised. In contrast to catechol, the linear measuring range for L-dopa was from 5 to 300nM, but the electrode response for L-dopa was twice as high as for catechol (Table 4.6). The response time for L-dopa is higher than that for catechol. The coefficient of variations of the measurements (3%) and the storage stability of several months, makes this sensor a potentially interesting analytical device for the detection of phenolic compounds.

Because of differences in reaction rates and diffusion velocities, the sensor measures various phenolic compounds with different sensitivity. To assess the analytical potential of our biosensor, different mono- and diphenolic compounds were investigated. The relative response of the electrode to monophenolic compounds related to catechol is shown in Table 4.7.

If the electrode response for a monophenolic compound is compared with its corresponding diphenolic compound, always similar sensitivities is obtained, e.g., p-cresol and 4-methylcatechol or L-tyrosine and L-dopa are determined with com-
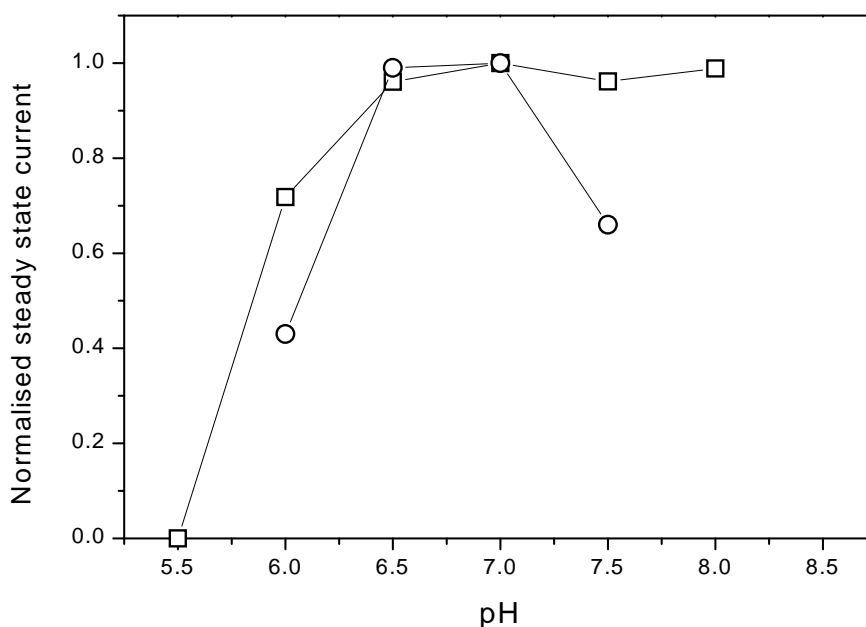
Figure 4.25: pH dependence of the ST/GDH-sensor response for 100nM L-dopa (○) and 250nM catechol (□) in 50mM phosphate buffer containing 10mM glucose.
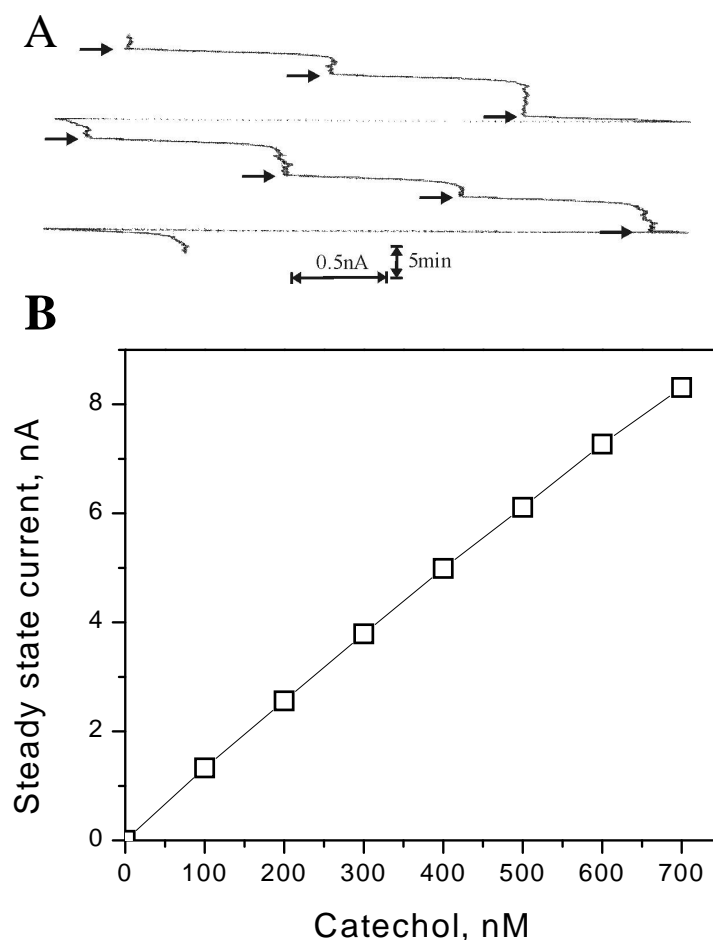
Figure 4.26: Current-time response of the ST/GDH-sensor on successive catechol injections measured with the stationary system (**A**) and the corresponding calibration graph (**B**)

parable sensitivities. P-cresol and p-aminophenol then followed, for which the detection is 3 and 2.5 times more sensitive than for catechol. Phenol is detected with a sensitivity in the same order of magnitude as catechol. Remarkably different however is the sensitivity for p-nitrophenol and p-nitrocatechol. The electrode response for p-nitrocatechol is almost the same as that for catechol. Whereas, the electrode response for p-nitrophenol is less than 1% of the response measured for 100nM catechol. This result may be explained by the fact that p-nitrophenol is a strong competitive inhibitor for catechol oxidation by tyrosinase [238].

Among the diphenolic compound are analytes with importance for medical diagnostic, e.g., the catecholamines dopamine and adrenaline. Dopamine and

Table 4.6: Sensor characteristics of the *S. antibioticus* tyrosinase/GDH-sensor (ST/GDH-sensor)

Parameter	**Substrate**	**Sensor characteristics**
Lower detection limit	L-Dopa	5nM
	Catechol	10nM
Linear measuring range	L-Dopa	5 - 300nM
	Catechol	10 - 700nM
Response time (100nM)	L-Dopa	6min
	Catechol	2min
Coefficient of variations	L-Dopa and Catechol	3% (n=9)
Storage stability		several months at 4°C

adrenaline will be quantified with the ST/GDH-sensor in the nanomolar range with a detection limit of 10nM and 5nM. This is more sensitive than other tyrosinase sensors and in the same order of magnitude of other enzyme sensors, at which often laccase is used. A detection limit of 1nM and 50nM for dopamine and adrenaline was obtained for example with an other tyrosinase sensor base on enzymatic-chemical recycling [240]. In contrast to the ST/GDH-sensor, at which the highest difference in the sensitivity of catecholamine detection was obtained for adrenaline and noradrenaline, this sensor has shown the highest difference between dopamine and adrenaline (Adrenaline and noradrenaline were measured in the same order of magnitude.).

Also other enzyme sensors are described which were used for catecholamine detection. Under this there are laccase sensors which are based on bioelectro-catalytic recycling [107]. Furthermore, a laccase/GDH Clark type oxygen electrode base on biocatalytic recycling is described [241]. In comparison to the enzyme sensors based on laccase, in which the substrate range of laccase allows mostly only a quantification of monophenolic compounds, the ST/GDH-sensor can be used more flexible. With the ST/GDH-sensor a sensitive quantification of monophenolic as well as diphenolic compounds is possible.

Table 4.7: Relative response of the ST/GDH-sensor for 100nM of different phenolic compounds. The response is related to catechol. A comparison to a published tyrosinase electrode is included.

	Relative response related to 100nM Catechol, %	Relative response related to 100nM Catechol, % [151]
Mono-phenolic compounds		
Phenol	107	100
p-Aminophenol	250	25
Hydroquinone	28	1
p-Chlorophenol	190	225
p-Cresol	330	185
L-Tyrosine	430	1
p-Nitrophenol	0.8[a]	0.0
Di-phenolic compounds		
Catechol	100	100
L-Dopa	228	4.5
Dopamine	65	12
Noradrenaline	11	n.d.
Adrenaline	170	n.d.
4-Metylcatechol	300	n.d.
4-Nitrocatechol	130	n.d.

[a] The relative response marked was calculated (simply by division through 10) from the signal measured with $1 \mu M$ of the compound and than related to 100nM catechol.

4.4 Cloning of the mutated tyrosinase gene in *S. antibioticus*

A general problem for many tyrosinase electrodes is the sensitivity needed for commercial exploitation. Therefore amplification systems were developed, e.g. bioelectrocatalytic recycling or biocatalytic recycling. Further improvements of the sensor performance could be achieved by controlled immobilisation of tyrosinase onto a sensor surface as well as by site to site fixation of two enzymes (tyrosinase and GDH). In boths cases the reduction of intermediate channeling distances will lead to an amplification system with more effective signal transduction.

The aim of this part is to show a pathway to the development of mutants of tyrosinase, which can be used for site-oriented fixation of tyrosinase onto a sensor surface as well as for site to site fixation of two enzymes. This means replacing one of the six histidins of tyrosinase, which are assigned to be the copper ligands (for explanation see paragraph 3.1.1), with glycin that creates a ′hole′ through which copper becomes directly accessible from the outside for a large variety of ligands. Such a mutant has the opportunity to insert a spacer in the vicinity of the active centre for a site-oriented fixation of tyrosinase.

In *S. antibioticus* the structural gene (*melC*2) for tyrosinase is part of a polycistronic operon (*melC*), preceded by the *melC*1 gene, which encodes a conserved protein (MELC1), a chaperone needed for transport and copper incorporation. *MelC* is about 1300bp long. If the whole *melC* operon had been used as starting material for the mutagenesis, then the sequencing step, which is necessary to control the result of the used mutagenesis procedure, would have been difficult. One of the difficulties is the length of the operon, since sequencing in one run is applicable for DNA with a length of 700 - 900bp. Furthermore it is known that sequencing of *melC*1 is difficult [242]. For these reasons the strategy was to do the mutagenesis at first on *melC*2, followed by cloning of the *melC*2 mutant in a *Streptomyces - E. coli* shuttle vector together with *melC*1, because of the essential function of MELC1 as a chaperone. For this a unique cleavage site (N=*Nde*I) was introduced between *melC*1 and *melC*2. Figure 4.27 shows a scheme of the strategy. The left site illustrates the work on *melC*1 and the work on *melC*2 is shown at the rigth site. For the mutagenesis three different methods were used, but a mutation was achieved only with the Mega Primer Method. After sequencing, to control the quality of the *melC*2-mutant, *melC*1 and the *melC*2-mutant were ligated and cloned in different *Streptomyces - E. coli* shuttle vectors (pUWL219 and pUCS75). Then these plasmids were used for transformation of different *Streptomyces* strains. The following paragraphs (4.4.1, 4.4.2 and 4.4.3) provide a more detailed description of this steps.
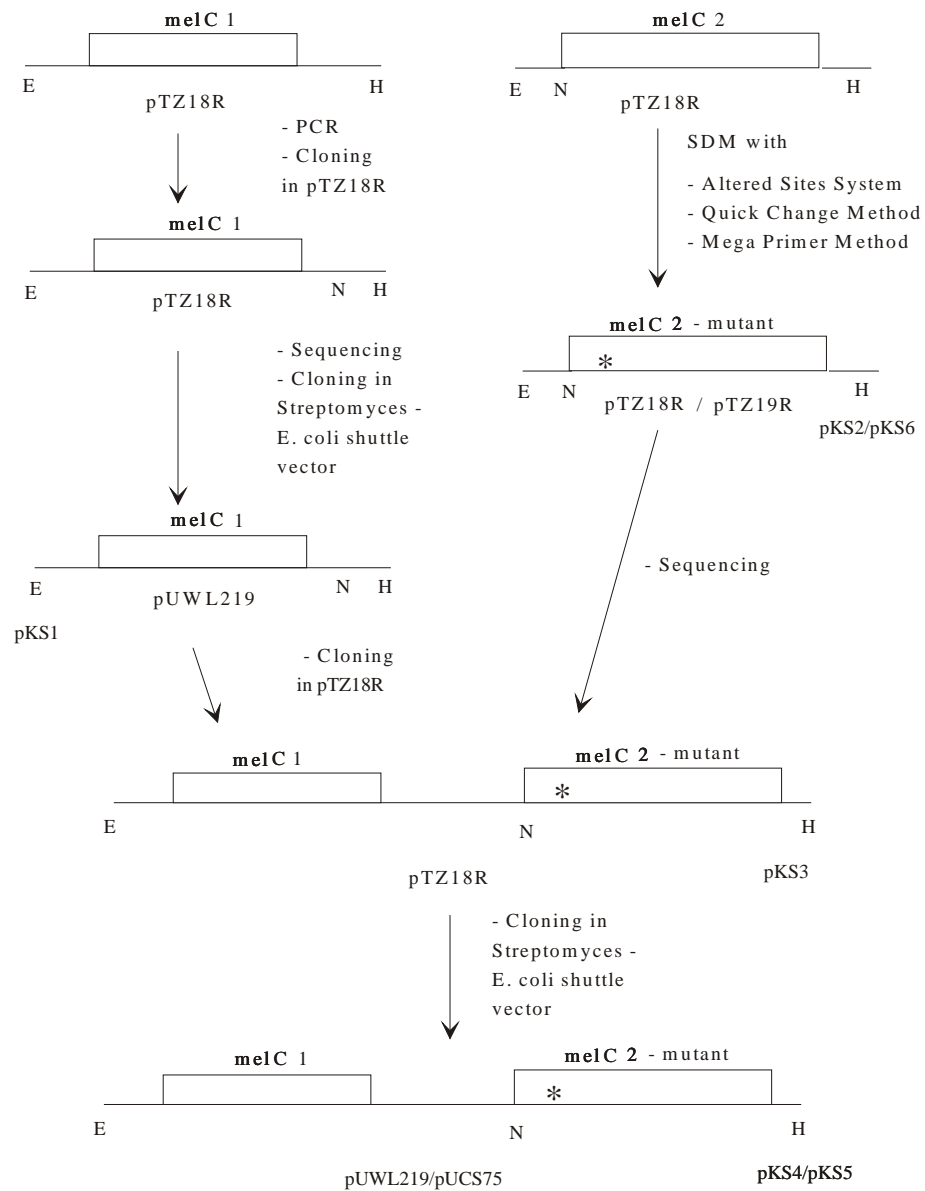
Figure 4.27: Strategy of cloning of the tyrosinase gene in *Streptomyces antibioticus* (E=*EcoR*I, H=*Hind*III, N=*Nde*I, ∗=mutation)

4.4.1 Cloning of *melC*1 with an introduced *Nde*I site in a *Streptomyces - E. coli* shuttle vector

The starting material to clone *melC*1 in a *Streptomyces - E. coli* shuttle vector was pMEL110, a pTZ18R vector with the whole *melC* operon as insert. As it is mentioned above before cloning the introduction of a *Nde*I site between *melC*1 and *melC*2, which makes a later ligation possible was required. This was done by PCR with pMEL110 digested with *EcoR*I as DNA template and MELC1-11 and MELC1-14 as primer. (The exact procedure is described in paragraph 7.3.5.) MELC1-11 anneals at the beginning of the *melC* operon sequence and has an *EcoR*I site for cloning. MELC1-14 introduce a *Nde*I site at ATG of *melC*2 and a *Xba*I site for cloning. After digestion of the PCR product with *EcoR*I and *Xba*I and purification, the *EcoR*I/*Xba*I-fragment was cloned in pTZ18R.

To examine the PCR product, one must duplicate this new plasmid. This was done by transformation of *E. coli* JM109 with this plasmid. Transformed JM109 have been selected on agar plates containing Ampicillin, Xgal and IPTG, because the pTZ18R vector contains a gene for Ampicillin resistance. Furthermore a successful ligation of the pTZ18R with a DNA fragment leeds to an interruption within the lacZ gene. The lacZ gene is the responsible gene for production of β-galactosidase, an enzym which is able to convert the colourless XGal in a blue dye. Therefore, bacterial colonies harboring the pTZ18R vector including the PCR product as insert, remain white and the plasmids with inserts were isolated from eight white colonies. In Figure 4.28 the steps described above are illustrated. Now the the pTZ18R vector including the PCR product as insert, shown at the end of the Figure, was analysed.

A first analysis was carried out by digestions with *Bgl*II and *Hind*III (340bp, 2940bp), with *EcoR*I and *Hind*III (770bp, 2900bp) and with *EcoR*I and *Nde*I (750bp, 2900bp). Then single stranded DNA was isolated to sequence the insert of pTZ18R. The sequence analysis, made by BaseClear (BaseClear, Leiden, The Netherlands), showed that the *melC*1-fragment between the *Bgl*II and *Xba*I restriction sites had the correct sequence.

But for the further steps the whole *melC*1 with an introduced *Nde*I site was necessary. For this reason a *Streptomyces - E. coli* shuttle vector was choosed which contains the *EcoR*I/*Mlu*I-fragment of the *melC* operon as insert of pUWL219. The 7200bp fragment of pMEL107 and the 313bp fragment of *melC*1, both digested with *Bgl*II and *Xba*I, were ligated, followed by the transformation of *E. coli* JM109 and selection on LB$_{Amp}$. Individual colonies were grown in LB and plasmids were isolated. Now they were analysed again by digestion with *Bgl*II and *Hind*III (340bp, 6750bp), with *EcoR*I and *Hind*III (770bp, 6320bp) and with *EcoR*I and *Nde*I (750bp, 6340bp). According to this analysis the first part, *melC*1 with an introduced *Nde*I site at ATG of *melC*2 in a *Streptomyces - E. coli* shuttle
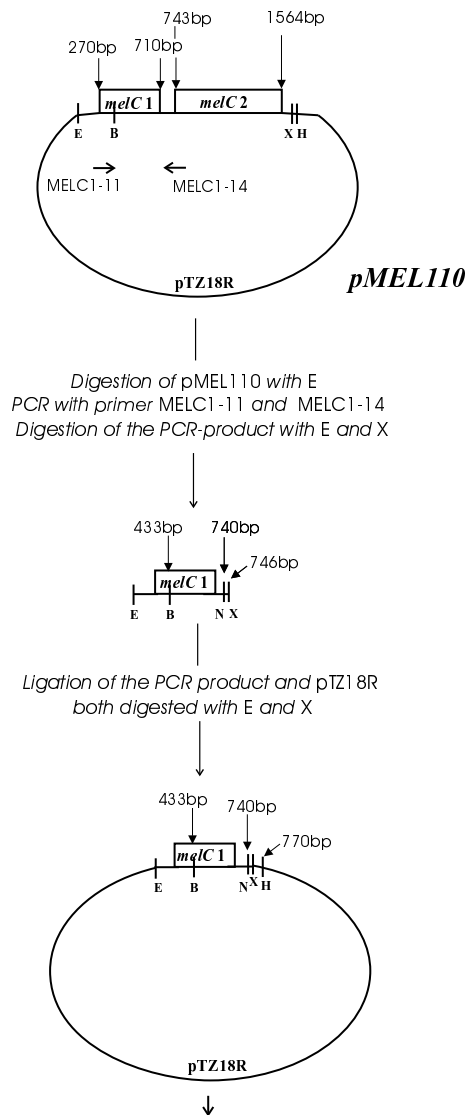
Figure 4.28: Part 1 of the strategy of cloning of *melC*1 with an introduced *Nde*I site in a *Streptomyces - E. coli* shuttle vector (B=*Bgl*II, E=*EcoR*I, H=*Hind*III, N=*Nde*I, X=*Xba*I

vector was achieved. This plasmid is designated pKS1. The above described steps are represented in Figure 4.29.

4.4.2   SDM of *melC*2 to substitute histidin[37] (His[37]) with glycin (Gly)

Three different methods for in-vitro-mutagenesis were used for the substitution of His[37] with Gly in *melC*2: the Altered Sites System (Promega, USA), the Quick-Change Method (Stratagene, USA) and the Mega-Primer Method according to Picard et al. [243]. In contrast to Tsai and Lee [41] no mutagenesis was obtained with the Altered Sites System (Promega, USA). The Quick Change Method (Stratagene, USA) was also not successful. But with the Mega-Primer Method the change of **CAC** (His[37]) into **GGC** (Gly) was obtained.

As it is shown in Figure 4.30 the first step of this method was the synthesis of a mega-primer. This was done by PCR with pMEL113 digested with *Hind*III as DNA template and MUT5 and TZ18R as primer. MUT5 hybridises in the 830bp-883bp region of *melC*2. It destroys the *Mlu*I site at 858bp and it is the responsible primer for the desired mutation (change of **CAC** (His[37]) into **GGC** (Gly)). TZ18R hybridises 270bp downstream of *EcoR*I of MCS and reads into MCS. It was used because it is a matching and known primer. (The exact procedure of the PCR is described in paragraph 7.3.5.) The result of step 1 was a mega-primer of 390bp containing the desired mutation. After purification of the 390bp mega-primer, this primer and MELC2-7 were used for step 2, a second PCR, again with pMEL113 digested with *Hind*III as DNA template. MELC2-7; hybridises at the end of *melC*2 and introduces a *Xba*I site immediately after stopcodon of *melC*2. (More detailed explanations about procedure conditions of the PCR are given in paragraph 7.3.5.) A 1080bp fragment was the result of step 2. In Figure 4.31 the 1% agarose gel is shown, where both, the 390bp band of the mega-primer and the 1080bp band of the fragment, can be seen.

For the ligation of pTZ18R and the fragment obtained with the Mega-Primer Method both were digested with *EcoR*I and *Xba*I. In Figure 4.33 the ligation is illustrated and a scheme of pKS2, the resulted plasmid is given.

To examine the mutations of *melC*2, one must duplicate this new plasmid pKS2. This was done by transformation of *E. coli* JM109 with pKS2. Transformed JM109 have been selected on agar plates containing Ampicillin, Xgal and IPTG, as it is also described above and plasmids (pKS2) were isolated.

Because of the properties of MUT5 (two mutations with one primer) one could assume that if one mutation is achieved also the second mutation should be there. This means, if pKS2 is missing one *Mlu*I-site, it then can be assumed that the desired mutation (the change of **CAC** (His[37]) into **GGC** (Gly)) also had success.

Isolated plasmids were analysed by digestion with *Mlu*I (220bp,3500bp), with *EcoR*I and *Mlu*I (220bp, 240bp, 3260bp), with *EcoR*I and *Hind*III (820bp, 2900bp),
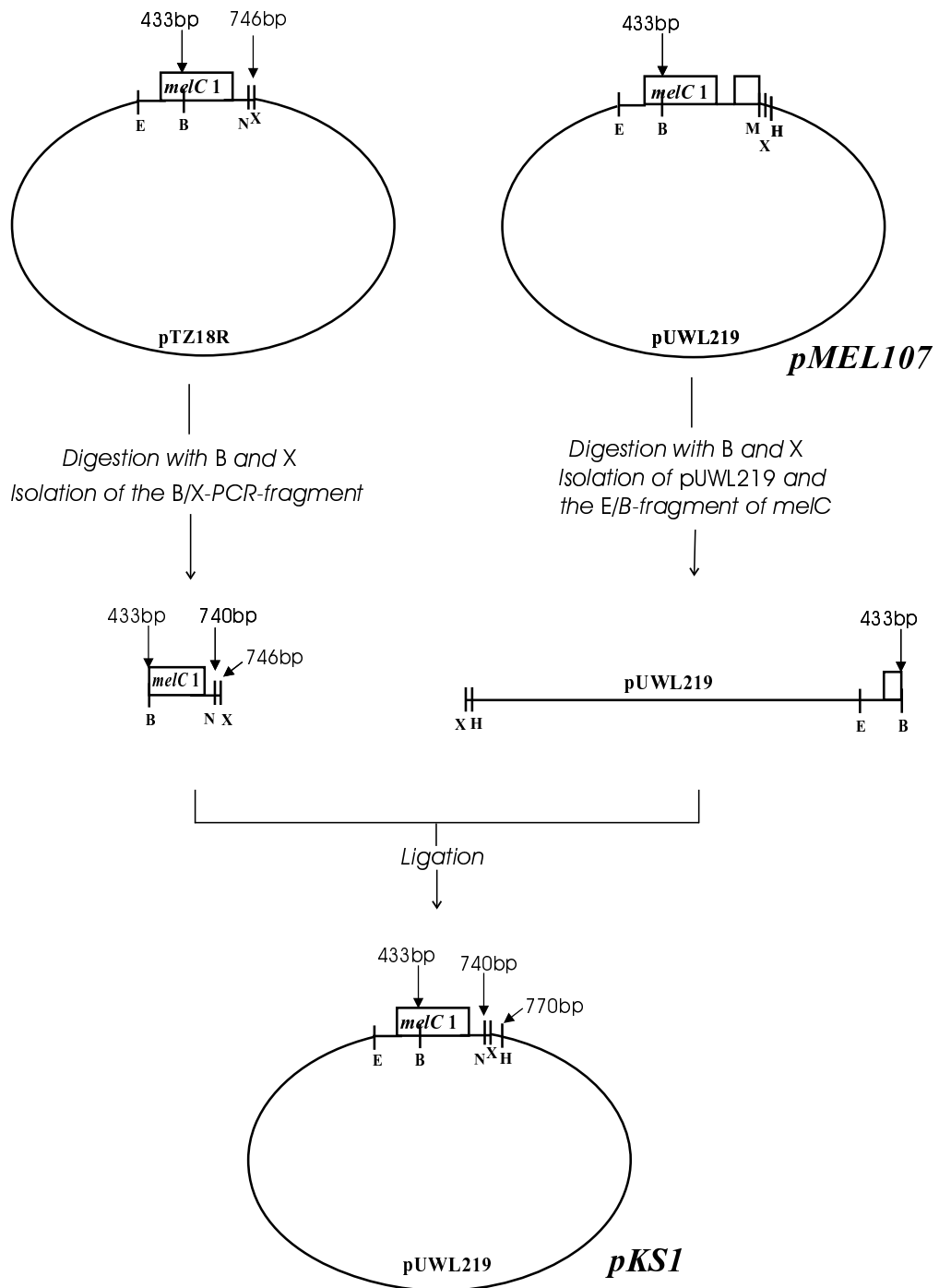
Figure 4.29: Part 2 of the strategy of cloning of *melC*1 with an introduced *Nde*I site in the *Streptomyces - E. coli* shuttle vector pUWL219 (B=*Bgl*II, E=*EcoR*I, H=*Hind*III, M=*Mlu*I, N=*Nde*I, X=*Xba*I)

Figure 4.30: Part 1 of the strategy of SDM of *melC*2 to substitute His[37] with Gly
(E=*EcoR*I, H=*Hind*III, M=*Mlu*I, N=*Nde*I, X=*Xba*I
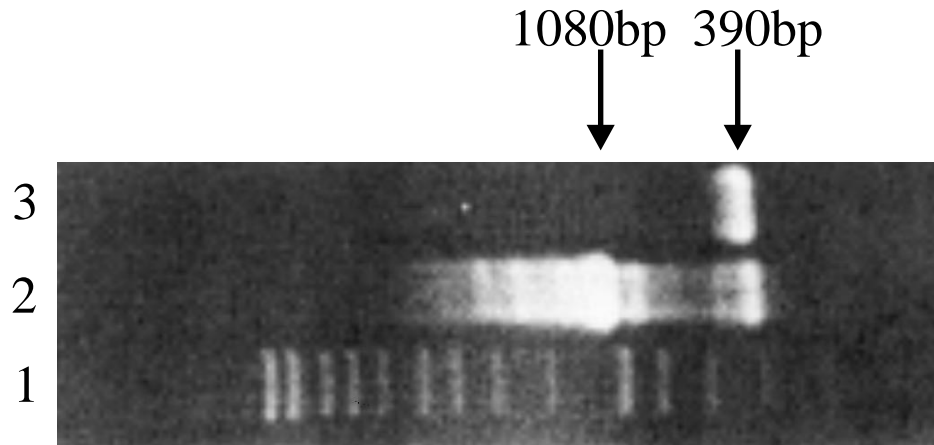
Figure 4.31: Illustration of the agarose gel obtained by agarose gel electrophoresis of the marker (lane 1), the PCR-product after the synthesis of the mutated mega-primer with a theoretically length of 390bp (lane 3, marked with a arrow) and of the PCR-product after the synthesis of the mutated DNA-fragment with a theoretically length of 1080bp (lane 2, marked with a arrow).

with *Nde*I and *Hind*III (820bp, 2900bp) and with *EcoR*I and *Sal*I (120bp, 270bp, 460bp, 2870bp) and agarose gel electrophoresis, shown in Figure 4.32. Special attention was put on the digestion with *EcoR*I and *Mlu*I, because of the missing *Mlu*I-site it should result in a fragment of 240bp instead of two fragments of about 120bp. This is visible on the 1% agarose gel, shown in Figure 4.32B. A 1% agarose gel leads aspecially to a high separation of the short DNA fragments. In Figure 4.32B the line of 200bp is missed because the amount of marker-DNA was not high anough. For this reason the lines of the marker start with 400bp. Nevertheless, the lower line of pKS2 digested with *EcoR*I and *Mlu*I must be the line for 220bp and 240bp. A line for 120bp should have to be found considerably below, but there is nothing. This result was a first indication for the success of this SDM procedure.

But a definite assessment about the results, whether the mutations had success or whether the quality of the DNA, can only achieved by sequence analysis. But sequence analysis is a technique which do not work fault-freely. For this reason three independet clones with the mutated *melC*2 as insert were isolated, to have the opportunity to start at different length of *melC*2 with sequence analysis. Beside *melC*2 in pTZ18R (pKS2), the *EcoR*I/*Hind*III-fragment of pKS2 was cloned in
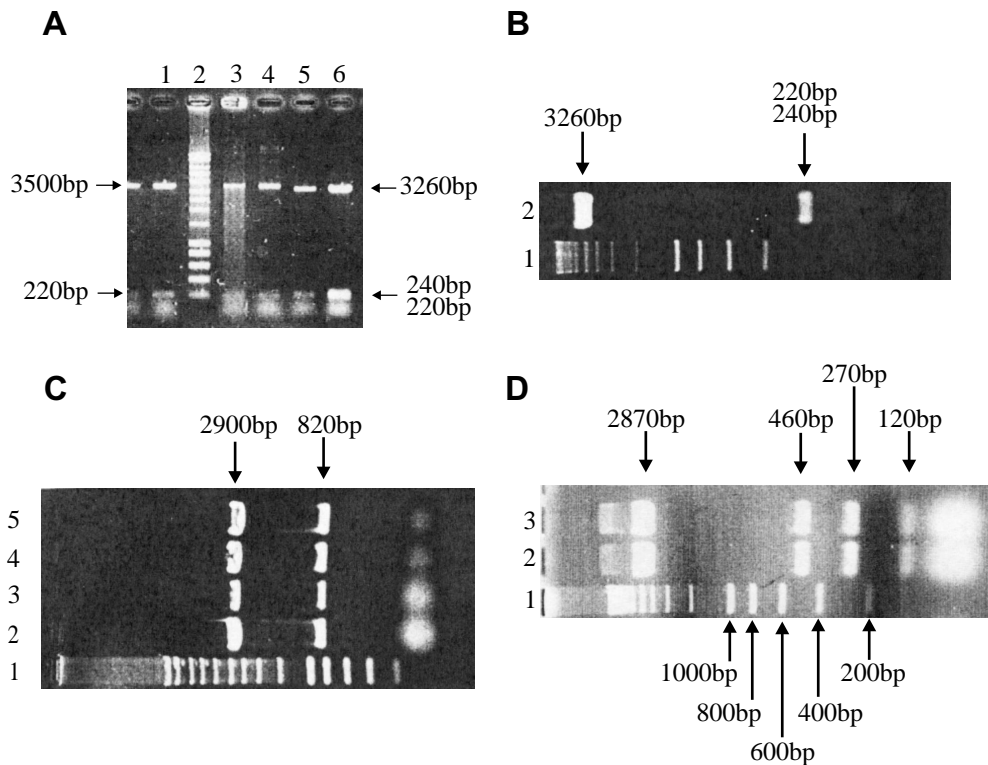
Figure 4.32: Agarose gel electrophoresis of pKS2 digested with: *Mlu*I (gel A, lane 1, 3 and 4), *EcoR*I and *Mlu*I (gel A, lane 5 and 6, gel B), *Nde*I and *Hind*III (gel C, lane 2 and 3), *EcoR*I and *Hind*III (gel C, lane 4 and 5) and gel D, lane 2 and 3. The marker can be seen in gel A, lane 2; gel B, lane 1; gel C, lane 1 and in gel D, lane1 (The description of the correspondens of DNA length and line of the marker is written in paragraph 7.1.1.). The numbers written at the site of the gels correspond to the length which were theoretically expected.

pTZ19R (this plasmid is designated pKS6) and the *EcoR*I/*Sal*I-fragment of the insert of pKS2 was also cloned in pTZ19R (this plasmid is designated pKS7). Then from all clones single stranded DNA (ssDNA) was isolated to sequence the inserts. The sequence analyses of pKS2 started from the beginning of *melC*2. With pKS6 the sequencing was allowed to start from the end of *melC*2 and pKS7 allowed sequence analyses from the middle of *melC*2 back to the start.

A comparison of the sequence analyses, made by BaseClear (BaseClear, Leiden, The Netherlands), confirmed the mutations at position 854 and 855 in *melC*2 (CAC encoding for His was substituted by GGC encoding for Gly) as well as the mutation at position 862 in *melC*2 (ACGCGT encoding for a *Mlu*I-site was sub-
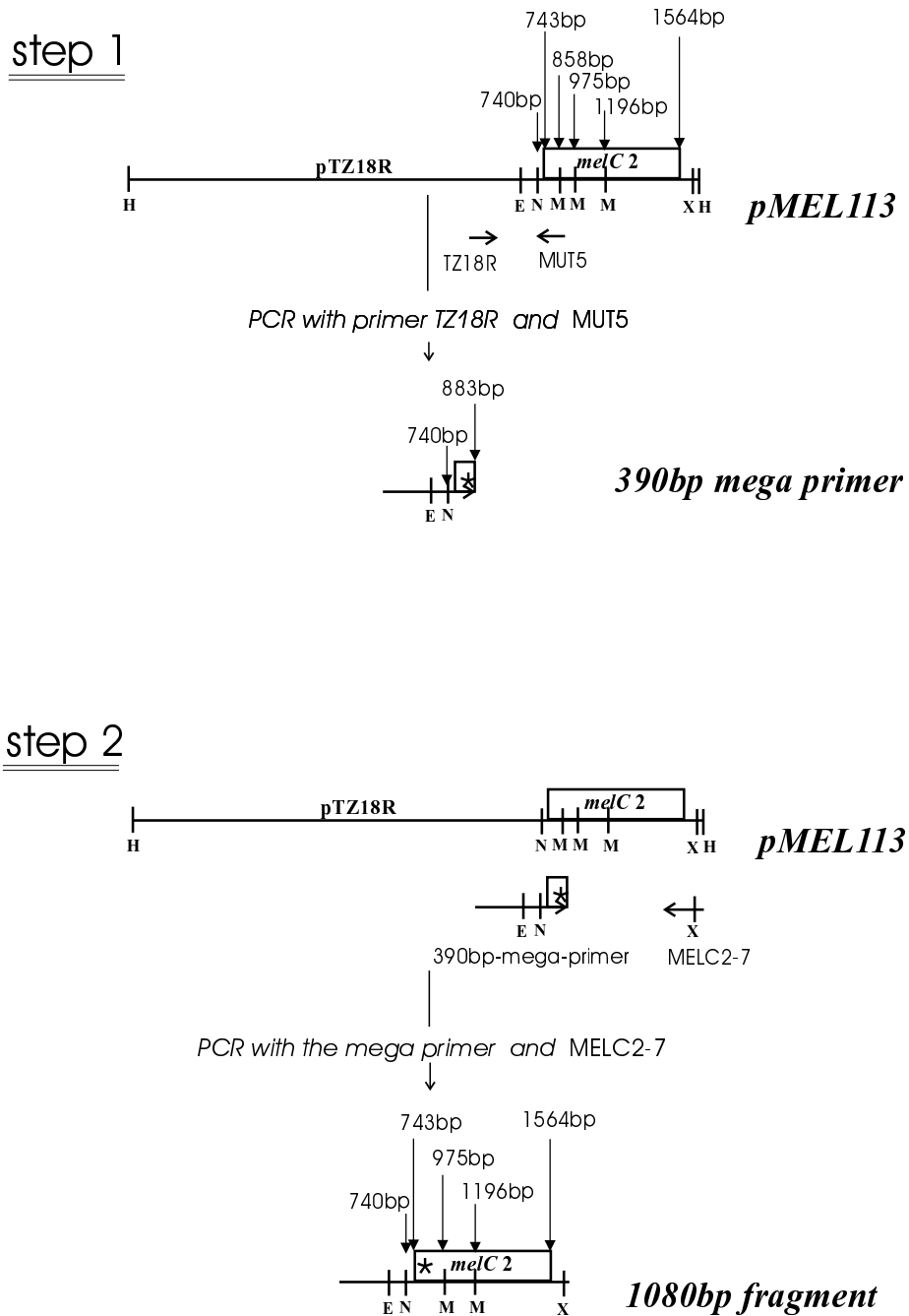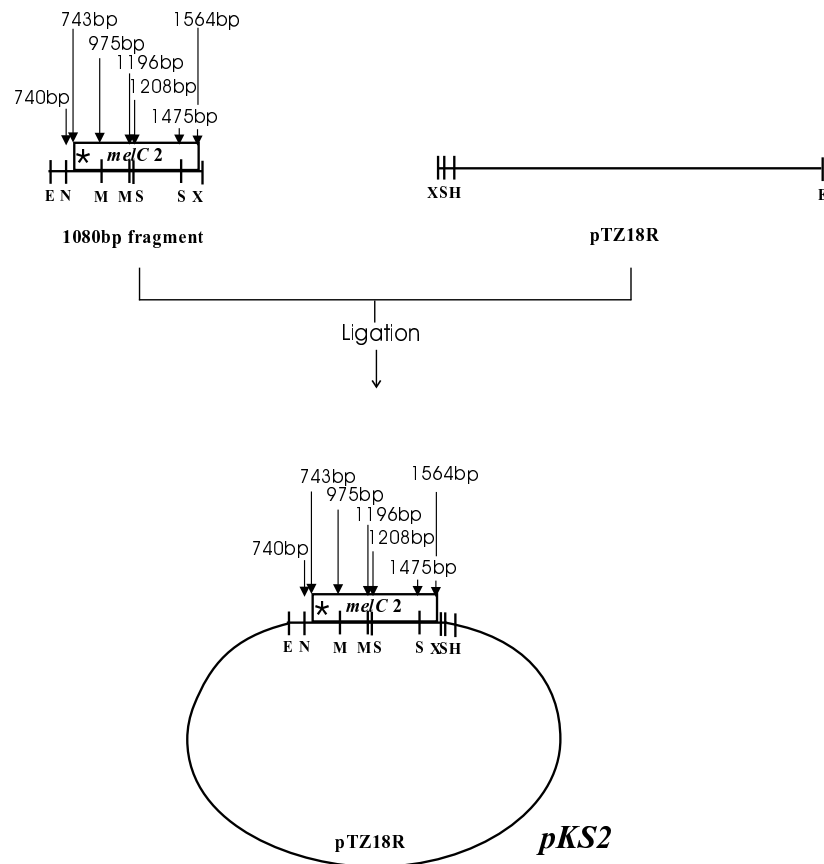
Figure 4.33: Part 2 of the strategy of SDM of *melC*2 to substitute His[37] with Gly (E=*EcoR*I, H=*Hind*III, M=*Mlu*I, N=*Nde*I, S=*Sal*I, X=*Xba*I

stituted by ACGCCT which destroy the *Mlu*I-site). Now it was clear that beside pKS1 also pKS2 was available. The prerequisites for cloning of *melC*1 and *melC*2 mutant in *Streptomyces - E. coli* shuttle vectors were fulfilled now.

4.4.3   Cloning of *melC*1 and *melC*2 mutant in *Streptomyces - E. coli* shuttle vectors

The scheme illustrated in Figure 4.27 shows that the next step in the cloning strategy was to combine *melC*1 with the mutated *melC*2 gene in pTZ18R. Before ligation pKS1 was digested with *EcoR*I and *Nde*I, pKS2 with *Nde*I and *Hind*III and pTZ18R with *EcoR*I and *Hind*III. Then they were separated by agarose gel elec-

trophoresis and ligated. Ligation mixture was used to transform *E. coli* JM109 and a selection on LB$_{Amp}$ followed. Then colonies were picked up to isolate plasmids which were analysed by digestion with *Bgl*II and *Hind*III (1170bp, 2990bp), *EcoR*I and *Mlu*I (240bp, 1000bp, 2920bp), *EcoR*I and *Hind*III (1300bp, 2900bp), with *Nde*I and *Hind*III (820bp, 3340bp) and with *EcoR*I and *Sal*I (120bp, 545bp, 665bp, 2730bp). The mutated *melC* operon cloned in pTZ18R was named pKS3.

The last task to be done was to digest both pKS3 and the *Streptomyces - E. coli* shuttle vector with *EcoR*I and *Hind*III (both pUWL219 and pUCS75), isolate the *melC* fragment and the digested pUWL219 and pUCS75 to perform the ligation. Again ligation mixture was used to transform *E. coli* JM109 and *E. coli* ES1301 and a selection on LB$_{Amp, IPTG \, and \, XGal}$ for pUWL219 or on LB$_{Gm, IPTG \, and \, XGal}$ for pUCS75 followed. Then white colonies were picked up to isolate plasmids, which were analysed by digestion with *EcoR*I and *Hind*III (1300bp and 6800bp if pUWL219 was used and 13 900bp if pUCS75 was used). The mutated *melC* operon cloned in pUWL219 was named pKS4 and in pUCS75 pKS5.

In Table 4.8 all plasmids, constructed in the context of this work are listed.

4.4.4 Transformation of protoplasts of *S. lividans* and *S. coelicolor* with pKS4 and pKS5

The *Streptomyces - E. coli* shuttle plasmids pKS4 and pKS5 were used to transform protoplasts of *S. lividans* and *S. coelicolor*. The protoplasts were allowed to re-generate on R2YE agar plates for 15hours. Thereafter transformants which were selected by overlaying with thiostrepton (50μg/ml) for pUWL219 or gentamycin (50μg/ml) for pUCS75. After eight days spores of one colony were spread on a fresh plate containing the appropriate antibiotic. On the fifteenth day spores were isolated and new sporulation plates were started. This time SAS plates were used for *S. lividans* and *S. coelicolor* containing pKS5, because sporulation is more abundant on this medium.

The following cultures were started in TSBS medium inoculated with fresh spores:

A: *S. lividans* containing pKS4

B: *S. lividans* containing pKS5

C: *S. coelicolor* containing pKS4

D: *S. coelicolor* containing pKS5.

They were grown in 10ml medium for 36hours at 30°C. The medium and the mycelium were tested for tyrosinase activity and samples of medium and

Table 4.8: Plasmids with insert

Name	Resistance	Vector-insert	Source + Information
pMEL2	Tc^R	pALTER-melC1-melC2	(*Bcl*I fragment of pIJ702) orientation: melC sequence = complement of ssDNA, i.e. *EcoR*I- *Hind*III
pMEL102	Tc^R	pALTER-melC1	*Xba*I (MCS)-*Mlu*I fragment of pMEL2
pMEL107	Amp^R	pUWL219-P_{mel}melC1	*EcoR*I-*Hind*III fragment of pMEL102
pMEL110	Amp^R	pTZ18R-melC1-melC2	*EcoR*I-*Hind*III fragment of pMEL2
pMEL113	Amp^R	pTZ18R-melC2	+ an additional *Nde*I side in the beginning of melC2
pKS1	Amp^R	pUWL219-melC1	+ an additional *Nde*I side at the end of melC1
pKS2	Amp^R	pTZ18R-melC2-mutant	*EcoR*I-*Xba*I fragment of the 1080bp fragment (obtained with the Mega-Primer-Method) in pTZ18R
pKS3	Amp^R	pTZ18R-melC-mutant	*EcoR*I-*Nde*I fragment of pKS1 and *Nde*I-*Hind*III fragment of pKS2
pKS4	Amp^R	pUWL219-melC-mutant	*EcoR*I-*Nde*I fragment of pKS1 and *Nde*I-*Hind*III fragment of pKS2
pKS5	Gm^R	pUCS75-melC-mutant	*EcoR*I-*Nde*I fragment of pKS1 and *Nde*I-*Hind*III fragment of pKS2
pKS6	Amp^R	pTZ19R-melC2-mutant	*EcoR*I-*Hind*III fragment of pKS2 in pTZ19R
pKS7	Amp^R	pTZ19R-melC2-mutant	*EcoR*I-*Sal*I fragment of pKS2 in pTZ19R

mycelium were analysed by SDS-PAGE western blotting, but neither tyrosinase nor MELC1 was detected.

Next, a 2 liter culture of *S. lividans* pKS4 was grown and tyrosinase isolation was started immediately after 37hours of growth. The rationale behind this approach was that the negative results of the small scale experiments could be due to instability of the tyrosinase mutant. The purification was carried out by the standard purification protocol for wildtype tyrosinase (description of the procedure in paragraph 7.3.1 and of the results in paragraph 4.1.1). In Figure 4.34 the elution profile of the chromatography is shown. As can be seen, the elution profile shows two clearly seperated peaks which is in contrast to the purification of wildtype tyrosinase that shows only one peak (for comparison see paragraph 4.1.1). Fractions containing protein were tested for tyrosinase activity, but no activity was detected. Further analyses such as SDS-PAGE and western blotting were performed, but no bands corresponding to tyrosinase were observed.

I have never detected MELC1 in culture overexpressing tyrosinase and MELC1. The reason for that is most likely that the half life of MELC1 (after transfer of the coppers and translocation over the cell membrane) is verry short.

To ensure the integrety of pKS4, the plasmid was isolated from the same culture and analysed by agarose gel chromatography (digestion with *Bgl*II and *Hind*III (1170bp, 6.8kb), *EcoR*I and *Mlu*I (240bp, 1kb, 6,8kb), *EcoR*I and *Hind*III
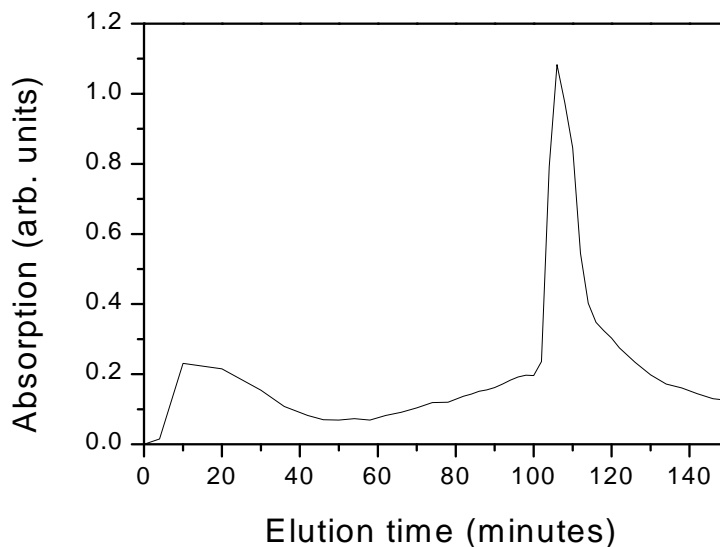
Figure 4.34: Elution profile of the chromatography of the expressed protein, which is presumeably the mutated tyrosinase

(1300bp, 6.8kb), with *Nde*I and *Hind*III (820bp, 7.2kb) and with *EcoR*I and *Sal*I (270bp, 545bp, 665bp, 6.8kb). According to the agarose gel chromatography results, the plasmid was perfect.

5   Discussion

5.1   Investigation of tyrosinase

The present work describes investigations of mushroom tyrosinase (MT), a commercially available enzyme and *S. antibioticus* tyrosinase (*S*.T) which has been isolated. The two tyrosinases show a number of differences in their characteristics:

- Molecular weight (MT: 118kD, *S*.T: 30,6kD)

- Sub-unit composition (MT: 4, *S*.T: 1)

- Substrate specificity (MT: significant differences of the enzymatic response for different phenolic compounds, *S*.T: the enzymatic response was usually in the same order of magnitude, except for three substrates)

- Specific activity for L-dopa (MT: 5.2U/mg lyophilisate, *S*.T: 1225U/mg protein).

- Used enzyme purity (MT: 10-15%, *S*.T: 98%)

Summarising these characteristics, *S. antibioticus* tyrosinase is the smaller and more purified enzyme and has with respect to L-dopa a significantly higher specific activity than mushroom tyrosinase. Furthermore *S. antibioticus* tyrosinase is the stabler enzyme and it is a monomeric enzyme.

Long-term storage investigations of the two tyrosinases revealed the storage of a dried enzyme sample at temperatures below zero turned out to be the best. If it is necessary, however, to store tyrosinase in solution, a temperature of -18°C should never be used. Otherwise a complete loss of activity of both tyrosinases will be the result. Storage at 4°C or at -80°C is possible.

All these characteristics make *S. antibioticus* tyrosinase to an interesting enzyme for analytical applications.

Additionally surface plasmon resonance was used to investigate the binding of tyrosinase to an immobilised inhibitor. For biosensor development the reversible binding of an enzyme via an inhibitor is very interesting. In this case for example oriented binding of an enzyme to the surface is possible. Since surface plasmon resonance detection allows the observation of weak molecular interactions [244] the interaction between both tyrosinases and immobilised kojic acid have been studied. A specific binding of both mushroom and *S. antibioticus* tyrosinase could be observed (see Figure 4.11 in paragraph 4.1.4).

5.2 Application of tyrosinase in enzyme electrodes

5.2.1 Enzyme electrodes prepared with mushroom tyrosinase

Monoenzyme electrodes   Various mushroom tyrosinase electrodes were developed, which are primarily based on different tyrosinase immobilisation schemes onto Clark type oxygen electrodes or screen printed electrodes. The maximum sensitivity was obtained for all electrodes between a pH of 5.0 to 7.5 with the substrate catechol for tyrosinase. The detection limit for catechol of the screen printed electrodes was in the nanomolar range whereas the detection limit for catechol of the Clark type oxygen electrode (electrode COE_MT_PVA) was $1\,\mu$M. All developed monoenzyme electrodes allow the detection of phenolic compounds in the lower micromolar range. The shortest response time of only 40sec was obtained with electrode COE_MT_PVA, in contrast to 3.5 to 4min for the screen printed electrodes. Regarding the application it is important, that a storage of the enzyme-membranes, used for the electrode COE_MT_PVA, is possible for several months at $4°$C.

In summary tyrosinase-modified SPE's based on carbon material have measured phenolic compounds with higher sensitivity than the tyrosinase-modified COE due to the applied amplification principle (bioelectrocatalytic recycling, for explanation see paragraph 3.3.2). Also a comparison of the developed monoenzyme electrodes (SPE_MT_N, SPE_MT_PU and COE_MT_PVA) with tyrosinase electrodes described in literatur has shown that most of them use bioelectrocatalytic recycling for amplification and allow the detection of phenolic compounds in the lower micromolar range with a detection limit in the nanomolar range. This is comparable to the results described in this work (for comparison see Table 3.3 in paragraph 3.4.3). Nevertheless, the challenges for tyrosinase-modified carbon electrode development in the future concerning the operational stability as well as the reproducibility from one batch of carbon paste to another still have to be overcome.

Bienzyme electrodes   The development of a bienzyme electrode, consisting of mushroom tyrosinase and glucose dehydrogenase, is described in this work (in the following called the MT/GDH-sensor). This application of two enzymes, which were used for building a very effective amplification system based on biocatalytic recycling (as described in paragraph 3.3.3), in combination with a COE is another way of increasing the sensitivity. The results of measurements with the MT/GDH-sensor will be discussed in the following.

The MT/GDH-sensor has been used in the stationary system as well as in the flow-through set-up. Measurements in the lower nanomolar range are possible with both systems and the higher detection limit of 5nM catechol of the flow-

through set-up (in contrast to 0.6nM of the stationary system) is mostly due to the shorter contact time of the measuring solution with the sensor. On the other hand the main advantage of the flow-through set-up is the very short response time of only 30sec.

In addition with the flow-through set-up a sample frequency is achieved which is much higher than with the stationary system because of the faster cleaning procedure and because of the necessary regeneration time of the membrane in the stationary system. Furthermore the reproducibility is excellent. If one concentration was measured several times the standard deviation is only 1.8% (n=11, catechol concentration = 100nM). In contrast all other following measurements with the stationary system have shown a standard deviation of 5% (n=8, catechol concentration = 100nM). Furthermore it should be mentioned, that the bi-enzyme membranes can be stored for several months at 4°C, which is also important for the application.
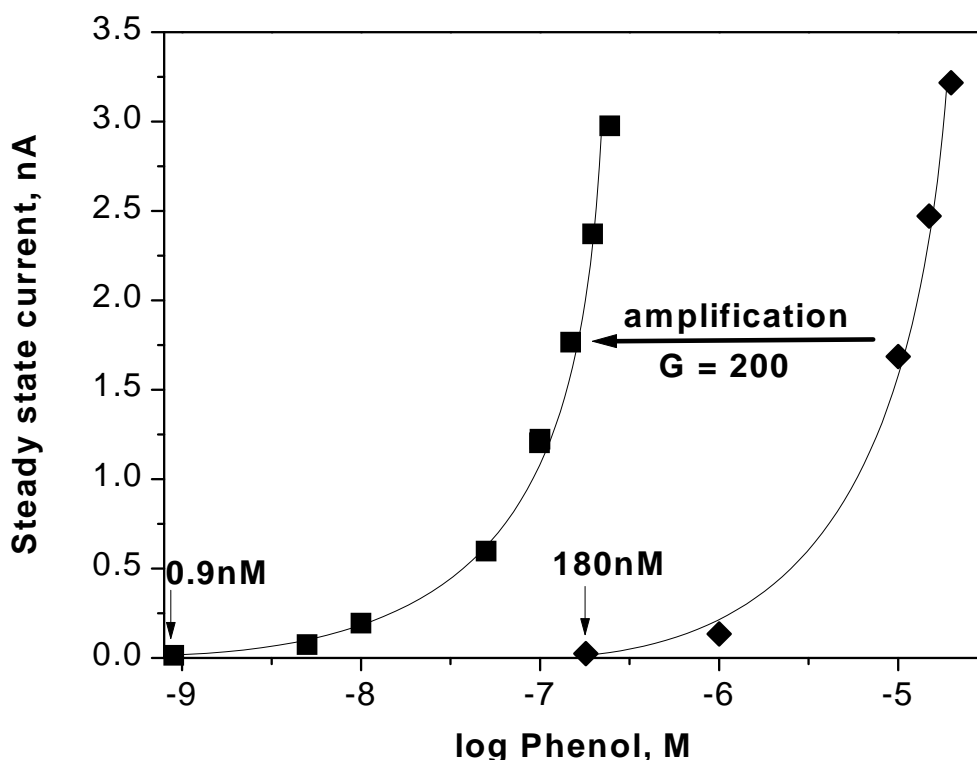

Figure 5.1: The calibration graphs for phenol measured with the bienzyme electrode (MT/GDH-sensor) (■) and the monoenzyme electrode (COE_MT_PVA) (♦)

In Figure 5.1 calibration graphs for phenol detection are shown. On the left measured with the bienzyme electrode (MT/GDH-sensor) and on the right measured with the monoenzyme electrode (electrode COE_MT_PVA). The difference in the sensitivity of about two orders of magnitude is clearly visible.

The principle of biocatalytic recycling, as it is applied in the MT/GDH-sensor, is only one possible method to amplify weak signals. Other principles of substrate recycling are also used by various groups. A choice of tyrosinase electrodes, developed during the last five years, is described in paragraph 3.3 and a summary is given in the Tables 3.3-3.5. It can easily be seen, that low detection limits are obtained with tyrosinase electrodes using tyrosinase entrapped within polypyrrole (10nM phenol [157]), tyrosinase mixed with graphite powder and an osmium complexed phenanthroline dione (6nM phenol [152], 10nM phenol and 10nM catechol [232]) and tyrosinase immobilised on graphite electrodes (15nM catechol [145]). With the detection limit of 0.6nM for catechol and 0.9nM for phenol the MT-sensor can be integrated in the group of most sensitive tyrosinase electrodes. A linear measuring range of more than four orders of magnitude for the MT/GDH-sensor is also competitive to the other tyrosinase electrodes.

Because of the characteristics of the bienzyme electrode, e.g., the excellent results in sensitivity, response time and reproducibility, the MT/GDH-sensor was applied in the field of environmental control. Different river and see water samples were analysed and compared with the Standard Method DIN 38409-H16-1. In all cases the concentrations of phenolic compounds determined with the MT/GDH-sensor were in the same order of magnitude as the one determined with the Standard Method DIN 38409-H16-1, but the MT/GDH-sensor offers a number of advantages. Using the MT/GDH-sensor than a μl volume of a water sample has only to added to the buffer solution and within minutes a result will obtained. In contrast to that, the Standard Method DIN 38409-H16-1 is based on a color reaction which is evaluated photometrically after a extraction with chlorform. Furthermore, a sample volume of half a liter is needed for only one measurement. Summarised one can say, that measurements with the MT/GDH-sensor are easier, faster and also cheaper. Moreover no sample preparation is necessary and with the sensor an opportunity is given for on-line monitoring.

The MT/GDH-sensor has also been used for the investigation of tyrosinase inhibitors. For the first time the principle of biocatalytic recycling has been applied as an amplification system for inhibitor studies. Inhibitors are measurable down to sub-micromolar concentrations. Benzoic acid, a widely used preservative and a reversible inhibitor of tyrosinase ($I_{50} = 20\mu M$), can be measured with a detection limit of 100nM. The I_{50} of $20\mu M$ for the MT/GDH-sensor was lower than the value determined for mushroom tyrosinase in solution [85] and for the enzyme added to the carbon ink of a screen printed electrode [160]. However, a tenfold lower value has been found when the enzyme was used in an organic

solvent [143]. Obviously, the micro- environment drastically affects the binding efficiency of the inhibitor. On the other hand, one should point out that the I_{50} obtained with the bienzyme electrode is a value apparently due to the combination of mass transport, enzyme kinetics, matrix and immobilisation effects. Hasebe et al. [97] also used an entrapment procedure with oxygen consumption measurements but applied ascorbic acid as a reducing agent instead of an enzyme. In the MT/GDH-sensor quinone reduction was performed by a fast enzymatic reaction using GDH. Therefore, the catechol sensitivity of the bienzyme sensor is higher and small changes in the catechol oxidation rate are more clearly distinguishable.

Inhibitors of tyrosinase were also investigated in solution (see paragraph 4.1.2) so that a comparison of both investigations (inhibition of tyrosinase immobilised in the bienzyme electrode as well as tyrosinase in solution) is possible.

Aromatic carboxylic acids, like benzoic acid, inhibit tyrosinase to a similar extent. Kojic acid also showed a similar inhibition of the immobilised and the dissolved enzyme. In contrast, 2-O- octanoyl kojic acid was a much stronger inhibitor of tyrosinase in solution than of the immobilised enzyme where the ester is even weaker than kojic acid itself. This could be caused by a restricted access of the compound to the membrane bound enzyme. On the other hand, the inhibition by 5-O-octanoyl kojic acid is higher than that by kojic acid, both in the membrane and in solution. The reason for this apparently contradictory result remains unclear. The di-ester of kojic acid showed no inhibition of the dissolved and the immobilised enzyme.

Thioureas are the strongest inhibitors for mushroom tyrosinase in solution as has also been shown by Wang et al. [160]. 1-Phenyl-2-thiourea is the most effective inhibitor of tyrosinase in solution as well as of the MT/GDH-sensor. The response of the bienzyme electrode was similar for 1- allyl-2-thiourea but it inhibited less in solution. N,N'-Diphenylthiourea and thiourea are the weakest inhibitors for both the immobilised (MT/GDH-sensor) and enzyme in solution.

With these results it is proofed that bienzyme systems with an analyte regenerating cycle can be used to measure enzyme inhibitors because the gain of the coupled enzyme reaction is influenced by an inhibitor.

5.2.2 Enzyme electrodes prepared with *S. antibioticus* tyrosinase

Monoenzyme electrodes *S. antibioticus* tyrosinase, immobilised onto a Clark type oxygen electrode (electrode COE_ST_ PVA), has a measuring range comparable to electrode COE_MT_ PVA. Even the detection limit of catechol is in the same order of magnitude, $1\mu M$ for electrode COE_MT_ PVA and $0.5\mu M$ for electrode COE_ST_ PVA. Other characteristics like the response time or the possible storage time are comparable. Only the shape of response measured by the electrode COE_ST_ PVA, especially in the beginning of catechol quantification, has shown some difference. Up to now the reason for this remains unclear.

In addition the sensitivity according to different analytes of both sensors (electrode COE_ST_ PVA and electrode COE_MT_ PVA) was similar. The sensitivity order of both electrodes was: p-cresol > phenol > catechol > L-dopa , which was similar to that described by Kotte et al. [151] for a mediator-modified tyrosinase electrode. A different ranking in the sensitivity has been described for tyrosinase-graphite electrodes: this may be caused by the hydrophobic environment of the graphite-epoxy resin [191, 192] or by the direct reduction of quinones at the carbon material [171].

Bienzyme electrodes   For the ST/GDH bienzyme electrode (ST/GDH-sensor) a similar amplification system as described for the MT/GDH-sensor was applied with glucose dehydrogenase as the second enzyme (for explanation see paragraph 3.3.3). In the following the electrode made of *S. antibioticus* tyrosinase and glucose dehydrogenase is called: ST/GDH-sensor.

Figure 5.2 shows the calibration graphs obtained with the bienzyme electrode (ST/GDH-sensor, Figure 5.2**A**) and the monoenzyme electrode (COE_ST_PVA electrode, Figure 5.2**B**) with the substrates L-dopa and catechol. When comparing the calibration graphs, it is obvious that the quantification of both substrates in the nanomolar range was possible with the ST/GDH-sensor (Figure 5.2**A**), whereas the monoenzyme electrode COE_ST_PVA has only determined concentrations in the micromolar level 5.2**B**).

For the ST/GDH-sensor a sensitivity of 16.5nA/μM was found for L-dopa and for catechol the sensitivity was 6.6nA/μM, i.e. the ST/GDH-sensor has a *higher* sensitivity for L-dopa. The sensitivity of the corresponding monoenzyme electrode COE_ST_PVA was determined to be 0.06nA/μM for L-dopa and 0.15nA/μM for catechol, i.e. the electrode COE_ST_PVA has a *lower* sensitivity for L-dopa. The explanation for the revealed change in selectivity on the introduction of the GDH can be found in the working principle of the two electrodes.

First the focus will be on monoenzyme electrodes. In the case of monoenzyme electrodes the amount of tyrosinase is high enough, that every substrate which reaches the enzyme layer will be converted by the enzyme immediately. This sensors work diffusion controlled. In tyrosinase/GDH bienzyme electrodes tyrosinase is limiting the recycling rate, which is underlined by the result that the enzyme loading as well as inhibitors effects the measuring signal directly, which cannot be observed in enzyme electrodes working diffusion controlled [2].

The higher sensitivity of the bienzyme electrode (ST/GDH-sensor) for L-dopa in comparison to catechol therefore reflects the higher affinity of *S. antibioticus* tyrosinase to L-dopa, whereas the lower sensitivity of the monoenzyme electrode (COE_ST_PVA) reflects the differences in the diffusion characteristics of catechol and L-dopa in polyvinylalcohol membranes.

For applications a higher specific activity for L-dopa is very useful, especially if it is possible to detect neurotransmitters like catecholamines in the lower
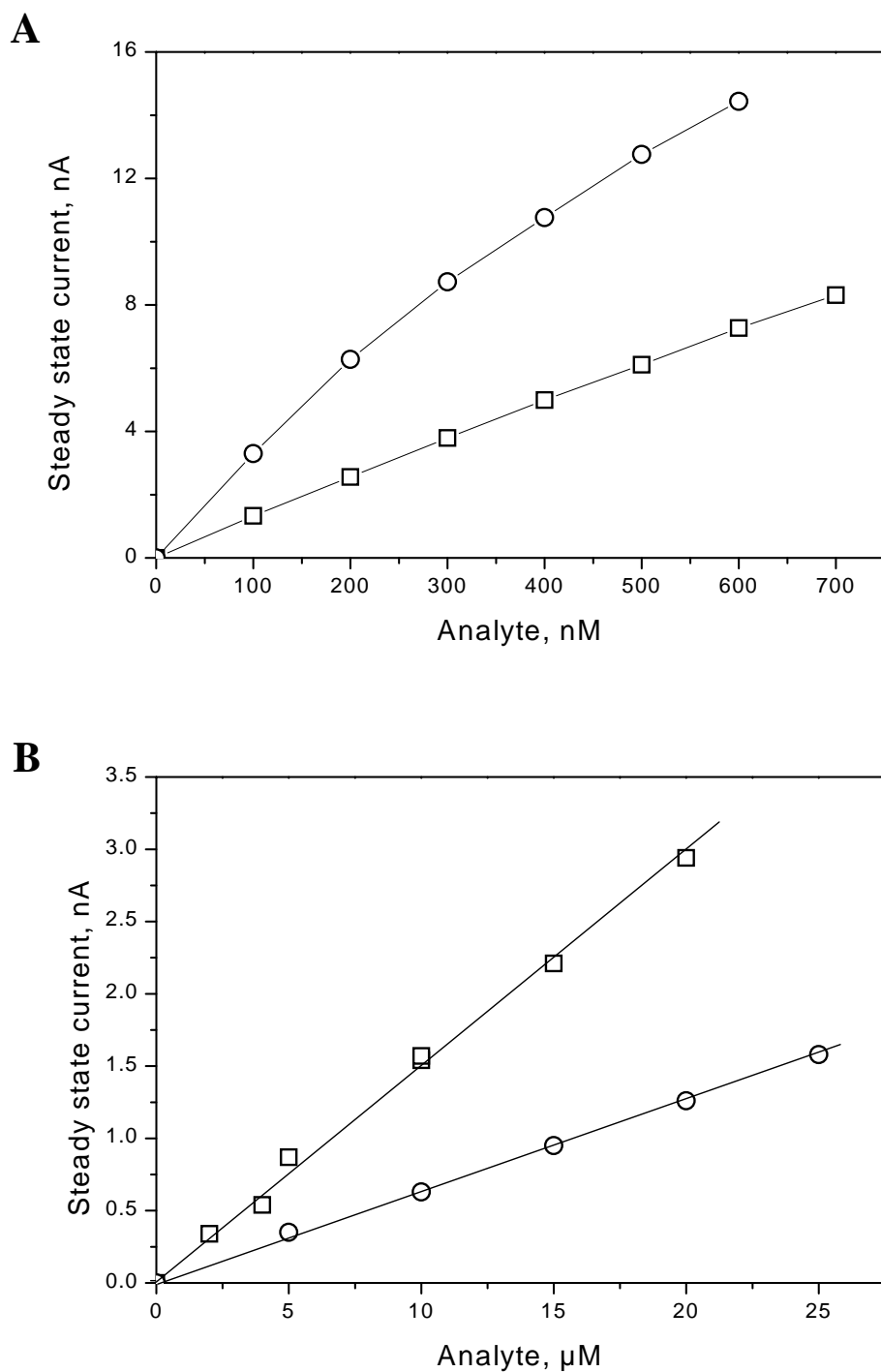
Figure 5.2: The calibration graphs for L-dopa (○) and catechol (□) measured with the bienzyme electrode (ST/GDH-sensor) (**A**) and with the monoenzyme electrode (COE_ST_ PVA electrode) (**B**)

nanomolar range, which is important in clinical analysis. But an application in other fields, e.g. environmental control, is also possible, because other phenolic compounds, like p-cresol, p-aminophenol or hydroquinone can be determined. Thus this newly developed sensor can be used as a detector for the sum of phenolic compounds, which is important especially in environmental control.

Compared with other tyrosinase electrodes, described in paragraph 3.3 and summarised in Tables 3.3-3.5 the ST/GDH-sensor belong to the group of most sensitive tyrosinase electrodes. Measurments in the nanomolar range with detection limits of 5nM for L-dopa and 10nM for catechol are comparable with tyrosinase electrodes developed in the last five years.

5.3   Modification of the tyrosinase gene

In this molecular-biological part of the thesis a pathway for the modification of the *S. antibioticus* tyrosinase by site directed mutagenesis (SDM) is described. A new restriction site (NdeI) is introduced in melC1. Also a protocol for the SDM of the tyrosinase gene was established and the change of **CAC** (His^{37}) into **GGC** (Gly) was obtained. The EcoRI - HindIII fragment was cloned in the *Streptomyces - E. coli* shuttle vectors both in pKS4 and in pKS5 for transformation of *Streptomyces*. During the efforts seven new plasmids were obtained, listed in Table 4.8 in paragraph 4.4.3.

The substitution of histidine residues in tyrosinase (MELC2) of the *S. antibioticus* melC operon was described for the first time by Tsai and Lee [41]. They substituted each of the six histidine residues in the tyrosinase coding operon melC (His^{37}, His^{53}, His^{62}, His^{189}, His^{193} and His^{215}) employing the Altered Site System (Promega) for in vitro mutagenesis. The most interesting information of this article was that the change of one histidine in the active site of tyrosinase led to an expression of a tyrosinase-MELC1 complex which is not able to dissociate. This is one reason, why they did not find any tyrosinase activity.

The article of Tsai and Lee [41] is focussed on tyrosinase-MELC1 complexes in the extracellular medium. No information is given about tyrosinase inside the cell. In addition *Streptomyces lividans* TK64 is used but it is known that *Streptomyces lividans* has a problem with tyrosinase expression [242]. For example wildtype tyrosinase is expressed in *S. antibioticus* with a ratio of extracellular : intracellular of 100:0. This is completely different in comparison to the expression of wildtype tyrosinase in *Streptomyces lividans*. The next problem was the antibody used for the immunoblotting of tyrosinase. The authors used an anti-MELC1/anti-tyrosinase-mixture for tyrosinase, which made a distinction between MELC1-dimer and tyrosinase (MELC2) impossible. Likewise other questions according to experimental work of this article are still open.

Because of the problems with the choice and the execution of the experimental

work of Tsai and Lee [41] a new start is worthwhile. In the context of these studies the mutated tyrosinase gene was obtained and is available in various plasmids for expression in *Streptomyces*. Several experiments were carried out to express and purify the modified tyrosinase in amounts sufficient for further characterisation. However, the work on expression of tyrosinase mutants turned out to be not as straight forward as purification of the wild type enzyme. Expression levels were extremely low and remained low despite changes in the expression protocol that have been shown to be successful in other expression attempts. It seems that as soon as the active site is altered, either the expression level is reduced, or the maturation and transport across the cell membrane is diminished or the stability of the protein is lost to a great extend (the latter could be protein degradation in either the cell or the medium). To remove these obstacles in obtaining sufficient modified tyrosinase further cooperation with the group of Prof. Dr. G.W. Canters has been arranged. Recent results have demonstrated that successful expression and purification of tyrosinase mutants is possible.

One of the main topics in the field of bio-analytics is to search for and implement improvements in sensor performance. With the tyrosinase mutant gene in our hands, the first step into the bio-analytical work is made. Molecular engineering is one of the most promising directions in this field. It pavings the way to the site-oriented fixation (SOF) of an enzyme for further investigations. This SOF is a new technique for tyrosinase and underlines the innovative aspect of our approach to biosensor development. It also opens the way for the introduction of a suitable linker molecule. Furthermore a site-to-site fixation of two enzymes is conceivable. In this respect the tyrosinase/GDH system is very promising.

6   Summary and outlook

The aim of the present studies was the development of a tyrosinase sensor, which can be used for the determination of phenolic compounds in the subnanomolar range. This measuring range is necessary because of the limit of phenolic compounds in drinking water (0.5nM acccording to the EU-Trinkwasserverordnung, 2001). Moreover it is useful to have a sensor with a large linear measuring range, which makes this sensor to a flexible measuring instrument. In this case the sensor can be used for the examination of phenolic compounds in various water samples without additional calibrations in between or without additional dilution steps. Such a sensor is also of great interest for catecholamine quantification in the clinical diagnostic.

To accomplish these goal, two tyrosinases were examined in regard to their later application in the sensor development:

- Mushroom tyrosinase and

- S. antibioticus tyrosinase

and three different types of tyrosinase sensors were investigated:

- Two monoenzyme electrodes without an amplification system (based on mushroom tyrosinase: COE_MT_PVA and on S. antibioticus tyrosinase: COE_ST_PVA)

- Two monoenzyme electrodes with a bioelectrocatalytic recycling system based on mushroom tyrosinase immobilised in nafion: SPE_MT_N and in polyurethane: SPE_MT_PU) and

- Two bienzyme electrodes with a biocatalytic recycling system (based on mushroom tyrosinase: MT/GDH-sensor and on S. antibioticus tyrosinase: ST/GDH-sensor)

The best results referred to the sensitivity were achieved with the two bienzyme electrodes. According to the best of my knowledge no other tyrosinase sensor is described up till now, with a comparable or higher sensitivity for catechol then the MT/GDH-sensor (for comparison see Table 3.3, 3.4 and 3.5 in paragraph 3.4.3. With this sensor a detection limit of 0.6nM was obtained for catechol. Furthermore a linear measuring range over four orders of magnitude was obtained, which also was achieved with a tyrosinase sensor for the first time. The MT/GDH-sensor was applied for the quantification of phenolic componds in see, river as well as in urban waste water. All results of these measurements were comparable with the results determined by the Standard Method DIN 38409_H16-1.

But the MT/GDH-sensor offers a number of advantages compared to the Standard Method.

A μl volume of a water sample added to the buffer solution is sufficient for the MT/GDH-sensor and the result will be obtained accurately within minutes. In contrast to that, the Standard Method DIN 38409-H16-1 is based on a color reaction which is evaluated photometrically after a extraction with chlorform which takes several hours. Furthermore, a sample volume of half a liter is needed for a single measurement. Summarised one can say, that measurements with the MT/GDH-sensor are easier, faster and much cheaper. Moreover the only sample preparation was filtration and dilution and with the sensor an opportunity is given for on-line monitoring of phenolic compounds in, e.g. see, river as well as urban waste water.

The second bienzyme electrode, the ST/GDH-sensor can also quantifiy phenolic compounds in the lower nanomolar range and is part of the most sensitive tyrosinase electrodes developed during the last five years [145, 152, 157, 223, 232]. A detection limit of 10nM was obtained for catechol. The main advantage of the ST/GDH-sensor in comparison to the MT/GDH-sensor is the sensitivity for catecholamines which are important in clinical diagnostic. The detection limit of 10nM and 5nM was achieved for dopamine and adrenaline (MT/GDH-sensor: 25nM and 125nM for dopamine and adrenaline). This is more sensitive than other tyrosinase sensors and in the same order of magnitude of other enzyme sensors, where often laccase is used (for explanation see paragraph 4.3.2). In comparison to the enzyme sensors based on laccase, in which the substrate range of laccase allows in most cases only a quantification of monophenolic compounds, the ST/GDH-sensor can be used more flexible. With the ST/GDH-sensor a sensitive quantification of monophenolic as well as diphenolic compounds is possible.

A further task in the context of this studies was the investigation, whether one of the tyrosinase sensors can also be of use for the quantification of tyrosinase inhibitors. Benzoic acid and derivatives, kojic acid and derivatives, azide and flouride as well as thiourea and derivatives were chosen for the measurements. It could be established, that the high sensitivity of the tyrosinase sensor for substrats of tyrosinase leads also to a high sensitivity for inhibitors of tyrosinase. Benzoic acid, a widely used preservative and the model compound for the MT/GDH-sensor, was detected with a detection limit of 100nM. A comparison of this result with results of other tyrosinase sensors used for inhibitor measurement, described during the last ten years, has shown, that only one sensor could also be used for the determination of benzoic acid in the nanomolar range, but the detection limit of this sensor was only 700nM ([97]).

The results of the examination of the two tyrosinases in regard to their later application in the sensor development have shown the advantages of *S. antibioticus* tyrosinase in comparison to mushroom tyrosinase especially for future re-

search. Beside the advantages described in paragraph 5.1 a very important advantage is the available information about the structure, the active centre and kinetic behaviour, while these information are not available for mushroom tyrosinase. Furthermore, the purification protocol and the good reproducibility also make *S. antibioticus* tyrosinase to an interesting enzyme for analytical applications. The purification procedure is very fast and yields an enzyme with a very high purity. Moreover, it is possible to obtain, with every new purification, the same quality of the enzyme preparation [1, 245]. This is an important advantage in comparison to the commercially available mushroom tyrosinase, because it is known that the sensitivity and the selectivity of tyrosinase-modified electrodes are highly dependent on the purity of the tyrosinase preparation [163].

A further result of these studies was the receipt of the mutated tyrosinase gene. It is available now in various plasmids for expression in *Streptomyces*. Several experiments were carried out to express and purify the modified tyrosinase in amounts sufficient for further characterisation. However, the work on expression of tyrosinase mutants turned out to be not as straight forward as purification of the wild type enzyme. To remove these obstacles in obtaining sufficient modified tyrosinase further cooperation with the group of Prof. Dr. G.W. Canters has been arranged. Recent results have demonstrated that successful expression and purification of tyrosinase mutants is possible.

In my opinion future research will focus on new techniques of enzyme immobilisation, including the development of new material for ultra-thin coating of the electrode surface. This is of particular importance in the miniaturisation of biosensors. Furthermore, studies will be carried out to manipulate the enzymatic substrate selectivity, for instance by protein engineering. For future developments of tyrosinase based biosensors it is imperative that an expression system is available combined with an excellent and fast purification procedure, which is the case for *S. antibioticus* tyrosinase.

7 Experimental

7.1 Materials and reagents

7.1.1 Enzymes and chemicals

Tyrosinase from *Agaricus bisporus* (TYR, EC 1.14.18.1), L-proline, L-tyrosine, catechol, L-ascorbic acid disodium salt, 2,6-dichlorophenolindophenol, p-amino-phenol, p-nitrophenol, p-nitrocatechol, hydroquinone, 4-hydroxybenzoic acid pro-pylester, N-ethyl-N-(3-diethylaminopropyl) carbodiimide, N-[2-hydroxyethyl]pi-perazine]-N-[2-ethanesulfonic acid] (HEPES), thiourea and 1-phenyl-2-thiourea were purchased from Sigma (Germany). Nafion was obtained from Du Pont (France). Polyurethane (PU-M20) was a kind gift from BioSensor Technologie (Germany). The molecular weight marker (The lines of the marker correspond to 7.4kD, 20.9kD, 34kD, 49kD, 82kD, 113kD and 200kD molecular weigth of a protein.) and the DNA marker (The lines of the marker correspond to 200bp (20ng), 400bp (40ng), 600bp (60ng), 800bp (80ng), 1000bp (100ng), 1500bp (15ng), 2000bp (20ng), 2500bp (25ng), 3000bp (30ng), 4000bp (40ng), 5000bp (50ng), 6000bp (60ng), 8000bp (80ng) and 10000bp (100ng) length (amount) of DNA.) were purchased from Pharmacia (Sweden). *S. antibioticus* tyrosinase was purified according to a modified version of published procedures [18, 238, 245] (for explanation see in section Methods paragraph 7.3.1). The quinoprotein glu-cose dehydrogenase *Acinetobacter calcoaceticus* (GDH, EC 1.1.99.17) was a kind gift from Roche (USA).

11-aminoundecanoic acid, N-hydroxysuccinimide, L-dopa, p-chlorophenol, p-cresol, N,N-diphenylthiourea and 1-allyl-2-thiourea and 4-methylcatechol were obtained from Aldrich (Germany), oxoid soya broth from Oxoid Ltd (UK) and dopamine, adrenalin, methyl- and propyl-4-hydroxybenzoates and sucrose from Fluka (Switzerland). Phenol, glucose, disodiumhydrogenphosphate, sodiumdihy-drogenphosphate and kojic acid (5-hydroxy-2-(hydroxymethyl)-4H-pyran-4-one) were received from Merck (Germany), pyrrolquinolin quinone (PQQ) from (Boeh-ringer Mannheim), benzoic acid from Riedel-de Häen (Germany), sodium azide and poly(vinyl)alcohol from Serva (Germany) and potassium fluoride from Chemie-werk Nünchritz (Germany)

Thiostrepton was a kind gift from Bristol-Meyers Squibb (USA) to Gerard W. Canters and E. Vijgenboom. Kojic acid derivatives were synthesised by Kaatz et al. [185].

All chemicals purchased were of analytical grade and used without further purification, if not stated otherwise.

7.1.2 Strains, plasmids and primers

Primers used for PCR are listed in Table 7.1. Plasmids with inserts which are used as target DNA for PCR experiments can be found in Table 4.8 on page 94, whereas

plasmids which are used for cloning (of PCR fragments for example) and for isolation of single strand DNA and *S. antibioticus - E. coli* shuttle vectors are listed in Table 7.2. Plasmid preparations from *E. coli* are essentially done according to protocols described in a laboratory manual [246]. The isolation procedure for plasmid DNA from *S. antibioticus* are done according to Kieser et al. [247].

E. coli strain JM109 was used for cloning experiments.

Streptomyces strains were provided by E. Vijgenboom and are listed in Table 7.3. *S. coelicolor* and *S. lividans* originate from the strain collection of the John Innes Centre (Norwich, UK). *S. antibioiticus* was obtained from the Kluyver Laboratory of Biotechnology (TU Delft, The Netherlands).

Table 7.1: Primer used for PCR

Primer	T_m	Sequence	Informations about the primers
MEL 1-11	63.9°C	5'-GCC-GAA-TTC-GGA-TCA-CGT-CAG-TTT-TCG-CAC-GTG-AGC	Anneals at the beginning of the *melC* operon sequence
MEL 1-14	67.0°C	5'-CGC-TCT-AGA-**CAT-ATG**-CGG-GTG-CTC-CAA-AAG-TGC-GGG-G	Introduction of a *Nde*I site at ATG of *melC*2 and a *Xba*I site for cloning
MUT 5	74.7°C	5'-GTC-GGT-GTC-GCC-CAG-GAT-GAA-*GGC*-GTT-**GCC**-CGT-GGT-GAC-GAA-GGC-GTC-GTA-GCG	SDM of *melC*2 (in italics is the mutation = change of CAC (His37) into GGC (Gly)) and in bold is the destroyed *Mlu*I site (change of *GCG* into *GCC*
TZ18R	62.3°C	5'-GAC-CGA-GCG-CAG-CGA-GTC-AGT-GAG-CG	Hybridises about 270bp downstream of the *EcoR*I site of MCS and reads into MCS
MELC 2-7	63.0°C	5'-CGC-TCT-AGA-TCA-GAC-GTC-GAA-GGT-GTA-GTG-C	Introduction of a *Xba*I site immediately after stopcodon *melC*2, underlined

Table 7.2: Plasmids

Plasmid	Length	Ref.
pTZ18R	2.9kb	(Pharmacia, Sweden)
pTZ19R	2.9kb	(Pharmacia, Sweden)
pALTER	5.6kb	(Promega, USA)
pUWL219	6.8kb	[248]
pUCS75	13.9kb	[249]

Table 7.3: Streptomyces strains

Strain		Phenotype
S. lividans 66	1326	wild type containing endogenous plasmids SLP2 and SLP3
S. coelicolor A3(2)	M145	wild type, plasmid free
S. antibioticus		wild type

7.2   Apparatus and instruments

7.2.1   Biosensorpreparation

Membrane preparation and assembly of the biosensor   Membranes containing immobilised glucose dehydrogenase (GDH) and tyrosinase were prepared by mixing $30\mu l$ PQQ (0.5mM), the enzymes and $30\mu l$ PVA (20%). An aliquot ($2\mu l$) of the solution was spread onto a polyacrylate plate (4mm in diameter). UV exposure was carried out for 30min to incorporate the enzymes in the PVA crosslinked matrix. The membranes containing approximately 1.6U mushroom tyrosinase or 1U *S. antibioticus* tyrosinase according to the proline-assay and 23U GDH according to the standard assay with 2,6-dichlorophenolindo-phenol as electron-acceptor. They were removed from the polyacrylate plates and stored at $4°C$. The tyrosinase/GDH membrane was fixed onto a Clark type oxygen electrode (COE, Elbau GmbH, Germany) between a polypropylene (thickness 6 μm) and regenerated cellulose (thickness 8 μm) membrane.

Monoenzyme electrodes based on COE's are biosensors which containing tyrosinase and GDH but only tyrosinase is active. The monoenzyme electrode prepared with mushroom tyrosinase is called COE_MT_PVA. If *S. antibioticus* tyrosinase is used than COE_ST_PVA was chosen as name for the monoenzyme electrode.

The bienzyme electrode prepared with mushroom tyrosinase and GDH is called MT/GDH-sensor. If *S. antibioticus* tyrosinase is used in combination with GDH than ST/GDH-sensor was chosen as name for the bienzyme electrode.

Immobilisation of tyrosinase on screen printed electrodes (SPE's)

Immobilisation in nafion   1mg mushroom tyrosinase (48U according to the proline-assay) was dissolved in $50\mu l$ water. Than $20\mu l$ enzyme solution and $20\mu l$ phosphate buffer/methanol mixture (20% phosphate buffer; 50mM containing 0.1% Nafion; pH = 6.5 and 80% methanol) were mixed and dripped three times (including drying in between) on the electrode. This monoenzyme electrode is called SPE_MT_N.

Immobilisation in polyurethan   1mg mushroom tyrosinase (48U according to the proline-assay) was dissolved in $50\mu l$ polyurethane (BST, Germany). Than $2\mu l$ enzyme/polyurethane mixture was dripped on the electrode. This monoenzyme electrode is called SPE_MT_PU.

Immobilisation of tyrosinase on a kojic acid linker   The investigations according to the immobilisation of 11-aminoundecanoic acid (5-hydroxy-4-oxo-4*H*-pyran-2-yl)-methyl ester (in the following called kojic acid linker) on different surfaces followed by the immobilisation of tyrosinase on the kojic acid linker were done with a BIAcore 2000. (With a BIAcore 2000, a combination of SPR detection, sensor chip chemistry and an integrated flow system in one measuring instrument, it is possible to simultaneously detect interaction events on four different spots located in different flow cells (FC), on the sensor surface [244].)

Immobilisation of the kojic acid linker on a carboxylated dextran matrix
A continuous-flow ($10 \mu l$/min) of HBS buffer was maintained over the sensor surface of the CM5-chip H14.

The carboxylated dextran matrix on the sensor surface in flow cell 2 (in the following called FC2), FC3 and FC4 were activated by a 2min injection of a aqueous solution containing 400mM N-ethyl-N-(3-diethylaminopropyl) carbodiimide (EDC) and 0.1M N-hydroxysuccinimide (NHS) (activation procedure). This was followed in FC2 and FC4 by the reaction *vs.* the aminogroup of 11-aminoundecanoic acid ($100 \mu M$) with the activated carboxylic group of the dextran matrix.

Specific surfaces in FC3 were obtained by 5min injection of kojic acid linker ($100 \mu M$) in 10mM HEPES, pH=8.0 containing 150mM NaCl, 0.1% ethanol and 0.05% TWEEN 20. In FC4 a second activation procedure was followed by the reaction of the kojic acid linker under identical conditions as described for FC3.

Then a third activation procedure was done this time by 3min injection and the immobilisation procedure was completed by a 5min injection of 10mM ethanolamine in 10mM HEPES, pH=8.0 containing 150mM NaCl, 0.1% ethanol and 0.05% TWEEN 20 to block remaining ester groups in FC2-4.

Finally FC1, which at first remained untreated, was activated (the same activation procedure as described above) and then reaction between the activated carboxylic group of the dextran matrix and the amino group of the linker of kojic acid linker took place for 30min in DMSO. Also here a 5min injection of 10mM ethanolamine in 10mM HEPES, pH=8.0 containing 150mM NaCl, 0.1% ethanol and 0.05% TWEEN 20 took place to block remaining ester groups.

In Figure 7.1 a scheme of the modified sensor surface is given.

Immobilisation of the kojic acid linker on a gold surface of the gold-chip J3   The sensor J3 was a gold chip without further treatment. For this reason at first the gold surface was incubated with DMSO containing 3,3-dithiodipropionic acid-di-(N- succinimidylester (DTSP, 20mM)) for 2.5hours.

Then four different solutions were prepared in 10mM HEPES, pH=8.0 containing 150mM NaCl, 0.1% ethanol, 0.05% TWEEN 20 and a nucleophilic com-

pound (in the case of FC1 the nucleophilic compound was ethanolamine (10mM),
in the case of FC4 kojic acid linker (100μM), in the case of FC3 a mixture of
ethanolamine and kojic acid linker, 20%:80% and in the case of FC2 a mixture of
ethanolamine and kojic acid linker, 80%:20%). Nucleophilic compound are able
to react with the activated carboxylic acids.

The immobilisation procedure was completed by a 5min injection of 10mM
ethanolamine in 10mM HEPES, pH=8.0 containing 150mM NaCl, 0.1% ethanol
and 0.05% TWEEN 20 to block remaining ester groups.

In Figure 7.2 a scheme of the modified sensor surface is given.
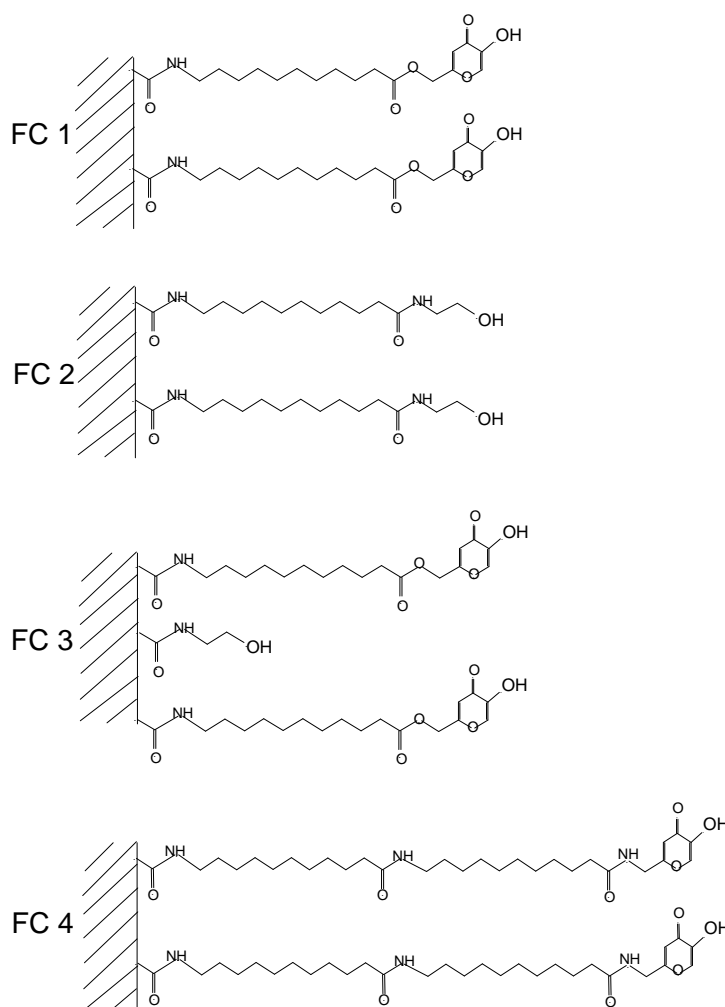
Figure 7.1: Scheme of the modified sensor surface of sensor H14

Immobilisation of tyrosinase on a kojic acid linker   Tyrosinase (2mg/ml in the case of mushroom tyrosinase and 0.2mg/ml in the case of *S. Antibioticus* tyrosinase) in 5mM phosphate buffer, pH=6.5 containing 150mM NaCl and 0.05% TWEEN 20 was injected at a constant flow rate of 10μl/min (binding process). The dissociation process started with the injection of only buffer solution (5mM phosphate buffer, pH=6.5 containing 150mM NaCl and 0.05% TWEEN 20) at a constant flow rate of 10μl/min. To regenerate the surface the flow cells were rinsed with NaOH and HCl in the change (respectively 1min injection of a 10mM solution at a constant flow rate of 10μl/min).
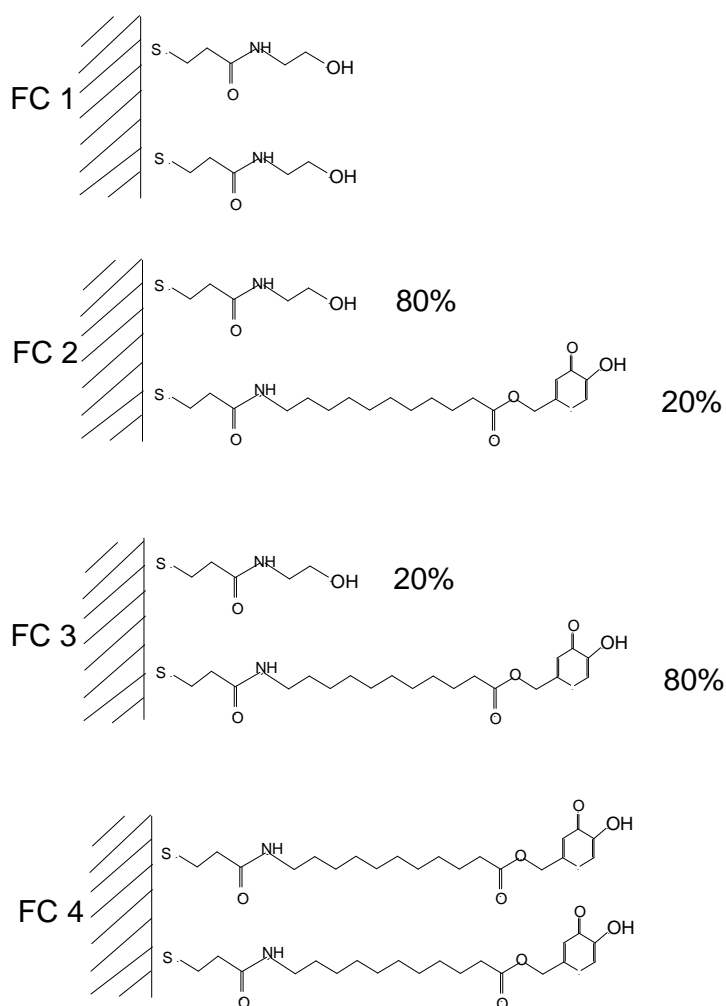

Figure 7.2: Scheme of the modified sensor surface of sensor J3

Investigations according to the character of tyrosinase binding (specific or unspecific) were made as it is described above, but a step is added before the binding experiment started. Tyrosinase (0.5mg/ml, 2mg/ml, 5mg/ml and 7mg/ml) was at first incubated with 2mM tropolone (one of the strongest inhibitors of tyrosinase) for 2 hours at room temperature and then injected in 5mM phosphate buffer, pH=6.5 containing 150mM NaCl and 0.05% TWEEN 20 to the different flow cells.

7.2.2   Measurement systems used for Clark type oxygen electrodes (COE's)

Stationary system   Monoenzyme electrodes (COE_MT_PVA and COE_ST_PVA) as well as bienzyme electrodes (MT/GDH-sensor and ST/GDH-sensor) were fixed into a stirring cell from plexiglas (diameter 6mm, 1ml volume, making by H. Bolien, University of Potsdam). The working platinum electrode (diameter of 0.5mm) with a integrated Ag/AgCl reference electrode (SME 2, Elbau, Berlin, Germany) was covered with a enzyme-membrane (e.g. section 7.2.1), which was embedded between a 10μm thick polyethylene membrane (Metra, Radebeul, Germany) and a 8μm thick regenerated cellulose membrane (BioSensor Technologie, Berlin, Germany). These three membranes were stretched on a separate distance holder before (see Figure 3.12 in paragraph 3.2.2). The in this way prepared biosensor was screwed into the measuring cell containing 1ml of measuring solution and polarised at a potential -600mV (vs. Ag/AgCl reference electrode) using a potentiostat GKM 01 (ZWG, Berlin, Germany). The solution inside the cell was stirred with a magnetic stirrer and transient currents were allowed to decay to a steady-state value. The decrease in current at the electrode upon application of the analyte was monitored by the potentiostat at room temperature and recorded by a chart recorder (Kipp & Zonen, Delft, The Netherlands). Before measurement, the biosensor was incubated for 2h in 50mM sodium phosphate buffer (pH = 6.5). The measurement was made by addition of low volumes of sample solution ($\leq$ 2% of the total volume) after a constant base current of ca 70 ± 10nA has stabilised.

Flow-through set-up   In Figure 7.3 the scheme for the flow-through set-up is shown. Buffer or analyte/buffer mixtures were transported by a peristaltic pump (pump 1 in Figure 7.3, Minipuls 3, Gilson, USA) through the flow cell at a flow rate of 0.3ml/min. The MT/GDH-sensor was polarised at a potential -600mV (vs. Ag/AgCl reference electrode) using a potentiostat GKM 01 (ZWG, Berlin, Germany) and transient currents were allowed to decay to a steady-state value. To stabilise the measurements against varying oxygen concentration, the buffer-mixtures were enriched with air [250]. For this a membrane pump (pump 2 in Figure 7.3, membrane pump 2002G-0206, ASF Thomas, Puchheim, Germany) is used. The measurement was started after about 2h if a constant base current of ca
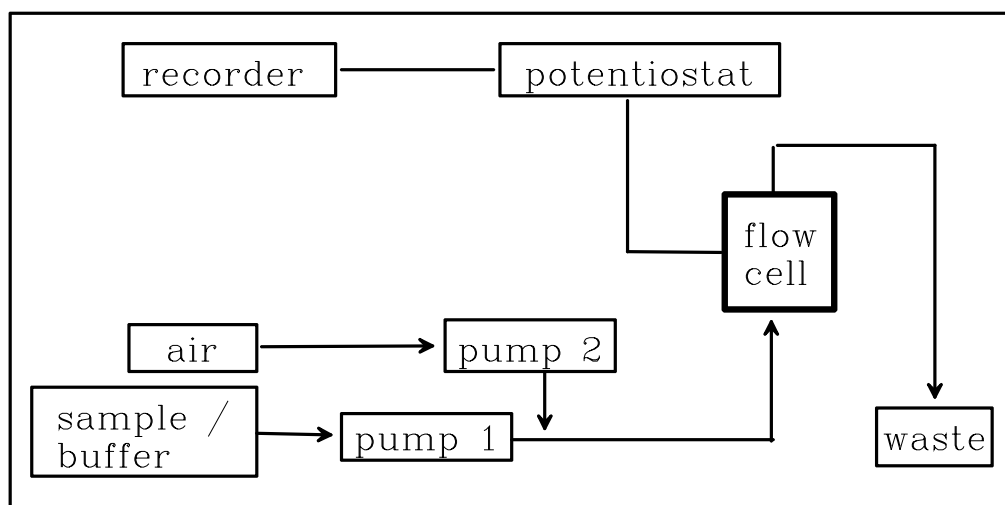
Figure 7.3: Scheme of the Flow-through set-up

7010nA has stabilised. The decrease in current at the electrode upon application of the analyte was monitored by the potentiostat at room temperature and recorded by a chart recorder (Kipp & Zonen, Delft, The Netherlands).

The flow-through set up was also used for inhibitor analysis. Two different measurment methods were applied which were different from each other mainly in the order of the single steps. Both methods are explained in the following:

Method 1 First, the phosphate buffer was exchanged for phosphate buffer containing 10mM glucose. After 5min, the glucose containing phosphate buffer was substituted for phosphate buffer containing 10mM glucose and 100nM catechol (buffer 1). After 10min the inhibitor incubation was performed for 30s by switching to a glucose, catechol and inhibitor containing phosphate buffer (buffer 1 + inhibitor). The sensor was then equilibrated with buffer 1 for (non-inhibited) catechol measurement and the assay can be repeated. The current decrease in the presence of an *inhibitor* was detected.

Method 2 This method was a variation of Method 1 with the following differences:

1. Buffer 1 was substituted by phosphate buffer containing the inhibitor instead of catechol (buffer 2).

2. Different concentrations of catechol (buffer 2 + catechol) were incubated for 30sec instead of the inhibitor.

3. The measuring signal for addition of *catechol* to the inhibitor containing buffer was detected.

The control experiment for catechol without inhibitor is performed after each inhibitor measurement.

7.2.3   Measurement systems used for screen printed electrodes (SPE's)

First the working carbon electrode was covered with a enzyme-membrane (see above paragraph 7.2.1). The prepared biosensors (SPE_MT_N and SPE_MT_PU) were fixed into a stirring cell from plexiglas (diameter 6mm, 1ml volume, making by H. Bolien, University of Potsdam) containing 1ml of measuring solution. The carbon electrode was polarised at a potential -50mV (vs. Ag/AgCl reference electrode) using a potentiostat GKM 01 (ZWG, Berlin, Germany). The solution inside the cell was stirred with a magnetic stirrer and transient currents were allowed to decay to a steady-state value. The increase in current at the electrode upon application of the analyte was monitored by the potentiostat at room temperature and recorded by a chart recorder (Kipp & Zonen, Delft, The Netherlands). Before measurement, the biosensor was incubated for 2h in 50mM sodium phosphate buffer containing 100mM KCl (pH = 6.5). The measurement was made by addition of low volumes of sample solution ($\leq$ 2% of the total volume) after a constant base current has stabilised.

7.3   Procedures

7.3.1   Isolation of *S. antibioticus* tyrosinase, adapted from [1]

The protein was purified according to a modified version of published procedures [18, 238, 245]. The plasmid pIJ703 containing the melC operon encoding tyrosinase from *S. antibioticus* was a kind gift from Prof. Dr. E. Katz [251]. The plasmid was transformed to *S. antibioticus* by Standard Methods [252] and tyrosinase was expressed in 2l medium containing 30g/l oxoid soya broth, 10% w/v sucrose, 50μM cupric sulfate and 5μg/ml thiostrepton. After 28hours of growth, the bacterial mycelium was removed from the growth medium by vacuum filtration using a glass filter (type P2) funnel containing glass wool. Efficient and selective binding of tyrosinase from the growth medium is achieved by diluting the medium ten-fold with water and bringing the pH of the solution to 6.25. The dilution step results in a decrease in the ionic strength of the medium, which otherwise would be too high for the protein to bind to carboxymethylsepharose (in the following called CM). After dilution and changing pH, the CM (equilibrated with 10mM phosphate buffer at pH=6.0) was added to the medium where the total amount added typical constituted 0.5 to 1.0 % of the total volume of the diluted medium.

Tyrosinase bound to CM was filtered on a glass funnel and washed two times with around 100ml of cold 10mM phosphate buffer (pH=6.0). Then the column was poured and equilibrated with 10mM phosphate buffer (pH=6.0). The first elution was started with a linear phosphate gradient (10mM phosphate pH=6.0 to 100mM phosphate pH=7.2, 500ml of each). After concentration of collected fractions, which showing tyrosinase activity, the buffer was exchanged to 10mM phosphate buffer with pH=7.2 by Amicon filtration prior the binding to the second CM column. This time the enzyme was eluted with a linear phosphate gradient (10mM phosphate pH=7.2 to 100mM phosphate pH=7.2, 500ml of each). Again all fractions showing tyrosinase activity were pooled and concentrated to around 25ml by Amicon filtration. Then the buffer was changed to 40mM phosphate buffer with a pH of 7.2 and again the enzym solution was concentrated to around 25ml by Amicon filtration. At the end 20% of glycerol was added and tyrosinase was stored at -80°C.

7.3.2   Determination of the protein concentration

The protein concentration of *S. antibioticus* tyrosinase was determined from the optical absorption at 280nm in 10mM sodium phosphate buffer, pH = 6.8, by using a molar absorption coefficient of $82000M^{-1}cm^{-1}$ according to Jackman et al. [253]. For mushroom tyrosinase the total amount of lyophilisate was used for calculations, e.g. to determine the specific activity. Previous investigations in our group have demonstrated that only ten to fifteen percent of the lyophilisate actually consists of tyrosinase [236]. Also for GDH the total amount of lyophilised enzyme was used for the calculations.

7.3.3   Determination of the specific activity of different enzymes

Tyrosinase

Proline-assay   Proline-assay used for the estimation of the tyrosinase activity in solution is based on the reaction of proline and quinones according to Rezepecki and Waite [50]. For the measurements a cuvette was filled with 1.44ml sodium phosphate buffer (100mM; pH=6.5 containing 1M sodium chloride), 30μl proline (1M) and 15μl catechol solution (10mM). The solutions were mixed in the cuvette for 1 min. To start the assay, 0.5μg to 2.5μg of tyrosinase was added and the solution was stirred again. After 10s, the differential absorption at 525nm was measured using a Beckman DU 640 spectrophotometer (Beckman, USA). The solution containing only 1.44ml sodium phosphate buffer (100mM; pH=6.5 containing 1M sodium chloride), 30μl proline (1M) and 15μl catechol solution (10mM) was used as the reference solution. The stock solutions were stored on

ice in dark containers. Measurements were performed at 22°C. Calculation of activity was based on an extinction coefficient of $5\,400\text{M}^{-1}\text{cm}^{-1}$ for 4-N-prolyl-o-quinone.

Dopachrome-assay   Dopachrome-assay was the Standard Dopachrome Method according to Fling et al. [27]. For the measurements a cuvette was filled with 1ml sodium phosphate buffer (100mM; pH = 6.8) containing 5mM L-dopa. To start the assay, 7.5μg to 22.5μg mushroom or 0.075μg to 0.225μg of Streptomyces antibioticus tyrosinase were added and the solution was mixed in the cuvette for 5sec. Then the increase in absorption at 475nm due to the formation of dopachrome ($\epsilon_{475} = 3\,600\text{M}^{-1}\text{cm}^{-1}$) was monitored as a function of time. The measurements were performed at 22°C and the solution containing only 1ml sodium phosphate buffer (100mM; pH = 6.8) with 5mM L-dopa was used as the reference solution. The activity was expressed as μmol of L-dopa oxidised per minute. For the determination of the pH-optimum of *S. antibioticus* tyrosinase a universal buffer (Davies-buffer) instead of phosphate buffer was used.

GDH

DCIP-assay   Activity was determined spectrophotometrically at room temperature by monitoring the reduction rate of 2,6-dichlorophenolindophenol (DCIP) at 610nm. The activity was expressed as μmol of DCIP reduced per minute based on an extinction coefficient of $21\,000\text{M}^{-1}\text{cm}^{-1}$ at a pH of 7.0 for DCIP [100]. The reaction mixture contained 0.066M Na_2HPO_4/KH_2PO_4 pH=7.0, 100μM $CaCl_2$, 200μM DCIP, 20mM glucose and enzyme 0.03μg to 0.228μg in a total volume of 1ml and the reaction mixture without the enzyme was used as the reference solution.

7.3.4   Determination of the content of phenolic compounds according to DIN 38409-H16-1

500mg copper sulfate were added to 500ml of the water sample under investigation (e.g. river water, see water etc.). (If a investigation of the water sample is not possible in the time of 4 hours (period of time between the sampling and the examination) then one has to acidify the water sample with hydrochloric acid up to a pH value of 4.) Then the pH of the solution was changed by the addition of buffer solution 1 (pH = 10) (perhaps completed by the addition of sodium hydroxide), 3ml aminoantipyrine solution was given to this and the mixture was shook for 30 seconds. In the following 3ml peroxodisulfate solution was added and the mixture was shook for 30 seconds again. This reaction mixture was left light protectedly

for 30 min and after that the resulted dye was extracted by shaking 5 min with 25 ml chloroform. Then the chloroform phase was filtered above 5 g of sodium sulfate into a measuring retort (nominal volume = 25 ml) and the measuring retort was filled up to the marking line by washing with chloroform. The content of phenolic compounds was determined spectrophotometrically at room temperature by measuring the adsorption of the dye at 460nm. For the reference solution destilled water is used instead of the water sample.

buffer solution 1: First 34g ammoniumchloride and 200g tartrate of potassium and sodium were dissolved in 700ml water. Then 150ml ammonia solution ($\varrho = 0.91$g/ml) were added and finally the mixture was filled up with water to 1l.

aminoantipyrine solution: 2g 4-Amino-2,3-dimethyl-1-phenyl-3-pyrazolin-5-on were dissolved in water and the solution was filled up with water to 100ml.

peroxodisulfate solution: 0.65g potassiumperoxosulfate were dissolved in 100ml water.

7.3.5 Cloning of the tyrosinase gene from *S. antibioticus*

Creation of a NdeI site in melC1 10μl PCR buffer (10 x), 4μl dNTPs (2.5mM), 2.5μl primer MEL1-11 (20μM),), 2.5μl primer MEL1-14 (20μM), 10ng plasmid DNA pMEL110 and 2.5U Taq-polymerase were mixed. Then the solution was filled up with water to a final volume of 100μl and the following protocol was used for the temperature cycling:

1 cycle:	1min denaturation at 94°C
20–40 Cycles:	1min 30sec denaturation at 94°C
	1min annealing at 55°C
	2min extension at 72°C
Last cycle:	1min 30sec denaturation at 94°C
	1min 30sec annealing at 55°
	5 min extension at 72°C
	storage on ice

Then the PCR-product was purified, monitored by agarose gel electrophoresis (AGE) and stored in 20μl TE buffer at -20°C.

SDM of melC2

Mega-Primer Method   1994 Picard et al. [243] described this method of a one-tube PCR-based mutagenesis technique. They presented an example where less than 4.5 hours were necessary for the whole procedure because for example a purification of intermediate products was not require. For the tyrosinase DNA the procedure was modified and the intermediate product, the mega- primer (390bp), was purified before the procedure for the fragment (1080bp) started. The single procedures are explained in the following paragraphs.

Synthesis of 390bp mega-primer $10\mu l$ thermo reaction buffer (10 x), $4\mu l$ dNTPs (2.5mM), $2.5\mu l$ primer of pTZ18R ($20\mu M$),), $2.5\mu l$ primer MUT5 ($20\mu M$) and 10ng plasmid DNA pMEL113 digested with HindIII were mixed. Then the solution was filled up with water to a final volume of $100\mu l$ and the following protocol was used for the temperature cycling:

1 cycle:	15min denaturation at 95°C
35 cycles:	1min denaturation at 94°C
	1min annealing at58°C
	2min extension at 72°C
	During the first cycle after the temperature in the tube cooled down up to 58°C the Pfu-polymerase (5U) were added.
Last cycle:	10min extension at 72°C
	storage on ice

The mega-primer was isolated from primers, nucleotides and polymerase by using a QIAquick column (Qiagen, USA) and concentrated up to $48\mu l$. $5\mu l$ of the solution were taken for agarose gel electrophoresis and the other $42\mu l$ were used for the synthesis of the 1080bp fragment, explained in the following section.

Synthesis of the 1080bp fragment $20\mu l$ Q-solution (5 x), $10\mu l$ thermo PCR buffer (10 x), $4\mu l$ dNTPs (5mM), $42\mu l$ mega-primer (solution described above in paragraph 7.3.5),), $2.5\mu l$ primer MELC2-7 ($20\mu M$), 10ng plasmid DNA pMEL113 digested with HindIII and 2.5U Hot Star taq-polymerase (Qiagen, USA) were mixed. Then the solution was filled up with water to a final volume of $100\mu l$ and the following protocol was used for the temperature cycling:

1 cycle:	15min denaturation and activation of Hot Star taq-polymerase at 95°C
35 cycles:	1min denaturation at 94°C
	1min annealing at 58°C
	1min extension at 72°C
Last cycle:	10 min extension at 72°C
	storage on ice

The solution was concentrated up to $20\mu l$ and then stored at -20°C.

References

[1] A. Tepper. *personal communication*. University of Leiden, The Netherlands, 1999.

[2] F. W. Scheller and F. Schubert. *Biosensors*. Elsevier, Amsterdam, The Netherlands, 1992.

[3] A. P. F. Turner, I. Karube, and G. S. Wilson, editors. *Biosensors - fundamentals and applications*. Oxford University Press, Oxford, England, 1987.

[4] U. Wollenberger, F. Schubert, D. Pfeiffer, and F. W. Scheller. Enhancing biosensor performance using multienzyme systems. *Trends in Biotechnology*, 11:255, 1993.

[5] L. C. Clark and C. Lyons. Electrode systems for continuous monitoring in cardiovascular surgery. *Annals of the New York Academy of Sciences*, 102:29, 1962.

[6] F. W. Scheller, D. Pfeiffer, R. Hintsche, I. Dransfeld, U. Wollenberger, and F. Schubert. Analytical aspects of internal signal processing in biosensors. *Annals of the New York Academy of Sciences*, 613:68, 1990.

[7] F. W. Scheller, U. Wollenberger, D. Pfeiffer, A. Makower, M. Paeschke, and B. Neumann. *Elektrochemische biosensoren - grundlagen, anwendungen und perspektiven*, page 201. VCH Verlagsgesellschaft, Weinheim, Germany, 1992.

[8] E. A. H. Hall. *Biosensors*. Open University Press, Manchester, England, 1990.

[9] H. J. Mason, W. B. Fowlks, and E. W. Peterson. Oxygen transfer and electron transport by the phenolase complex. *Journal of the American Chemical Society*, 77:2914, 1955.

[10] H. S. Mason, E. Spencer, and I. Yamazaki. Identification by electron spin resonance spectroscopy of the primary product of tyrosinase - catalyzed catechol oxidation. *Biochemical and Biophysical Research Communications*, 4:236, 1961.

[11] W. Korytowski, T. Sarna, B. Kalyanaraman, and R. C. Sealy. Tyrosinase-catalyzed oxidation of dopa and related catechol(amine)s: a kinetic electron spin resonance investigation using spin stabilization and spin label oximetry. *Biochimica et Biophysica Acta*, 924:383, 1987.

[12] K. Marumo and J. H. Waite. Optimisation of hydroxylation of tyrosine and tyrosine-containing peptides by mushroom tyrosinase. *Biochimica et Biophysica Acta*, 872:98, 1986.

[13] J. G. Cory and E. Frieden. Differential reactivities of tyrosine residues of proteins to tyrosinase. *Biochemistry*, 6:122, 1967.

[14] R. Z. Kazandijan and A. M. Klibanov. Regioselective oxidation of phenols catalysed by polyphenol oxidase in chlorophorm. *Journal of the American Chemical Society*, 107:5448, 1985.

[15] H. W. Duckworth and J. E. Coleman. Physicochemical and kinetic properties of mushroom tyrosinase. *The Journal of Biological Chemistry*, 245:1613, 1970.

[16] K. G. Strothkamp, R. L. Jolley, and H. S. Mason. Quarternary structure of mushroom tyrosinase. *Biochemical and Biophysical research Communications*, 70:519, 1976.

[17] C. W. G. van Gelder, W. H. Flurkey, and H. J. Wichers. Sequence and structural features of plant and fungal tyrosinases. *Phytochemistry*, 45:1309, 1997.

[18] V. Bernan, D. Filpula, W. Herber, M. Bibb, and E. Katz. The nucleotide sequence of the tyrosinase gene from *streptomyces antibioticus* and characterisation of the gene product. *Gene*, 37:101, 1985.

[19] K. Lerch. *Neurospora* tyrosinase: structural, spectroscopic and catalytic properties. *Molecular and Cellular Biochemistry*, 52:125, 1983.

[20] G. L. Woolery, L. Powers, M. Winkler, E. I. Solomon, K. Lerch, and T. G. Spiro. Extended x-ray-absorption fine structure study of the coupled binuclear copper active site of tyrosinase from *neurospora crassa*. *Biochimica et Biophysica Acta*, 788:155, 1984.

[21] L. Bubacco, J. Salgado, A. W. J. W. Tepper, E. Vijgenboom, and G. W. Canters. [1]h nmr spectroscopy of the binuclear cu(ii) active site of *streptomyces antibioticus* tyrosinase. *FEBS Letters*, 442:215, 1999.

[22] S. Bouchilloux, P. McMahill, and H. S. Mason. The multiple forms of mushroom tyrosinase. *The Journal of Biological Chemistry*, 238:1699, 1963.

[23] K. Lerch, C. Longoni, and E. Jordi. Primary structure of tyrosinase from *neurospora crassa*. *The Journal of Biological Chemistry*, 257:6408, 1982.

[24] U. Kupper, D. M. Niedermann, G. Travaglini, and K. Lerch. Isolation and characterisation of the tyrosinase gene from *neurospora crassa*. *The Journal of Biological Chemistry*, 264:17250, 1989.

[25] H. J. Wichers, T. van den Bosch, Y. A. M. Gerritsen, J. I. Oyevaar, M. C. E. M. Recourt, and R. W. Kerrigan. Enzymology and molecular biology of *agaricus bisporus* tyrosinase. *Science and Cultivation of Edible Fungi*, 2:723, 1995.

[26] D. Kertesz and R. Zito. Mushroom polyphenol oxidase: Purification and general properties. *Biochimica et Biophysica Acta*, 96:447, 1965.

[27] M. Fling, N. H. Horowitz, and S. F. Heinemann. The isolation and properties of crystalline tyrosinase from neurospora. *The Journal of Biological Chemistry*, 238:2045, 1963.

[28] M. Jimnez and F. Garcia-Carmona. Hydrogen peroxide-dependent 4-*t*-butylphenol hydroxylation by tyrosinase - a new catalytic activity. *Biochimica et Biophysica Acta*, 1297:33, 1996.

[29] N. Horowitz, M. Fling, and G. Horn. Tyrosinase (*neurospora crassa*). *Methods in Enzymology*, 17:615, 1970.

[30] R. S. Brown, K. B. Male, and J. H. T. Luong. A substrate recycling assay for phenolic compounds using tyrosinase and nadh. *Analytical Biochemistry*, 222:131, 1994.

[31] T. Barman. *Enzyme handbook*, volume 1. Springer, New York, 1969.

[32] A.S.Sussman. A comparison of the properties of two forms of tyrosinase from *neurospora crassa*. *Archives of Biochemistry and Biophysics*, 95:407, 1961.

[33] K. Streffer E. Vijgenboom, A. W. J. W. Tepper, A. Makower, F. W.Scheller, G. W. Canters, and U. Wollenberger. Determination of phenolic compounds using recombinant tyrosinase from *streptomyces antibioticus*. *Analytica Chimica Acta*, 427:201, 2001.

[34] E. S. Krol and J. L. Bolton. Oxidation of 4-alkylphenols and catechols by tyrosinase: ortho-substituents alter the mechanism of quinoid formation. *Chemico-Biological Interactions*, 104:11, 1997.

[35] V. Kahn and R. W. Miller. Tiron as a substrate for mushroom tyrosinase. *Phytochemistry*, 26:2459, 1987.

[36] Y.-H. W. Lee, B.-F. Chen, S.-Y. Wu, W.-M. Leu, J.-J. Lin, C. W. Chen, and S. J. Lo. A *trans*-acting gene is required for the phenotypic expression of a tyrosinase gene in *streptomyces*. *Gene*, 65:71, 1988.

[37] N. C. Eickman, E. I. Solomon, J. A. Larrabee, T. G. Spiro, and K. Lerch. Ultraviolet resonance raman study of oxytyrosinase. comparison with oxyhemocyanins. *Journal of the American Chemical Society*, 100:6529, 1978.

[38] R. S. Himmelwright, N. C. Eickman, C. D. LuBien, K. Lerch, and E. I. Solomon. Chemical and spectroscopic studies of the binuclear copper active site of neurospora tyrosinase: comparison to hemocyanins. *Journal of the American Chemical Society*, 102:7339, 1980.

[39] S. D. Longa, I. Ascone, A. Bianconi, A. Bonfigli, A. C. Castellano, O. Zarivi, and M. Miranda. The binuclear copper site structure of *agaricus bisporus* tyrosinase in solution probed by x-ray absorption spectroscopy. *The Journal of Biological Chemistry*, 271:21025, 1996.

[40] H. Decker and F. Tuczek. Tyrosinase/catecholoxidase activity of hemocyanins: structural basis and molecular mechanism. *Trends in Biochemical Sciences*, 25:392, 2000.

[41] T.-Y. Tsai and Y.-H. W. Lee. Roles of copper ligands in the activation and secretion of streptomyces antibioticus. *The Journal of Biological Chemistry*, 273:19243, 1998.

[42] R. L. Jolley, L. H. Evans, N. Makino, and H. S. Mason. Oxytyrosinase. *The Journal of Biological Chemistry*, 249:335, 1974.

[43] G. M. Jacobson, R. Iskandar, and M. K. Jacobsohn. Activity of mushroom tyrosinase on catechol and on a catechol estrogen in an organic solvent. *Biochimica et Biophysica Acta*, 1202:317, 1993.

[44] J. H. Waite. Calculating extinction coefficients for enzymatically produced o-quinones. *Analytical Biochemistry*, 75:211, 1976.

[45] D. F. Waugh. Protein-protein interactions. *Advances in Protein Chemistry*, 9:325, 1954.

[46] C. R. Dawson and R. J. Magee. Plant tyrosinase (polyphenol oxidase). *Methods in Enzymology*, 2:817, 1955.

[47] F. Richard-Forget F. Gauillard and J. Nicolas. New spectrophotometric assay for polyphenol oxidase activity. *Analytical Biochemistry*, 215:59, 1993.

[48] E. Valero and F. Garcia-Carmona. Kinetic study of a substrate cycle involving a chemical step: highly amplified determination of phenolic compounds. *Journal of Molecular Catalysis B: Enzymatic*, 6:429, 1999.

[49] P. G. Pfifferi and L. Baldassari. A spectrophotometric method for the determination of the catecholase activity of tyrosinase by bestorn's hydrazone. *Analytical Biochemistry*, 52:325, 1973.

[50] L. M. Rzepecki and J. H. Waite. A chromogenic assay for catecholoxidases based on the addition of l-prolin to quinones. *Analytical Biochemistry*, 179:375, 1989.

[51] E. Harel A. M. Mayer and R. Ben-Shaul. Assay of catechol oxidase - a critical comparison of methods. *Phytochemistry*, 5:783, 1966.

[52] G. P. Power and I. M. Ritchie. Electrochemical assay for catecholase activity of mushroom tyrosinase. *Analytical Chemistry*, 54:1985, 1982.

[53] M. H. Smit and G. A. Rechnitz. Benzoic acid determination through competetive inhibition of mediated bioelectrocatalysis. *Electroanalysis*, 5:747, 1993.

[54] C. J. Cooksey, P. J. Garratt, E. J. Land, S. Pavel, C. A. Ramsden, P. A. Riley, and N. P. M. Smit. Evidence of the indirect formation of the catecholic intermediate substrate responsible for the autoactivation kinetics of tyrosinase. *The Journal of Biological Chemistry*, 272:26226, 1997.

[55] E. Valero, R. Varon, and F. Garcia-Carmona. Characterization of polyphenol oxidase from airen grapes. *Journal of Food Science*, 53:1482, 1988.

[56] F. Garcia-Carmona, E. Pedreno, J. D. Galindo, and F. Garcia-Canvas. A new spectrophotometric method for the determination of cresolase activity of epidermis tyrosinase. *Analytical Biochemistry*, 95:433, 1979.

[57] F. Garcia-Canvas, F. Garcia-Carmona, and J: A. Lozano. Hysteresis of mushroom tyrosinase: lag period of cresolase activity. *Phytochemistry*, 20:1215, 1981.

[58] S. H. Pomerantz and M.C. Warner. 3,4-dihydroxy-l-phenylalanine as the tyrosinase cofactor; occurrence in melanoma and binding constant. *The Journal of Biological Chemistry*, 242:5308, 1967.

[59] A. Palumbo, G. Misuraca, M. D'Ischia, and G. Prota. Effect of metal ions on tyrosinase activity. *Biochemistry Journal*, 228:647, 1985.

[60] J. R. Ros, J. N. Rodriguez-Lopez, and F. Garcia-Canvas. Effect of ferrous ions on the monophenolase activity of tyrosinase. *Biochimica et Biophysica Acta*, 1163:303, 1993.

[61] A. Sanchez-Ferrer, J. N. Rodriguez-Lopez, F. Garcia-Canvas, and F. Garcia-Carmona. Tyrosinase: a comprehensive review of its mechanism. *Biochimica et Biophysica Acta*, 1247:1, 1995.

[62] J. Cabanes, F. Garcia-Canvas, J. A. Lozarno, and F. Garcia-Carmona. A kinetic study of the melanization pathway between l-tyrosine and dopachrome. *Biochimica et Biophysica Acta*, 923:187, 1987.

[63] S. Naish-Byfield and P. A. Riley. Oxidation of monohydric phenol substrates by tyrosinase. *Biochemical Journal*, 288:63, 1992.

[64] H. S. Mason. Structures and functions of the phenolase complex. *Nature*, 177:79, 1956.

[65] W. H. Vanneste and A. Zuberbühler. *Molecular mechanism of oxygen activation*, page 371. Academic Press, New York, 1974.

[66] D. E. Wilcox, A. G. Porras, Y. T. Hwang, K. Lerch, M. E. Winkler, and E. I. Solomon. Substrate analogue binding to the coupled binuclear copper active site in tyrosinase. *Journal of the American Chemical Society*, 107:4015, 1985.

[67] J. N. Rodriguez-Lopez, J. Tudela, R. Varn, F. Garcia-Carmona, and F. Garcia-Canvas. Analysis of a kinetic model for melanin biosynthesis pathway. *The Journal of Biological Chemistry*, 267:3801, 1992.

[68] J. G. Schiller and C. C. Liu. Immobilization of tyrosinase within polyacrylamide gels. *Biotechnology and Bioengeneering*, 18:1405, 1976.

[69] B. J. B. Wood and L. L. Ingraham. Labelled tyrosinase from labelled substrate. *Nature*, 205:291, 1965.

[70] C. R. Dawson and W. P. Tarpley. On the pathway of the catechol-tyrosinase reaction. *Annals of the New York Academy of Sciences*, 100:937, 1963.

[71] I. Asimov and C. R. Dawson. On the reaction inactivation of tyrosinase during the aerobic oxidation of catechol. *Journal of the American Chemical Society*, 72:820, 1950.

[72] G. Pfifferi, L. Baldassari, and R. Cultrera. Inhibition by carboxylic acids of an o-diphenol oxidase from *prunus avium* fruits. *Journal of the Science of Food and Agriculture*, 25:263, 1974.

[73] J. R. L. Walker and E. L. Wilson. Studies on the enzymatic browning of apples. inhibition of apple o-diphenol oxidase by phenolic acids. *Journal of the Science of Food and Agriculture*, 26:1825, 1975.

[74] J. R. L. Walker and R. F. McCallion. The selective inhibition of ortho- and para-diphenol oxidases. *Phytochemistry*, 19:373, 1980.

[75] J. S. Conrad, S. R. Dawso, E. R. Hubbard, T. E. Meyers, and K. G. Strothkamp. Inhibitor binding to the binuclear active site of tyrosinase: temperature, ph and solvent deuterium isotope effects. *Biochemistry*, 33:5739, 1994.

[76] C. Billaud, D. Lecornu, and J. Nicolas. Substrates and carboxylic acid inhibitors of a partially purified polyphenol oxidase from gum arabic. *Journal of Agricultural and Food Chemistry*, 44:1668, 1996.

[77] R. C. Hider and K. Lerch. The inhibition of tyrosinase by pyridinones. *Biochemical Journal*, 257:289, 1989.

[78] S. Shirota, K. Miyazaki, R. Aiyama, M. Ichioka, and T. Yokokura. Tyrosinase inhibitors from crude drugs. *Biological and Pharmaceutical Bulletin*, 17:266, 1994.

[79] T. Tada, M. Nomura, K. Shimomura, and Y. Fujihara. Synthesis of karahanaenone derivatives and their inhibition properties toward tyrosinase and superoxide scavenging activity. *Bioscience, Biotechnology and Biochemistry*, 60:1421, 1996.

[80] H. Morita, T. Kayashita, K. Takeya, and H. Itokawa. Conformational analysis of a tyrosinase inhibitory cyclic pentapeptide, pseudostellarin a, from *pseudostellaria heterophylla. Tetrahedron*, 50:12599, 1994.

[81] I. Kubo, I. Kinst-Hori, K. Ishiguro, S. K. Chaudhuri, Y. Sanchez, and T. Ogura. Tyrosinase inhibitory flavanoids from *heterotheca inuloides* and their structural functions. *Bioorganic and Medicinal Chemistry Letters*, 4:1443, 1994.

[82] G. Robinson, D. Leech, and M. R. Smyth. Electrically 'wired' tyrosinase enzyme inhibition electrode for the detection of respiratory poisons. *Electroanalysis*, 7:952, 1995.

[83] X. Hu and Z. Leng. Determination of cyanide using a tyrosinase ampero-metric biosensor with catechol as substrate. *The Analyst*, 120:1555, 1995.

[84] M. G. Peter and U. Wollenberger. *Phenol-oxidizing enzymes: mechanisms and applications in biosensors*, page 63. Birkhäuser Verlag, Basel, Switzerland, 1997.

[85] V. Kahn and A. Andrawis. Inhibition of mushroom tyrosinase by tropolone. *Phytochemistry*, 24:905, 1985.

[86] A. C. Allan and J. R. I. Walker. The selective inhibition of catechol oxidases by salicylhydroxamine acid. *Phytochemistry*, 27:3075, 1988.

[87] J. F. Maddaluno and K. F. Faull. Inhibition of mushrrom tyrosinase by 3-amino-l-tyrosine: Molecular probing of the active site of the enzyme. *Experientia*, 44:885, 1988.

[88] L. Macholan. Phenol-sensitive enzyme electrode with substrate cycling for quantification of certain inhibitory aromatic acids and thio compounds. *Collection of Czechoslovak Chemical Communications*, 55:2152, 1990.

[89] S. Naish-Byfield, C. J. Cooksey, and P. A. Riley. Oxidation of monohydric phenol substrates by tyrosinase: effect of dithiothreitol on kinetics. *Biochemical Journal*, 304:155, 1994.

[90] I. d. Cruz Vieira and O. Fatibello-Filho. L-cystein determination using polyphenol oxidase-based inhibition flow injection procedure. *Analytica Chimica Acta*, 399:287, 1999.

[91] M. Goetghebeur and S. Kermasha. Inhibition of polyphenol oxidase by copper-metallothionein from *aspergillus niger*. *Phytochemistry*, 42:935, 1996.

[92] J. S. Chen, C. Wei, R. S. Rolle, W. S. Otwell, M. O. Balaban, and M. R. Marshall. Inhibitory effect of kojic acid on some plant and crustacean polyphenol oxydases. *Journal of Agricultural and Food Chemistry*, 39:1396, 1991.

[93] J. S. Chen, C. Wei, and M. R. Marshall. Inhibition mechanism of kojic acid on polyphenol oxydase. *Journal of Agricultural and Food Chemistry*, 39:1897, 1991.

[94] J. Cabanes, S. Chazarra, and F. Garcia-Carmona. Kojic acid, a cosmetic skin whitening agent, is a slow-binding inhibitor of catecholase activity of tyrosinase. *Journal of Pharmacy and Pharmacology*, 46:982, 1994.

[95] Y. Kobayashi, H. Kayahara, K. Tadasa, T. Nakamura, and H. Tanaka. Synthesis of amino acid derivatives of kojic acid and their tyrosinase inhibitory activity. *Bioscience, Biotechnology and Biochemistry*, 59:1745, 1995.

[96] Y. Kobayashi, H. Kayahara, K. Tadasa, and H. Tanaka. Synthesis of n-kojic amino acid and n-kojic amino acid kojiate and their tyrosinase inhibitory activity. *Bioorganic and Medicinal Chemistry Letters*, 6:1303, 1996.

[97] Y. Hasebe, K. Oshima, O. Takise, and S. Uchiyama. Chemically amplified kojic acid responses of tyrosinase-based biosensor, based on inhibitory effect to substrate recycling driven by tyrosinase and l-ascorbic acid. *Talanta*, 42:2079, 1995.

[98] J.-L. Besombes, S. Cosnier, P. Labbe, and G. Reverdy. A biosensor as warning device for the detection of cyanide, chlorophenols, atrazine and carbamate pesticides. *Analytica Chimica Acta*, 311:255, 1995.

[99] D. Barcelo. *Environmental analysis: techniques, applications and quality assurance*. Elsevier, Amsterdam, The Netherlands, 1993.

[100] J. G. Hauge. Purification and properties of glucose dehydrogenase and cytochrome b from *bacterium anitratum. Biochimica et Biophysica Acta*, 45:250, 1960.

[101] P. Dokter, J. Franz, and J. A. Duine. Purification and characterisation of quinoprotein glucose dehydrogenase from *acinetobacter calcoaceticus* l.m.d. 79.41. *Biochemical Journal*, 239:163, 1986.

[102] P. Dokter, J. T. Pronk, B.J. van Schie, J. P. van Dijken, and J. A. Duine. The in vivo and in vitro substrate specificity of quinoprotein glucose dehydrogenase from *acinetobacter calcoaceticus* l.m.d. 79.41. *FEMS Microbiological Letters*, 43:195, 1987.

[103] K. Matsushita, E. Shinagawa, O. Adachi, and M. Ameyama. *Quinoprotein D-glucose dehydrogenase in Actinobacter calcoaceticus LMD 79.41: purification and characterisation of the membrane-bound enzyme distinct from the soluble enzyme in: pqq and quinoproteins*, page 122. Kluwer Academic Publishers, Dordrecht, The Netherlands, 1989.

[104] J. A. Duine, J. J. Frank, and J. K. van Zeeland. Glucose dehydrogenase from *acinetobacter calcoaceticus. FEBS Letters*, 108:443, 1979.

[105] J. G. Hauge. Glucose dehydrogenase of *bacterium anitratum*: an enzyme with a novel prosthetic group. *The Journal of Biological Chemistry*, 239:3630, 1964.

[106] A. L. Ghindilis, A. Makower, and F. W. Scheller. Nanomolar determination ofthe ferrocene derivatives using a recycling enzyme electrode. *Analytical Letters*, 28:1, 1995.

[107] F. Mizutani, S. Yabuki, and M. Asai. Highly-sensitive measurement of hydroquinone with an enzyme electrode. *Biosensors and Bioelectronics*, 6:305, 1991.

[108] A. V. Eremenko, A. Makower, and F. W. Scheller. Measurement of nanomolar diphenols by substrate recycling coupled to a ph-sensitive electrode. *Fresenius' Journal of Analytical Chemistry*, 351:729, 1995.

[109] U. Wollenberger and B. Neumann. Quinoprotein glucose dehydrogenase modified carbon paste electrode for the detection of phenolic compounds. *Electroanalyis*, 9:366, 1997.

[110] C. Anthony. *The role of quinoproteins in bacterial energy transduction*, page 223. Marcel Dekker, New York, 1993.

[111] K. Matsushita, E. Shinagawa, O. Adachi, and M. Ameyama. Quinoprotein d-glucose dehydrogenase of the *actinobacter calcoaceticus* respiratory chain: membran-bound and soluble forms are different molecular species. *Biochemistry*, 28:6276, 1989.

[112] P. Dokter, J. E. van Wielink, M. A. G. Kleef, and J. A. Duine. Cytochrome b-562 from *acinetobacter calcoaceticus* l.m.d. 79.41. *Biochemical Journal*, 254:131, 1988.

[113] A. Geerlof, P. Dokter, J. E. van Wielink, and J. A. Duine. Haem-containing protein complexes of *actinetobacter calcoaceticus* as secondary electron acceptors for quinoprotein glucose dehydrogenase. *Antonie van Leeuwenhoek*, 56:81, 1989.

[114] O. Geiger and H. Görisch. Reversible thermal inactivation of the quinoprotein glucose dehydrogenase from *acinetobacter calcoaceticus*. *Biochemical Journal*, 261:415, 1989.

[115] A. Oubrie, H. J. Rozeboom, K. H. Kalk, J. A. Duine, and B. W. Dijkstra. The 1.7 a crystal structure of the apo form of the soluble quinoprotein glucose dehydrogenase from acinetobacter calcoaceticus reveals a novel internal conserved sequence repeat. *Journal of Molecular Biology*, 289:319, 1999.

[116] A. J. J. Olsthoorn and J. A. Duine. On the mechanism and specificity of the soluble, quinoprotein glucose dehydrogenase in the oxidation of aldose sugars. *Biochemistry*, 37:13854, 1998.

[117] A. Oubrie, H. J. Rozeboom, K. H. Kalk, A. J. J. Olsthoorn, J. A. Duine, and B. W. Dijkstra. Structure and mechanism of soluble quinoprotein glucose dehydrogenase. *The EMBO Journal*, 18:5187, 1999.

[118] G. G. Guilbault. *Handbook of enzymatic methods of analysis*. Marcel Decker, New York, United States of America, 1976.

[119] F. W. Scheller, F. Schubert, D. Pfeiffer, R. Hintsche, I. Dransfeld, R. Renneberg, U. Wollenberger, K. Riedel, M. Pavlova, M. Kühn, H. G. Müller, P. Tan, W. Hoffmann, and W. Moritz. Research and development of biosensors - a review. *The Analyst*, 114:653, 1989.

[120] R. P. Buck, W. E. Hatfield, M. Umana, and E. F. Bowden, editors. *Biosensor technology - fundamentals and applications*. Marcel Decker, New York, United States of America, 1990.

[121] R. S. Sethi. Transducer aspects of biosensors. *Biosensors and Bioelectronics*, 9:243, 1994.

[122] M. P. Byfield and R. A. Abuknesha. Biochemical aspects of biosensors. *Biosensors and Bioelectronics*, 9:373, 1994.

[123] M. A. T. Gilmartin and J. P. Hart. Sensing with chemically and biologically modified carbon electrodes. *The Analyst*, 120:1029, 1995.

[124] N. Gajovic. *PhD Thesis*. University of Potsdam, Germany, 1999.

[125] W. Hartmeier. *Immobilisierte Biokatalysatoren*. Springer, Berlin, Germany, 1986.

[126] J. Woodward, editor. *Immobilised cells and enzymes*. IRL Press, Oxford, England, 1985.

[127] L. Gorton. Carbon paste electrodes modified with enzymes, tissues and cells. *Electroanalysis*, 7:23, 1995.

[128] W. H. Scouten, J. H. T. Luong, and R. S. Brown. Enzyme or protein immobilization techniques for applications in biosensor design. *Trends in Biotechnology*, 13:178, 1995.

[129] A. Walcarius. Analytical applications of silica-modified electrodes -a comprehensive review. *Electroanalysis*, 10:1217, 1998.

[130] U. Wollenberger. Electrochemical biosensors - ways to improve sensor performance. *Biotechnology and Genetic Engineering Reviews*, 13:237, 1995.

[131] T. Schulmeister. Mathematical treatment of concentration profiles and anodic current of amperometric enzyme electrodes with chemically-amplified response. *Analytica Chimica Acta*, 201:305, 1987.

[132] J. J. Kulis, V. V. Sorochinskii, and R. A. Vidziunaite. Transient response of bienzyme electrodes. *Biosensors*, 2:135, 1986.

[133] F. Liu, A. J. Reviejo, J. M. Pingarron, and J. Wang. Development of an amperometric biosensor for the determination of phenolic compounds in reversed micelles. *Talanta*, 41:455, 1994.

[134] A. J. Reviejo, C. Fernandez, F. Liu, J. M. Pingarron, and J. Wang. Advances in amperometric enzyme electrodes in reversed micelles. *Analytica Chimica Acta*, 315:93, 1995.

[135] J. M. Pingarron. Development of amperometric enzyme electrodes in reversed micelles media. *Journal de Chimie Physique et de Physico-Chimie Biologique*, 93:793, 1996.

[136] M. T. P. Pita, A. J. Reviejo, F. J. M. de Villena, and J. M. Pingarron. Amperometric selective biosensing of dimethyl- and diethyldithiocarbamates based on inhibition processes in a medium of reversed micelles. *Analytica Chimica Acta*, 340:89, 1997.

[137] F. Ortega, E. Dominguez, E. Burestedt, J. Emneus, L. Gorton, and G. Marko-Varga. Phenol oxidase-based biosensors as selective detection units in column liquid chromatography for the determination of phenolic compounds. *Journal of Chromatography A*, 675:65, 1994.

[138] J. Kulys and R. D. Schmid. A sensitive enzyme electrode for phenol monitoring. *Analytical Letters*, 23:589, 1990.

[139] P. Skladal. Mushroom tyrosinase-modified carbon paste electrode as an amperometric biosensor for phenols. *Collection of Czechoslovak Chemical Communications*, 56:1427, 1991.

[140] J. Wang, Y. Lin, and L. Chen. Organic phase biosensors for monitoring phenol and hydrogen peroxid in pharmaceutical antibacterial products. *The Analyst*, 118:277, 1993.

[141] J. Wang, Y. Lin, and L. Chen. Organic phase biosensors based on the entrapment of enzymes within poly(ester-sulfonic acid) coatings. *Electroanalysis*, 5:23, 1993.

[142] J. Wang and J. Reviejo. Organic-phase enzyme electrode for the determination of trace water in nonaqueous media. *Analytical Chemistry*, 65:845, 1993.

[143] J. Wang, E. Dempsey, A. Eremenko, and M. R. Smith. Organic-phase biosensing of enzyme inhibitors. *Analytica Chimica Acta*, 279:203, 1993.

[144] E. I. Iwuoha, O. Adeyoju, E. Dempsey, M. R. Smyth, J. Lui, and J. Wang. Investigation of the effects of polar organic solvents on the activity of tyrosinase entrapped in a poly(ester-sulphonic acid) polymer. *Biosensors and Bioelectronics*, 10:661, 1995.

[145] C. Nistor, J. Emneus, L. Gorton, and A. Ciucu. Improved stability and altered selectivity of tyrosinase based graphite electrodes for detection of phenolic compounds. *Analytica Chimica Acta*, 387:309, 1999.

[146] J. Wang and Q. Chen. Highly sensitive biosensing of phenolic compounds using bioaccumulation/chronoamperometry at a tyrosinase electrode. *Electroanalysis*, 7:746, 1995.

[147] Q. Deng and S. Dong. Construction of a tyrosinase-based biosensor in pure organic phase. *Analytical Chemistry*, 67:1357, 1995.

[148] Q. Deng, Y. Guo, and S. Dong. Cryo-hydrogel for the construction of a tyrosinase-based biosensor. *Analytica Chimica Acta*, 319:71, 1996.

[149] Q. Deng and S. Dong. The effect of substrate and solvent properties on the response of an organic phase tyrosinase electrode. *Journal of Electroanalytical Chemistry*, 435:11, 1997.

[150] G. E. De Benedetto, F. Palmisano, and P. G. Zambonin. Flow-through tyrosinase enzyme reactor based on reticulated vitreous carbon functionalized by an electrochemically synthesized film. *Analytica Chimica Acta*, 326:149, 1996.

[151] H. Kotte, B. Gründig, K. D. Vorlop, B. Strehlitz, and U. Stottmeister. Methylphenazonium-modified enzyme sensor based on polymer thick films for subnanomolar detection of phenols. *Analytical Chemistry*, 67:65, 1995.

[152] J. Parellada, A. Narvaez, M. A. Lopez, E. Dominguez, J. J. Fernandez, V. Pavlov, and I. Katakis. Amperometric immunosensors and enzyme electrodes for environmental applications. *Analytica Chimica Acta*, 362:47, 1998.

[153] B. Wang, B. Zhang, and S. Dong. Silica sol-gel composite film as an encapsulation matrix for the construction of an amperometric tyrosinase-based biosensor. *Biosensors and Bioelectronics*, 15:397, 2000.

[154] B. Wang and S. Dong. Organic-phase enzyme electrode for phenolic determination based on a functionalised sol-gel composite. *Journal of Electroanalytical Chemistry*, 487:45, 2000.

[155] S. Cosnier and C. Innocent. A new strategy for the construction of a tyrosinase-based amperometric phenol and o-diphenol sensor. *Bioelectrochemistry and Bioenergetics*, 31:147, 1993.

[156] S. Cosnier, A. Lepellec, B. Guidetti, and I. Rico-Lattes. Enhancement of biosensor sensitivity in aqueous and organic solvents using a combination of poly(pyrrole-ammonium) and poly(pyrrole-lactobionamide) films as host matrixes. *Journal of Electroanalytical Chemistry*, 449:165, 1998.

[157] S. Cosnier, J. J. Fombon, P. Labbe, and D. Limosin. Development of a ppo-poly(amphiphilic pyrrole) electrode for on site monitoring of phenol in aqueous effluents. *Sensors and Actuators B*, 59:134, 1999.

[158] J.-L. Besombes, S. Cosnier, and P. Labbe. Improvement of poly (amphiphillic pyrrole) enzyme electrodes via the incorporation of synthetic laponite- clay-nanoparticles. *Talanta*, 44:2209, 1997.

[159] E. A. Cummings, S. Linquette-Mailley, P. Mailley, S. Cosnier, and E. T. McAdams. A comperison of amperometric screen-printed, carbon electrodes and their application to the analysis of phenolic compounds present in beers. *Talanta*, 55:1015, 2001.

[160] J. Wang, V. B. Nascimento, S. A. Kane, K. Rogers, M. R. Smith, and L. Angnes. Screen-printed tyrosinase-containing electrodes for the biosensing of enzyme inhibitors. *Talanta*, 43:1903, 1996.

[161] M. Lutz, E. Burestedt, J. Emneus, H. Liden, S. Gobhadi, L. Gorton, and G. Marko-Varga. Effects of different additives on a tyrosinase based carbon paste electrode. *Analytica Chimica Acta*, 305:8, 1995.

[162] E. Burestedt, J. Emneus, L. Gorton, G. Marko-Varga, E. Dominguez, F. Ortega, A. Narvaez, H. Irth, M. Lutz, D. Puig, and D. Barcelo. Optimisation and validation of an automated solid phase extraction technique coupled on-line to enzyme-based biosensor detection for the determination of phenolic compounds in surface water samples. *Chromatographia*, 41:207, 1995.

[163] A. Lindgren, T. Ruzgas, J. Emneus, E. Csöregi, L. Gorton, and G. Marko-Varga. Flow injection analysis of phenolic compounds with carbon paste electrodes modified with tyrosinase purchased from different companies. *Analytical Letters*, 29:1055, 1996.

[164] M. B. Moressi, A. Zon, H. Fernandez, G. Rivas, and V. Solis. Amperometric quantification of alternaria mycotoxins with a mushroom tyrosinase modified carbon paste electrode. *Electrochemistry Communications*, 1:472, 1999.

[165] S. Ito, S. Yamazaki, K. Kano, and T. Ikeda. Highly sensitive electrochemical detection of alkaline phosphatase. *Analytica Chimica Acta*, 424:57, 2000.

[166] M. L. Pedano and G. A. Rivas. Amperometric biosensor for the quantification of gentisic acid using polyphenol oxidase modified carbon paste electrode. *Talanta*, 53:489, 2000.

[167] C. Petit, A. Gonzalez-Cortes, and J.-M. Kauffmann. Preparation and characterization of a new enzyme electrode based on solid paraffin and activated graphite particles. *Talanta*, 42:1783, 1995.

[168] A. I. Yaropolov, A. N. Kharybin, J. Emneus, G. Marko-Varga, and L. Gorton. Flow-injection analysis of phenols at a graphite electrode modified with co-immobilised laccase and tyrosinase. *Analytica Chimica Acta*, 308:137, 1995.

[169] J. Li, L. S. Chia, N. K. Goh, and S. N. Tan. Silica sol-gel immobilised amperometric biosensor for the determination of phenolic compounds. *Analytica Chimica Acta*, 362:203, 1998.

[170] A. Kaisheva, I. Iliev, S. Christov, and R. Kazareva. Electrochemical gas biosensor for phenol. *Sensors and Actuators B*, 44:571, 1997.

[171] F. Ortega, E. Dominguez, G. Jönsson-Pettersson, and L. Gorton. Amperometric biosensor for the detection of phenolic compounds using a tyrosinase graphite electrode in a flow injection system. *Journal of Biotechnology*, 31:289, 1993.

[172] W. R. Everett and G. A. Rechnitz. Mediated bioelectrocatalytic determination of organophosphorus pesticides with a tyrosinase-based oxygen biosensor. *Analytical Chemistry*, 70:807, 1998.

[173] J. Wang, F. Lu, and D. Lopez. Tyrosinase-based ruthenium dispersed carbon paste biosensor for phenols. *Biosensors and Bioelectronics*, 9:9, 1994.

[174] F. Schubert, S. Saini, A. P. F. Turner, and F. Scheller. Organic phase enzyme electrodes for the determination of hydrogen peroxid and phenol. *Sensors and Actuators B*, 7:408, 1992.

[175] L. Campanella, M. P. Sammartino, and M. Tomassetti. New enzyme sensor for phenol determination in non-aqueous and aqueous medium. *Sensors and Actuators B*, 7:383, 1992.

[176] L. Campanella, G. Favero, M. P. Sammartino, and M. Tomassetti. The effect of organic solvent properties on the response of a tyrosinase enzyme sensor. *Talanta*, 41:1015, 1994.

[177] L. Campanella, A. Fortuney, M. P. Sammartino, and M. Tomassetti. Tyrosinase biosensor response as a function of physical properties of organic solvents. *Talanta*, 41:1397, 1994.

[178] L. Stancik, L. Macholan, and F. Scheller. Biosensing of tyrosinase inhibitors in nonaqueous solvents. *Electroanalysis*, 7:649, 1995.

[179] F. Lisdat, U. Wollenberger, A. Makower, H. Hörtnagel, D. Pfeiffer, and F. W. Scheller. Catecholamine detection using enzymatic amplification. *Biosensors and Bioeletronics*, 12:1199, 1997.

[180] L. Campanella, T. Beone, M. P. Sammartino, and M. Tomassetti. Determination of phenol in wastes and water using an enzyme sensor. *The Analyst*, 118:979, 1993.

[181] L. Campanella, G. Favero, M. Pastorino, and M. Tomassetti. Monitoring the rancidification process in olive oils using biosensor operating in organic solvents. *Biosensors and Bioelectronics*, 14:179, 1999.

[182] L. Campanella, G. Favero, M. P. Sammartino, and M. Tomassetti. Further development of catalase, tyrosinase and glucose oxidase based organic phase enzyme elctrode response as a function of organic solvent properties. *Talanta*, 46:595, 1998.

[183] L. Campanella, G. Favero, M. P. Sammartino, and M. Tomassetti. Analysis of several real matrices using new mono-, bi-enzymatic, or inhibition organic phase enzyme electrodes. *Analytica Chimica Acta*, 393:109, 1999.

[184] Y. Hasebe, K. Yokobori, K. Fukasawa, T. Kogure, and S. Uchiyama. Highly sensitive electrochemical determination of *escherichia coli* density using tyrosinase-based chemically amplified biosensor. *Analytica Chimica Acta*, 357:51, 1997.

[185] H. Kaatz, K. Streffer, U. Wollenberger, and M. G. Peter. Inhibition of mushroom tyrosinase by kojic acid octanoates. *Zeitschrift für Naturforschung*, 54c:70, 1999.

[186] A. Makower, A. V. Eremenko, K. Streffer, U. Wollenberger, and F. W. Scheller. Tyrosinase-glucose dehydrogenase substrate-recycling biosensor: A highly-sensitive measurement of phenolic compounds. *Journal of Chemical Technology and Biotechnology*, 65:39, 1996.

[187] C. Capannesi, I. Palchetti, M. Mascini, and A. Parenti. Electrochemical sensor and biosensor for polyphenols detection in olive oils. *Food Chemistry*, 71:553, 2000.

[188] T. M. Anh, S. V. Dzyadevych, A. P. Soldatkin, N. D. Chien, N. Jaffrezic-Renault, and J. M. Chovelon. Development of tyrosinase biosensor based on ph-sensitive field-effect transistors for phenols determination in water solution. *Talanta*, 56:627, 2002.

[189] S. Wada, J. Ichikawa, and K. Tatsumi. Removal of phenols from wastewater by soluble and immobilised tyrosinase. *Biotechnology and Bioengineering*, 42:854, 1993.

[190] J. Wang and Q. Chen. Remote electrochemical biosensor for field monitoring of phenolic compounds. *Analytica Chimica Acta*, 312:39, 1995.

[191] J. Wang, L. Fang, and D. Lopez. Amperometric biosensor for phenols based on a tyrosinase-graphite-epoxy biocomposite. *The Analyst*, 119:455, 1994.

[192] P. Önnerfjord, J. Emneus, G. Marko-Varga, and L. Gorton. Tyrosinase graphite-epoxy based composite electrodes for detection of phenols. *Biosensors and Bioelectronics*, 10:607, 1995.

[193] M. Lutz and E. Dominguez. Development and optimization of a solid composite tyrosinase biosensor for phenol detection in flow injection systems. *Electroanalysis*, 8:117, 1996.

[194] D. Puig, T. Ruzgas, J. Emneus, L. Gorton, G. Marko-Varga, and D. Barcelo. Characterization of tyrosinase-teflon/graphite composite electrodes for the determination of catechol in environmental analysis. *Electroanalysis*, 8:885, 1996.

[195] Z. Yang and D. A. Robb. Comparison of tyrosinase activity and stability in aqueous and nearly nonaqueous environments. *Enzyme and Microbial Technology*, 15:1030, 1993.

[196] J. S. Dordick. Designing enzymes for use in organic solvents. *Biotechnology Progress*, 8:259, 1992.

[197] E. I. Iwuoha, M. R. Smyth, and M. E. G. Lyons. Organic phase enzyme electrodes: kinetics and analytical applications. *Biosensors and Bioelectronics*, 12:53, 1997.

[198] S. H. M. van Erp, E. O. Kamenskaya, and Y. L. Khmelnitsky. The effect of water content and nature of organic solvent on enzyme activity in low-water media. *European Journal of Biochemistry*, 202:379, 1991.

[199] G. A. Rechnitz. Bioselective membrane electrode probes. *Science*, 214:287, 1981.

[200] F. Mazzei, F. Botre, M. Lanzi, G. Lorenti, F. Porcelli, and C. Botre. Plant metabolism as an analytical tool: some applications of plant tissue electrodes for the selective determination of catecholamines. *Sensors and Actuators B*, 7:427, 1992.

[201] J. Wang, N. Naser, H. S. Kwon, and M. Y. Cho. Tissue bioelectrode for organic-phase enzymatic assays. *Analytica Chimica Acta*, 264:7, 1992.

[202] S. Canofeni, S. Di Sario, J. Mela, and R. Pilloton. Comparison of immobilisation procedures for development of an electrochemical ppo-based biosensor for on line monitoring of a depuration process. *Analytical Letters*, 27:1659, 1994.

[203] Y. Chen and T. C. Tan. Dopamine-sensing efficacy and characteristics of pretreated plant tissue powder sensors. *Sensors and Actuators B*, 28:39, 1995.

[204] Y. Chen and T. C. Tan. Dopamine-sensing and selectivity of nafion-coated plant tissue powder sensors. *Talanta*, 42:1181, 1995.

[205] F. Botre, F. Mazzei, M. Lanzi, G. Lorenti, and C. Botre. Plant-tissue electrode for the determination of catechol. *Analytica Chimica Acta*, 255:59, 1991.

[206] S. Uchiyama, Y. Hasebe, H. Shimizu, and H. Ishihara. Enzyme-based catechol sensor based on the cycling reaction between catechol and 1,2-benzoquinone, using l-ascorbate and tyrosinase. *Analytica Chimica Acta*, 276:341, 1993.

[207] E. S: Forzani, G. A. Rivas, and V. M. Solis. Amperometric determination of dopamine on an enzymatically modified carbon paste electrode. *Journal of Electroanalytical Chemistry*, 382:33, 1995.

[208] A. Navaratne, M. S. Lin, and G. A. Rechnitz. Eggplant-based bioamperometric sensor for the detection of catechol. *Analytica Chimica Acta*, 237:107, 1990.

[209] Z. Lin, W. Qiao, and M. Wu. The preparation of a spinach tissue-based carbon paste microelectrode and its performance in pharmacokinetic experiments in vivo. *Analytical Letters*, 25:1171, 1992.

[210] Y. Chen and T. C. Tan. Selectivity enhancement of an immobilised apple powder enzymatic sensor for dopamine. *Biosensors and Bioelectronics*, 9:401, 1994.

[211] O. Fatibello-Filho and I. d. Cruz Vieira. Flow injection spectrophotometric determination of l-dopa and carbidopa in pharmaceutical formulations using a crude extract of sweet potato root (*ipomoea batatas (l.) lam.*) as enzymatic source. *The Analyst*, 122:345, 1997.

[212] I. d. Cruz Vieira and O. Fatibello-Filho. Flow injection spectrophotometric determination of total phenols using crude extract of sweet potato root (*ipomoea batatas* (l.) lam.) as enzymatic source. *Analytica Chimica Acta*, 366:111, 1998.

[213] S. Uchiyama and S. Suzuki. Flow-injection determination of polyphenols using a plant juice carrier. *Analytica Chimica Acta*, 261:361, 1992.

[214] R. Rella, D. Ferrara, G. Barison, L. Doretti, and S. Lora. High-temperature operating biosensor for the determination of phenol and related compounds. *Biotechnology and Applied Biochemistry*, 24:83, 1996.

[215] E. I. Rainina, I. E. Badalian, O. V. Ignatov, A. Y. Fedorov, A. L. Simonian, and S. D. Varfolomeyev. Cell biosensor for detection of phenol in aqueous solution. *Applied Biochemistry and Biotechnology*, 56:117, 1996.

[216] K. Riedel, J. Hensel, S. Rothe, B. Neumann, and F. Scheller. Microbial sensors for determination of aromatics and their chloroderivatives. *Journal of Applied Microbiology and Biotechnology*, 38:556, 1993.

[217] G. P. Evans, M. G. Briers, and D. M. Rawson. Can biosensors help to protect drinking water? *Biosensors*, 2:287, 1986.

[218] M. J. Christophersen and T. J. Cardwell. Determination of total phenols in waters and wastewaters using flow injection with electrochemical detection; an alternative to the standard colorimetric procedure. *Analytica Chimica Acta*, 323:39, 1996.

[219] K. Schmidt-Bäumler, T. Heberer, and H. J. Stan. Occurence and distribution of organic contaminants in the aquatic system in berlin. part ii: substituted phenols in berlin surface water. *Acta hydrochimica et hydrobiologica*, 27:143, 1999.

[220] C. Martin and E. Dominguez. A new enzyme electrode for quantification of salicylic acid in a fia system. *Journal of Pharmaceutical and Biomedical Analysis*, 19:107, 1999.

[221] C. G. Bauer, A. V. Eremenko, E. Ehrentreich-Förster, F. F. Bier, A. Makower, H. B. Halsall, W. R. Heinemann, and F. W. Scheller. Zeptomole-detection biosensor for alkaline phophatase in an electrochemical immunoassay for 2,4- dichlorophenoxyacetic acid. *Analytical Chemistry*, 68:2453, 1996.

[222] J. Norberg, J. Emneus, J. A. Jönsson, L. Mathiasson, E. Burestedt, M. Knutsson, and G. Marko-Varga. On-line supported liquid membrane-liquid chromatography with a phenol oxidase-based biosensor as a selective detection unit for the determination of phenols in blood plasma. *Journal of Chromatography B*, 701:39, 1997.

[223] J. Wang, F. Lu, S. A. Kane, Y. K. Choi, M. R. Smith, and K. Rogers. Hydrocarbon pasting liquids for improved tyrosinase-based carbon-paste phenol biosensors. *Electroanalysis*, 9:1102, 1997.

[224] N. Pena, A. J. Reviejo, and J. M. Pingarron. Detection of phenolic compounds in flow systems based on tyrosinase-modified reticulated vitreous carbon electrodes. *Talanta*, 55:179, 2001.

[225] K. R. Rogers, J. Y. Becker, J. Cembrano, and S. H. Chough. Viscosity and binder composition effects on tyrosinase-based carbon paste electrode for detection of phenol and catechol. *Talanta*, 54:1059, 2001.

[226] P. Dantoni, S. H. P. Serrano, A. M. O. Brett, and I. G. R: Gutz. Flow-injection determination of catechol with a new tyrosinase/dna biosensor. *Analytica Chimica Acta*, 366:137, 1998.

[227] S. Cosnier and I. C. Popescu. Poly(amphiphilic pyrrole)-tyrosinase-peroxidase electrode for amplified flow injection-amperometric detection of phenol. *Analytica Chimica Acta*, 319:145, 1996.

[228] T. Huang, A. Warsinke, T. Kuwana, and F. W. Scheller. Determination of l-phenylalanine based on a nadh-detecting biosensor. *Analytical Chemistry*, 70:991, 1998.

[229] M. Bonakdar, J. L. Vilchez, and H. A. Mottola. Bioamperometric sensors for phenol based on carbon paste electrodes. *Journal of Electroanalytical Chemistry*, 266:47, 1989.

[230] M. H. Smit and G. A. Rechnitz. Toxin detection using a tyrosinase-coupled oxygen electrode. *Analytical Chemistry*, 65:380, 1993.

[231] I. M. Roberts, S. L. Jones, R. R. Premier, and J. C. Cox. A comparison of the sensitivity and specificity of enzyme immunoassays and time-resolved fluoroimmunoassay. *Journal of Immunological Methods*, 143:49, 1991.

[232] M. Hedenmo, A. Narvaez, E. Dominguez, and I. Katakis. Improved mediated tyrosinase amperometric enzyme electrodes. *Journal of Electroanalytical Chemistry*, 425:1, 1997.

[233] O. Adeyoju, E. I. Iwuoha, M. R. Smyth, and D. Leech. High-performance liquid chromatographic determination of phenols using a tyrosinase-based amperometric biosensor detection system. *The Analyst*, 121:1885, 1996.

[234] F. Daigle and D. Leech. Reagentless tyrosinase enzyme electrodes: effects of enzyme loading, electrolyte ph, ionic strength and temperature. *Analytical Chemistry*, 69:4108, 1997.

[235] F. Daigle, F. Trudeau, G. Robinson, M. R. Smit, and D. Leech. Mediated reagentless enzyme inhibition electrodes. *Biosensors and Bioelectronics*, 13:417, 1998.

[236] A. Makower. *personal communication*. University of Potsdam, Germany, 1999.

[237] S. Haebel. *personal communication*. University of Potsdam, Germany, 1997.

[238] K. Lerch and L. Ettlinger. Purification and characterisation of a tyrosinase from *streptomyces glaucescens*. *European Journal of Biochemistry*, 31:427, 1972.

[239] S. Nagai and T.Izumi. *Japanese Patent Application*, 79/82:257, 1979.

[240] Y. Hasebe, Y. Tanaka, and S. Uchiyama. Highly amplified spectrophotometry of polyphenols based on a cyclic reaction between polyphenols and o-quinone compounds using tyrosinase and l-ascorbic acid. *Analytical Letters*, 27:127, 1994.

[241] A. L. Ghindilis, A. Makower, C. G. Bauer, F. Bier, and F. W. Scheller. Determination of p-aminophenol and catecholamines at picomolar concentrations based on recycling enzyme amplification. *Analytica Chimica Acta*, 304:25, 1995.

[242] E. Vijgenboom. *personal communication*. University of Leiden, The Netherlands, 1999.

[243] V. Picard, E. Ersdal-Badju, A. Lu, and S.C. Bock. A rapid and efficient one-tube pcr-based mutagenesis technique using pfu dna polymerase. *Nucleic Acid Research*, 22:2587, 1994.

[244] R. Karlsson and R. Stahlberg. Surface plasmon resonance detection and multispot sensing for direct monitoring of interactions involving low-molecular-weight analytes and for determination of low affinities. *Analytical Biochemistry*, 228:274, 1995.

[245] L. Bubacco, E. Vijgenboom, C. Gobin, A. W. J. W. Tepper, J. Salgado, and G. W. Canters. Kinetic and paramagnetic nmr investigation of the inhibition of *streptomyces antibioticus* tyrosinase. *Journal of Molecular Catalyses B: Enzymatic*, 8:27, 2000.

[246] J. Sambrook, E. F. Fritsch, and T. Maniatis. *Molecular cloning: a laboratory manual*. Cold Spring Harbor Laboratory Press, New York, United States of America, 1989.

[247] T. Kieser, M. J. Bibb, M. J. Buttner, K. F. Chater, and D. A. Hopwood. *Practical Streptomyces genetics*. The John Innes Foundation, Norwich, United Kingdom, 2000.

[248] U. F. Wehmeier. New functional *escherichia coli - streptomyces* shuttle vectors allowing blue-white screening on xgal plates. *Gene*, 165:149, 1995.

[249] P. J. Dyson and M. Evans. pucs75, a stable high-copy-number *streptomyces - escherichia coli* shuttle vector which facilities subcloning from puc and m13 phage vectors. *Gene*, 171:71, 1996.

[250] D. Pfeiffer, F. Scheller, U. Wollenberger, D. Pfeil, S. Goan, J. Nentwig, N. Klimes, and K. Setz. *Designing and characterization of enzyme probes for different diagnostic relevance*, page 419. Akademiai Kiado, Mátrafüred, Hungary, 1992.

[251] E. Katz, C. J. Thompson, and D. A. Hopwood. Cloning and expression of the tyrosinase gene from *streptomyces antibioticus* in *streptomyces lividans*. *Journal of Genetic Microbiology*, 129:2703, 1983.

[252] D. A. Hopwood, M. J. Bibb, K. F. Chater, T. Kieser, C. J. Bruton, H. M. Kieser, D. J. Lydiate, C. P. Smith, J. M. Ward, and H. Schrempf. *Genetic manipulation of Streptomyces: a laboratory manual*. The John Innes Foundation, Norwich, United Kingdom, 1985.

[253] P. Jackman, A. Hajnal, and K. Lerch. Albino mutants of *streptomyces glaucescens* tyrosinase. *Biochemical Journal*, 274:707, 1991.